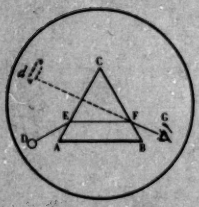

optics and spectroscopy

volume viii
number 2
february 1960

OPTICAL SOCIETY OF AMERICA

RUSSIAN EDITORIAL STAFF

Editor: S. E. FRISH

Assistant Editor: P. P. FEOFILOV
Corresponding Secretary: L. S. SAZONOV

Associate Editors:

M. M. GUREVICH M. A. EL'IASHEVICH A. A. LEBEDEV V. P. LINNIK
S. L. MANDEL'SHTAM I. V. OBREIMOV V. K. PROKOF'EV
N. N. SOBOLEV A. N. TERENIN A. I. TUDOROVSKII

Translated on the Initiative of
THE OPTICAL SOCIETY OF AMERICA, INC.
With a Grant-in-Aid from
THE NATIONAL SCIENCE FOUNDATION

TRANSLATION EDITORIAL STAFF

Scientific Editors

FRED W. BEHNKE, *Perkin-Elmer Corp.*

CYRUS FELDMAN, *Oak Ridge National Laboratory*

GEORGE HERRMAN, *Columbia University*

Administrative Editor: PATRICIA R. WAKELING, *OSA*

Published monthly by the Optical Society of America, Inc. Executive office: 1155 Sixteenth Street, N.W., Washington, D.C. Subscriptions for one year to members of the Society: Associates $13.00; Regular members and Fellows $17.00. Subscriptions for non-members of the Society: One year U. S. and Possessions, $25.00; Foreign $28.00. Back numbers: $3.00 per copy. Subscriptions, changes of address and undeliverable copies should be referred to the Executive offices in Washington, D.C. The office of publication is 2500 South State Street, Ann Arbor, Michigan. Second class postage paid at Ann Arbor, Michigan.

Printed in the U.S.A. by Edwards Brothers, Inc., Ann Arbor, Michigan.

CALCULATION OF PHOTOIONIZATION CROSS SECTIONS OF ALUMINUM AND GALLIUM ATOMS

L. A. Vainstein and G. E. Norman

Received 20 June 1959

The photoionization cross section of an atom is determined from the expression

$$\sigma = \frac{2\pi^2 a_0^2}{3 \cdot 137} \cdot \frac{\varepsilon - E_{nl'}}{g_{nl'}} \sum_{l=l'\pm 1} Q_{l'l} \left| \int_0^\infty P_{nl'}(r)\, P_{\varepsilon l}(r)\, r\,dr \right|^2, \quad (1)$$

where a_0 is the Bohr radius, $E_{nl'}$, $g_{nl'}$, $P_{nl'}(r)$ are respectively the energy, the statistical weight, and the radial function of the optical electron in the initial state of the atom; the radial function of the final state $P_{\varepsilon l}(r)$ is normalized to $\delta(\varepsilon - \varepsilon')$. In all that follows, the energy is expressed in Rydberg units, and all the other quantities are expressed in atomic units. The factor $Q_{l'l}$ depends only on the orbital and spin quantum numbers.[1] In the case of one electron outside of a filled shell $Q_{l'l} = 2 \max(l', l)$.

In order to find the radial function of a continuous spectrum $P_{\varepsilon l}(r)$, one must solve the Hartree-Fock equation numerically for each value of ε; this involves much computational work. As we know, in order to compute radial integrals of the type (1) we may use semi-empirical wave functions, the asymptotic behavior of which is determined in accordance with the experimental values of the energy terms. A method for determining these functions for a continuous spectrum, the so-called quantum defect method, was developed by Seaton. The general theory of the method is given in reference 2. In reference 3 it was used to calculate the photoionization cross section of Ca atoms.

For $\varepsilon \ll 4r^3$ the expression for $P_{\varepsilon l}(r)$ quoted in reference 2 can be put in the form

$$P_{\varepsilon l}(r) = A(\varepsilon, l)\,[u_{\varepsilon l}(r)\cos\pi\mu_l(\varepsilon) - v_{\varepsilon l}(r)\sin\pi\mu_l(\varepsilon)],$$

$$A^2(\varepsilon, l) = \prod_{s=0}^{l-1} [1 + (l-s)^2\varepsilon], \quad (2)$$

where $u_{\varepsilon l}(r)$ and $v_{\varepsilon l}(r)$ are linearly independent solutions of the radial Schrödinger equation with Coulomb field $-(1/r)$; $\mu_l(\varepsilon)$ is the quantum number defect extrapolated to the positive energy state of the optical electron. For the negative energy states E_{nl}

$$n_{nl} = n - n^*_{nl}; \quad n^*_{nl} = \frac{1}{\sqrt{-E_{nl}}}. \quad (3)$$

In most cases the extrapolation of $\mu_l(\varepsilon)$ to the positive energy state is reliable enough, since the function $\mu_l(\varepsilon)$ is close to being linear.

Equation (2) holds in the region where the field of the atomic remainder is close to being a Coulomb field. This region makes the major contribution to the radial integral for a dipole transition.

For small values of ε it is convenient to represent both $u_{\varepsilon l}(r)$ and $v_{\varepsilon l}(r)$ as series (Eq. (2) is asymptotic)

$$u_{\varepsilon l}(r) = \sum_{p=0}^{\infty} (-\varepsilon)^p \sum_{p=|q|}^{3p} a_{qp} \cdot (2r)^{\frac{p+1}{2}} J_{2l+1+p}(\sqrt{8r}), \quad (4)$$

$$v_{\varepsilon l}(r) = \sum_{p=0}^{\infty} (-\varepsilon)^p \sum_{p=|q|}^{3p} a_{qp} \cdot (2r)^{\frac{p+1}{2}} Y_{2l+1+p}(\sqrt{8r}), \quad (5)$$

$$a_{qp} = \frac{1}{4p}\,((2l+p)\,a_{q-1,\,p-2} - a_{q-1,\,p-3});$$

$$a_{00} = 1; \quad a_{12} = \frac{l+1}{4}; \quad a_{13} = -\frac{1}{12}, \quad (6)$$

where J_l and Y_l are Bessel functions of the first and second kind.

It is important that the functions $u_{\varepsilon l}(r)$ and $v_{\varepsilon l}(r)$ do not depend on the properties of a given atom. We have tabulated these functions for $l = 2$; $\varepsilon = 0$–0.1 (see Tables 1 and 2).

Table 1. Function $u_{\varepsilon 2}(r)$

r / $\sqrt{8r}$	0.00	0.02	0.04	0.06	0.08	0.10
2.0	0.264	0.262	0.261	0.259	0.257	0.255
2.5	0.652	0.641	0.629	0.619	0.608	0.597
3.0	1.086	1.042	0.999	0.958	0.917	0.877
3.5	1.218	1.107	0.996	0.894	0.798	+0.708
4.0	+0.743	+0.544	+0.366	+0.211	+0.076	−0.042
4.5	−0.248	−0.457	−0.611	−0.719	−0.786	−0.823
5.0	−1.170	−1.197	−1.147	−1.040	−0.896	−0.734
5.5	−1.311	−0.990	−0.621	−0.272	+0.04	+0.31
6.0	−0.441	+0.150	+0.802	+0.87	+1.00	+1.00

Table 2. Function $v_{\varepsilon 2}(r)$

r / $\sqrt{8r}$	0.00	0.02	0.04	0.06	0.08	0.10
2.0	−1.502	−1.463	−1.352	−1.256	−1.18	−0.11
2.5	−1.134	−1.029	−0.938	−0.859	−0.79	−0.73
3.0	−0.591	−0.482	−0.389	−0.306	−0.23	−0.17
3.5	+0.233	+0.330	+0.397	+0.460	+0.51	+0.55
4.0	1.026	1.039	1.026	0.999	0.96	0.92
4.5	1.383	1.114	0.836	0.754	+0.58	+0.42
5.0	+0.677	+0.323	+0.016	−0.24	−0.43	−0.56
5.5	−0.491	−0.818	−0.997	−1.05	−0.99	−0.8
6.0	−1.379	−1.305	−1.05	−0.69	−0.3	0.0

The photoionization of Al and Ga atoms was computed with the help of these tables and the ground state functions of a self-consistent field given in references 4 and 5. In both cases, $l' = 1$ for the ground state. Test calculations showed that of the two possible values $l = l' \pm 1$, only $l = 2$ contributes significantly to the cross section. Therefore, from then on, only the $p \to d$ transition of the optical electron was taken into account. The Figure shows the cross sections obtained as a function of the energy of the emitted electron.

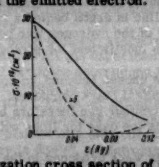

Photoionization cross section of aluminum atoms (solid line) and gallium atoms (dashed line) (× 5).

As is seen in the Figure, despite the similarity of the

outer shells of Al and Ga, their photoionization cross sections are considerably different. Unfortunately, at present we lack the experimental data for these atoms.

The authors express their gratitude to L. M. Biberman for many valuable discussions.

REFERENCES

1. E. Condon and G. Shortley. "Theory of Atomic Spectra." Izdatel'stvo Inostrannoi Literatury, Moscow, 1949.
2. M. J. Seaton and M. N. Roy. Astron. Soc. Pacific Leaflet, 118, 504 (1958).
3. M. J. Seaton. Ann. Astrophys. 18, 206 (1955).
4. L. Bierman and K. Lübeck. Z. Astrophys. 26, 43 (1949).
5. W. Hartree, D. R. Hartree, and M. F. Manning. Phys. Rev. 59, 299 (1941).

THE CONTOUR OF THE H_β HYDROGEN LINE BEHIND A SHOCK WAVE IN ARGON

V. N. Alyamovskii and V. F. Kitaeva

Received 22 June 1959

A study was made of the contour of the H_β hydrogen line behind a reflected shock wave in argon. It was established that a considerable part of the contour is satisfactorily described by Holtsmark's statistical theory. The concentration of charged particles in the argon behind the reflected shock wave was obtained from the experimental contour and half-width of this line. The values agree with calculated values obtained on the assumption of an ideal gas in thermal equilibrium.

The present research forms part of a program of the Physical Institute of the USSR Academy of Sciences on the spectroscopic study of the state of a gas behind a shock wave. A generalized line-reversal method has proven to be very effective.[1] However, at present this method is restricted to studying the state of a gas behind a shock wave at temperatures no higher than 5000°K. Spectroscopic methods must be developed which are suitable for studying the state of the plasma behind a shock wave at higher temperatures; in particular, methods based on studying the contours of spectral lines. The study of the contours of lines excited in a gas behind a shock wave is interesting from two points of view.

Firstly, by measuring the half-width of the line, we obtain information on the concentration of charged particles in the plasma behind the shock wave, and also on the plasma temperature if thermal equilibrium prevails. The line contours described by Holtsmark's statistical theory are determined exclusively by the concentration of particles, not by their velocity, and measuring the line width is therefore the only optical method available for measuring the concentration of charged particles in a plasma which is not in equilibrium.

Secondly, excitation conditions of the plasma lines behind a shock wave are very favorable for comparing experimental data with theories of line broadening, since the plasma behind the shock wave is highly uniform, and is not perturbed by any external fields; this is not true for the electrical light sources ordinarily used (arc, spark, etc.).

In the present investigation, we studied the contour of the H_β hydrogen line in argon behind a reflected shock wave. The intensity of the hydrogen line behind the incident shock wave was insufficient for photographic recording.

The H_β line was chosen because, in contrast to H_α, H_γ etc., it has no central Stark component, and its theoretical Holtsmark contour can therefore be calculated more reliably than is the case for lines with a central component.

The shock waves were produced in the shock tube described in reference 1. Hydrogen was used as the driver gas. The hydrogen pressure in the high pressure chamber was 80-110 atm. The low pressure chamber was filled with a mixture of argon and hydrogen. The pressure of the mixture was ~0.3-3 mm Hg. Hydrogen was added to the argon in small quantities, ~2-5% by pressure. The velocity of the incident shock wave was measured by ionization transducers. 0.3 volt was applied to the transducers. The pulses were recorded on an OK-17M oscillograph. Figure 1 is a diagram of the apparatus. Under these experimental conditions, the velocity of the incident shock wave varied from 3.6 to 4.8 km/sec, and the corresponding calculated temperature and pressure behind the reflected wave were ~12,000-13,000°K and 0.5-1.5 atm.

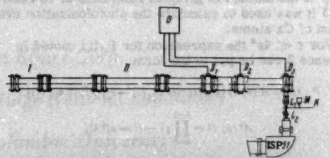

Fig. 1. Diagram of the apparatus. I—High pressure chamber; II—low pressure chamber; D_1, D_2—ionization transducers; O—oscillograph; L_1, L_2—lenses; ISP-51—spectrograph; M—motor; K—disc.

The H_β line was recorded photographically with an ISP-51 spectrograph, using the medium focal length camera (f = 270 mm). The dispersion of this spectrograph in the region of the H_β line was 40 A/mm. The spectral slit-width was 0.8 A. The radiation from an end segment (~1 cm) of the tube reached the spectrograph. An RF-3 plate was used. To scan the radiation spectrum in time, a disc 28 cm in diameter, with openings 0.5 mm wide set 5 mm apart, was placed in front of the spectrograph slit and rotated by an MU-100 motor. The speed of rotation of the disc (~1500 rpm) was selected so that images of successive slits did not overlap; the resolution obtained was ~25 μsec. Figure 2 shows the plasma radiation spectrum obtained behind the reflected shock wave. The Figure shows that the time-resolved spectrum consists of two distinct regions. The first region ~100 μsec long is due to radiation after the first reflection of the

shock wave from the end of the tube and is characterized by its constant intensity; the second region is due to radiation after the following reflections. The contour of the H_β line in the first region was measured photometrically.

Fig. 2. Spectrum of the luminescence in argon behind a reflected shock wave.

Figure 3 shows one of the H_β line contours obtained. Under our experimental conditions, the H_β line in the plasma behind the reflected shock wave is characterized by a considerable half-width (40-60 A), a dip in intensity in the middle of the line, and an asymmetry of about 6%, which is explained[3] by the quadratic Stark effect. The quantity $2(I_{blue} - I_{red})/(I_{blue} + I_{red})$ was used as a measure of asymmetry. The distance between the blue and red maxima of the H_β line increases in proportion to the increase in the half-width. The graph in Fig. 4 illustrates this. Due to the large scatter of the experimental points, the line was constructed by the least squares method.

The H_β line contour which we obtained in the gas behind the shock wave is similar to the contour given in references 2-5 for a high current confined arc, and the asymmetry has the same value. The dip in the center of the H_β line is caused by the fact that the central Stark component is absent.

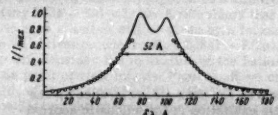

Fig. 3. Contour of the H_β line in argon behind a reflected shock wave. Solid curve—experimental contour; points—contour from Holtsmark's theory.

We compared our experimental H_β line contours with the theoretical contour calculated from Holtsmark's theory, which we took from reference 3. For the conditions of our experiments it was not necessary to use Kogan's more exact theory[6] which takes account of the movement of ions, since in our experiments the parameter $h_1 = N_1 (C_2/v_1)^3$ is greater than unity (here N_1 is the concentration of charged particles, C_2 is the Stark effect constant, v_1 is the ion velocity). Kogan's theory leads to the same line intensity distribution as Holtsmark's theory, which neglects the movement of the ions.

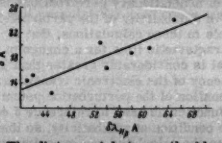

Fig. 4. The distance Δ between the blue and red maxima of the H_β line plotted against the line half width $\delta\lambda_{H\beta}$.

The comparison was made as follows: we chose the contour which agreed best with our experimental contours from the family of theoretical contours corresponding to different values of the normal field strength E_0. This gave us a value of E_0, and thus the concentration N_1 of charged particles in the plasma behind the reflected shock wave, since

$$E_0 = 2.61 e N_1^{\frac{2}{3}}.$$

The results are presented in the Table in the column "N_1 from E_0." The column "N_1 from $\delta\lambda_{H\beta}$" gives the values of N_1 calculated from a comparison of the experimental H_β line half-width with the Holtsmark value. We estimate the error in determining E_0 to be ~15%. This corresponds to an error of ~20% in determining N_1. The error in determining N_1 from the H_β line half-width $\delta\lambda_{H\beta}$ is ~15%. The Table also gives the values $N_{1\beta}$ for argon behind the reflected shock wave, which we obtained by linear extrapolation of the data given in reference 7; these data were calculated by using Saha's equation (neglecting atomic excitation) and the equation of state for an ideal gas; heat conduction and radiation losses were neglected in these calculations.* Our experimental results

*The argon parameters behind the reflected shock wave are marked with the subscript 5 in the Table, in agreement with reference 7.

can be compared with these calculated values since we have estimated that adding 2% of hydrogen does not appreciably alter the parameters of argon behind the reflected shock wave.

Expt. No.	High pressure (atm)	Low pressure of argon + 2% hydrogen (mm Hg)	Incident shock wave: ν (km/sec)	Incident shock wave: Mach number M	$\delta\lambda_{H\beta}$ (A)	Field strength E_0 (kv/cm)	Concentration $N_1 \times 10^{-15}$: from E_0 (cm^{-3})	Concentration $N_1 \times 10^{-15}$: from $\delta\lambda_{H\beta}$ (cm^{-3})	Parameters of argon behind the reflected shock wave: $(N_1 + N_e)_5 \times 10^{-15}$ (cm^{-3})	Density $N_5 \cdot 10^{-18}$ (cm^{-3})	Degree of ionization α_5	Temp. T_5 (°K)	Pressure P_5 (atm Hg)
79	75	0.26	4.52	14.1	45	108	1.6	1.2	1.4	3.8	0.36	12700	490
81	84	0.26	4.80	14.4	63	144	2.5	1.9	1.5	4.0	0.37	12900	530
83	110	0.26	4.78	14.9	65	180	3.3	2.0	1.7	4.2	0.41	13300	570
77	75	0.45	—	—	41	96	1.3	1.0	—	—	—	—	—
78	90	0.45	4.06	12.7	42	108	1.6	1.0	1.3	4.9	0.26	12600	640
86	115	0.78	3.82	11.9	54	126	2.0	1.5	1.4	6.6	0.21	12500	870
87	110	1.16	3.60	11.2	52	144	2.5	1.4	1.4	8.5	0.17	12300	1070

DISCUSSION OF RESULTS

Figure 3 and the Table show agreement between theory and experiment, in the first approximation. The experimental contour of the line is described adequately by Holtsmark's theory; the concentrations of charged particles determined either from the half-width $\delta\lambda_{H\beta}$ or from the H_β line contour agree with the data calculated using Saha's gas dynamics. Therefore, the method of determining the concentration of charged particles from the broadening of the H_β hydrogen line, using Holtsmark's theory, is completely reliable for studying plasma behind a shock wave.

However, a more detailed analysis of the results obtained shows that for all the experiments, the concentrations of charged particles determined from the intensity distribution at the edges of the line exceed those obtained from the half-width. A similar situation was noticed in reference 5 in determining the concentration of charged particles in the plasma of a high current confined arc. This discrepancy is due[2,3] to distortion of the pure Holtsmark contour by two factors:[10] (1) Debye screening of the ion field which leads to narrowing of the contour, and (2) collision with electrons, which leads to collision broadening of the contour. At the center of the line, these two factors almost compensate each other and the half-

width remains close to the Holtsmark value. However, the shapes of the edges of the lines change, since the electron broadening leads to a distribution with a slower fall in intensity than predicted by Holtsmark, which leads to an increase in the intensity of the edges, and so to increased values for the concentration.

Further, the Table shows satisfactory agreement, within the experimental accuracy between the values of N_i calculated from the H_δ line half-width (from $\delta\lambda_{H_\delta}$), which we will consider the true values for the reasons mentioned above, and the values calculated theoretically. This agreement may be the result of the compensation of two effects: firstly, heat conduction and radiation losses (which are neglected in the calculations) lower the value of N_i; secondly, the effects of easily ionized impurities and of a reduction in ionization potential observed in our conditions, which are neglected in the calculations, increase N_i. However, in the first place the low contamination of the spectrum with lines of impurity elements shows that the concentrations of these elements were low; in the second place, the reduction in the ionization potential (~6%) should, under our conditions, lead to approximately the same percentage increase in the concentration of charged particles, since for our values of α, the total gas energy behind the wave reflected from the end of the tube $E \approx N_i \alpha \chi$ to an accuracy ~20% (χ is the ionization potential and E is a fixed quantity for a given velocity).

Therefore, within the experimental accuracy, neglecting losses, the calculated ion concentrations in the plasma behind the reflected wave agree with the experimental values.

The authors sincerely thank N. N. Sobolev for his advice and interest.

REFERENCES

1. N. N. Sobolev, A. V. Potapov, V. F. Kitaeva, F. S. Faizullov, V. N. Alyamovskii, E. T. Antropov, and I. L. Isaev. Izvest. Akad. Nauk SSSR, Ser. Fiz. 22, 730 (1958); Opt. i Spektr. 6, 284 (1958).
2. H. Grim. Z. Physik 137, 280 (1954).
3. G. Jürgens. Z. Physik 134, 21 (1952).
4. P. Bogen. Z. Physik 149, 62 (1957).
5. P. J. Dickerman. J. Appl. Phys. 29, 598 (1958).
6. V. I. Kogan. Sb. Fizika plazmy i problema upravlyaemykh termoyadernykh reaktsii 4, 258 (1958).
7. E. L. Resler, Shao-Chi Lin, and A. Kantrowitz. J. Appl. Phys. 23, 1390 (1952).
8. W. Lochte-Holtgreven. Repts. Progr. Phys. 21, 312 (1958).
9. H. Grim. Proc. Conf. on Extremely High Temperatures, New York 93 (1958).
10. G. Ecker. Z. Naturforsch. 12a, 346 (1957); Z. Physik. 148, 593 (1957); Z. Physik. 149, 254 (1957).

ON A POSSIBLE MECHANISM OF ELECTRONIC EXCITATION IN SLOW ATOMIC COLLISIONS

E. E. Nikitin

Received 28 May 1959

As follows from the general theory of atomic collisions (cf., for example, reference 1), the effective threshold E_{eff} of the cross section, σ, for electronic excitation in the adiabatic approximation exceeds the real threshold E_0 by a significant amount. For intermediate energies E of the colliding atoms ($E_0 < E < E_{eff}$), σ varies exponentially with E, so that the cross section, averaged over the Maxwellian energy distribution of the colliding atoms, is characterized by a temperature dependence of the Landau-Teller type.[2] The latter is well known from the theory of inelastic molecular collisions.

In some cases, however, the experimental results do not agree with these conclusions. In reference 3, for example, the luminescence of xenon behind a shock wave front was studied. The mechanism proposed by the authors for the production of this radiation consists of a radiative transition from an excited Xe_2^* molecule, whose electronic state corresponds to the formation of a chemical bond, into the ground state characterized by mutual repulsion of the two Xe atoms. As the first step in the process, electronic excitation of a xenon atom must take place according the reaction

$$Xe + Xe \rightarrow Xe^* + \chi v.$$

The relatively low efficiency of this reaction explains the existence of a delay period τ between the passage of the shock-wave front and the maximum of the luminosity. It is significant that an investigation of the temperature dependence of the time τ leads to the relation

$$\frac{1}{\tau} \sim \exp\left(-\frac{E_0}{kT}\right), \qquad (1)$$

in which the activation energy E_0 is equal to the energy of the first resonance transition of Xe. It is well known that this form of temperature dependence is obtained only when $E \approx E_0$; i.e., when the corss section σ is relatively weakly dependent (as compared with the Boltzmann factor) on the energy near the threshold. This conclusion agrees with the experimental data on the ionization of He and A in atomic collisions.[4]

Experimental values of the cross section obtained in reference 4 show satisfactory agreement with calculated values of the cross section for ionization.[5] In reference 5, the method of nonstationary perturbations is used. The assumption of adiabaticity of the perturbation plays an essential role in these calculations; that is, it is assumed that the characteristic time for a change in the perturbation potential is considerably greater than the reciprocal of the frequency of the electronic transition. However, the approximation of the perturbation potential by a discontinuous function as used in reference 5 effectively nullifies the condition of adiabaticity, so that the agreement between the calculated and experimental values of the cross sections does not appear to have much significance.

It thus appears that the adiabatic approximation is not applicable in some cases of inelastic atomic collisions.

The simplest nonadiabatic process which can be realized in atomic collisions is a multiple (and, in particular, a double) charge transfer. In this case, the atoms are located on different potential curves before and after the collision, and the transition from one potential curve to the other takes place by way of the potential curve of the ionic state. The probability of such a transition, which involves a double passage through the point of intersection, is determined by the Landau-Zener formula[4] and is equal to

$$P = e^{\eta}(1 - e^{\eta}). \qquad (2)$$

For $\eta \ll 1$, this expression takes the form

$$P = \eta = \frac{2\pi\,(\Delta U)^2}{\hbar v \left|\frac{d}{dr}(U_1 - U_2)\right|} = 247\,\frac{\sqrt{m}}{\sqrt{E}}\,\frac{(\Delta U)^2}{(\Delta E)^2}, \qquad (3)$$

where U_1 and U_2 are the potential curves of the two electronic states, v is the relative velocity of the colliding atoms at the point $U_1(r) = U_2(r)$, and ΔU is the matrix element of the perturbation. In numerical estimations of η one can use the last equality in Eq. (3), which has been taken from reference 7; in this expression the energy and reduced mass of the colliding atoms are expressed in electron volts and atomic units, respectively.

A model reaction involving a double transfer of charge is

$$H(1s) + H(3s) \rightarrow H^- (1s^2) + H^+ \rightarrow H(1s) + H(2s)$$

which has been considered by Bates and Lewis.[5] These authors found that the reaction constant is very weakly dependent on the temperature and is equal to 2×10^{-11} cm^3/sec at 500°K; this corresponds to a relatively high probability $P(3s \rightarrow 2s) \approx 1/10$. It is evident that the speed of the reverse reaction will be given by a formula of type (1) with an activation energy $E_0 = E(3s) - E(2s)$.

We will consider the ionization of the helium atom from this point of view (cf. the Figure). If we choose the energy U_1 of the system $He(1s^2) + He(1s^2)$ as the zero level, neglecting the exchange energy which plays a significant role only at small distances, we obtain $U_2 = 24.5$ ev for the energy of the system $He(1s^2) + He^+(1s)$. The energy $U_3(R)$ of the ionic state of the system $He^- + He^+$ as $R \rightarrow \infty$ is found by summing the energy of He^+ and the energy of the negative ion He^-. Only the excited He atom possesses an electron affinity; this corresponds to the ion $He^-(1s2s2p)$(cf., for example, reference 9) with an energy of about 20.5 ev. Thus we find $U_3(\infty) = 45$ ev. For $R \rightarrow \infty$ the curve for the ionic state U_3 intersects first the straight line U_1, and then the straight line U_2. Ionization in the collision He + He is thus described by the two-stage process

$$He(1s^2) + He(1s^2) \rightarrow He^-(1s2s2p)$$
$$+ He^+(1s) \rightarrow He(1s^2) + He^+(1s) + e.$$

We will now estimate the magnitude of η in expression (3). We will consider the case of the transition from

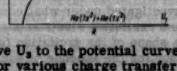

the potential curve U_3 to the potential curve U_2. Calculation shows that for various charge transfer reactions which have been studied, the value of ΔU ranges from 10^{-2} to 1 ev.[7, 8, 10] If we assume for definiteness that the translational energy before collision exceeds the threshold energy necessary for ionization by 0.5 ev, we obtain $\eta \ll 1$. For the transition $U_3 - U_1$, the magnitude of η will be still smaller. From expressions (2) and (3), then, it follows that the probability of a double transfer of charge will be relatively weakly dependent on the energy. A comparison with the deactivation reaction of hydrogen considered above indicates that the value of the ionization probability observed experimentally in helium can be reasonably explained in terms of this scheme (the experimental ionization probability of helium in a single gas-kinetic collision is approximately 10^{-4}).[4] To calculate the cross section, and to obtain the explicit form of the function $\sigma = \sigma(E)$, it is of course necessary to use approximate electronic functions for He, He^+, and He^-. In this case, however, it must be assumed that the basic qualitative conclusions concerning the weak dependence of the cross section on the energy, and its relatively large value as a result of nonadiabaticity, still hold good.

In just the same way, it is possible to interpret qualitatively the observed temperature dependence[3] of the efficiency of the electronic excitation of Xe. In this case, the double charge transfer arises as a result of the reaction

$$Xe(5p^6) + Xe(5p^6) \rightarrow Xe^- + Xe^+(5p^5) \rightarrow Xe(5p^56s) + Xe(5p^6),$$

where Xe^- is the negative excited ion of Xe (in the normal state, Xe has no electron affinity).

As far as actual calculation of the value of the cross section is concerned, one must note the following: The adiabatic approximation and the introduction of charge transfer in collisions are conceptually contradictory as approximations in the calculation of the probability amplitude by the general formula of the theory of nonstationary perturbations

$$a_{ps} = \frac{1}{i\hbar}\int_{-\infty}^{+\infty} W_{ps}(t)\exp(i\omega t)\,dt.$$

In the first case, the frequency ω is considered to be independent of the time. In the second case the dependence of the matrix element of the perturbation $W_{ps}(t)$ on time is neglected, and it is assumed that ω is proportional to t at the point of intersection of the potential curves. By means of concrete examples, Bates[11] has recently shown the importance of the simultaneous calculation of the time dependence of the off-diagonal terms of the perturbation matrix W_{ps}, as well as that of the diagonal elements which determine the frequency of the transition. From what has been said, it thus follows that although the concept of double charge transfer is more accurate than that of adiabatic electronic excitation, it nevertheless appears to be unsatisfactory, in its simplest form, for an accurate calculation of the cross section

The author is grateful to Professor N. D. Sokolov for discussions of this investigation.

REFERENCES

1. H. S. W. Massey and E. H. S. Burhop. "Electronic and Ionic Impact Phenomena." Clarendon Press, Oxford, 1952.
2. L. Landau and E. Teller. Physik. Z. Sowjetunion 10, 34 (1936).
3. W. Roth and P. Gloersen. J. Chem. Phys. 29, 820 (1958).
4. A. Rostagni. Nuovo cimento 11, 821 (1934).
5. P. Rosen. Phys. Rev. 109, 348, 351 (1958).
6. L. Landau and E. Lifshitz. "Kvantovaya Mechanika." (Quantum Mechanics), Moscow, 1948.

7. D. R. Bates and B. L. Moiseiwitsch. Proc. Phys. Soc. (London) A67, 805 (1954).
8. D. R. Bates and J. T. Lewis. Proc. Phys. Soc. (London) A68, 173 (1955).
9. N. S. Buchel'nikova. Uspekhi Fiz. Nauk 65, 351 (1958).
10. A. Dalgarno. Proc. Phys. Soc. (London) A67, 1010 (1954).
11. D. R. Bates. Proc. Phys. Soc. (London) 73, 227 (1959).

PHOTOELECTRIC DETERMINATION OF THE EXCITATION FUNCTIONS OF THE BANDS OF THE NEGATIVE SYSTEM N_2^+

S. M. Kishko

In this paper, the excitation functions of the bands (0 – 0) and (0 – 1) of the negative system N_2^+ are studied, and the effect of a monoenergetic beam of electrons and of nitrogen pressure on their behavior are examined. Five maxima, lying at various energies of the exciting electrons, were observed in the excitation functions under investigation.

When a molecular gas is excited by a beam of electrons, the intensity of the radiation bands depends on the energy of the electron beam. This functional relationship is called the excitation function of the band.

Data on excitation functions of bands are needed in solutions of many problems in spectroscopy,[1] astrophysics, and gas discharge physics;[2] they are also needed for explaining the glow of the night sky, aurora polaris, etc. In spite of this, molecular excitation functions have not been studied extensively.[3-9]

Our goal was to obtain reliable data on the excitation functions of the various bands in the negative system N_2^+, which arise from the transition $B^2\Sigma - X^2\Sigma$.

EXPERIMENTAL METHOD

All the basic information about the experimental apparatus and the method of measurement were given in reference 1. Here we shall consider in detail only the photometric apparatus, which was used for recording the radiation under investigation. Figure 1 shows the electric circuit of the photometer, which consisted of a photomultiplier Type FEU-17 and a dc amplifier constructed from a single vacuum tube Type 2E2P.* With an input

*Translator's Note: This is the Russian tube designation.

resistor $R = 3.3 \times 10^{10}$ ohms the amplification factor of the amplifier was equal to 5×10^4. In order to limit the fluctuation in the spectra, a condenser of a capacity such that the time constant RC was equal to 4 sec was connected in parallel with the input resistor of the amplifier. In the case under discussion, the photometer contained a photomultiplier with an integral sensitivity of 50 amp/lumen and a dark current of 7×10^{-11} amp at a sensitivity of 1 amp/lumen. The measured photocurrent was read on an M-95 galvanometer. The dark current of

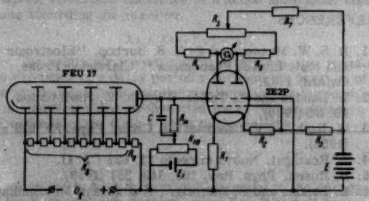

Fig. 1. Photometer circuit diagram.

the photomultiplier was compensated by means of an external constant current source E_1 with the aid of the potentiometer R_{10}. The photomultiplier supply consisted of a battery of dry cells of the type BAS-80, and the dc amplifier was supplied by a large capacity acid battery.

To ensure a uniform voltage distribution among all the photomultiplier electrodes, the resistors in the potential divider were selected to have a single value of resistance to within an accuracy of 2%. The resistance between the last emitter and ground was doubled and equal to 600 kohms. In the case of the FEU-17 photomultiplier, the total voltage applied across the potential divider was 720 volts. In order to reduce dark current fluctuations, our photomultiplier was cooled in dry ice with the help of a simple apparatus whose basic part was a copper cylindrical conductor fitted over the photomultiplier in such a way as to completely surround it as far as the fourth emitter. The accuracy of photocurrent measurements was about 2%.

The excitation tube was filled with nitrogen obtained by heating sodium azide.[11] Molecular nitrogen ions are formed and are excited according to the reaction:

$$N_2 + e \rightarrow (N_2^+)^* + 2e$$

under the condition that the energy of the exciting electrons exceeds the excited state energy $B^2\Sigma$, which is 18.7 ev.

The molecular nitrogen ion concentration and the probability of the transition $B^2\Sigma - X^2\Sigma$ were sufficiently large, so that the radiation of the negative system N_2^+ [1] could be photographed on photoplates of "spectral Type III" by using an exposure of about 20 min.

In order to study the properties of the electron beam by means of which the molecular gas under investigation was excited, the uniformity and the degree to which the beam was monoenergetic were determined for various accelerating potentials.

Measurements of the degree to which the beam was monoenergetic[12] were made with a nitrogen pressure of 1×10^{-3} mm Hg, an electron current density of 10^{-3} amp/cm^2 and an applied voltage of 40 volts. It was found that under these conditions in the excitation tube more than 90% of the electrons in the beam had velocities in a band that was from 1 to 1.2 ev wide.

We also investigated under what conditions the nitrogen pressure and excitation electron current density have no effect on the shape of the excitation functions.

The criterion for the absence of such an effect is a linear dependence of the intensity on pressure and electron current density. Separate measurements of ours showed that in order to preserve linearity between the

indicated quantities, it is necessary for the nitrogen pressure in the excitation tube to be less than 4.5×10^{-3} mm Hg and for the current density to be less than 3.3×10^{-3} amp/cm^2 (see Figs. 2, 3).

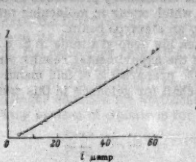

Fig. 2

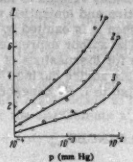

Fig. 3

Fig. 2. Intensity of radiation from the I(0 – 1) band as a function of the electron current density i for a pressure of 0.8×10^{-1} mm Hg.
Fig. 3. Intensity of radiation from the I(0 – 1) band as a function of nitrogen pressure p for various electron current densities. Current density (in μamp) curve 1—35; curve 2—30; curve 3—25.

EXPERIMENTAL RESULTS AND DISCUSSION

The relative excitation functions of the bands (0 – 0) and (0 – 1) of the negative system N_2^+, were investigated; the edges of these bands were at 3914.4 and 4278.1 A respectively. The results of the measurements are shown in Fig. 4, which was obtained for a nitrogen pressure of 0.8×10^{-3} mm Hg and a current density of 10^{-3} amp/cm^2; the experimental points were taken at 3 volt intervals.

From the results which were obtained it can be seen that the excitation functions of both bands have several sharply defined maxima, which lie at 49.56 and 67 volts. Beyond these sharp maxima, there follows a broad maximum whose highest point lies in the 80 to 90 volt region. The onset of the excitation functions of both bands occurs at about 19 volts which is in good agreement with the excitation potential of the level (18.7 volts[34]). The investigation of the excitation functions was conducted in different tubes, without affecting the results.

Because a small bump was observed on the excitation functions in the region of 30 volts, we investigated their leading edges with considerably better energy homogeneity in the electron beam (the energy spread was less than 1 ev), and the experimental points were taken between 1.5 and 2 volts apart. As a consequence of this work, as is seen in Fig. 5, still another narrow maximum was observed for both bands at an excitation potential of 29 volts. Thus, five maxima were found in the excitation functions of the (0 – 0) and (0 – 1) bands of the negative system N_2^+.

All the maxima described here were observed in many measurements at the same energies of exciting electrons, and therefore their existence cannot be doubted. The accuracy of determination of the excitation potential was ±0.5 ev.

If the nitrogen pressure was gradually increased, the maxima in the curves merged together. The results of measurements on the (0 – 1) band obtained at various nitrogen pressures (from 0.8×10^{-3} to 9×10^{-3} mm Hg)

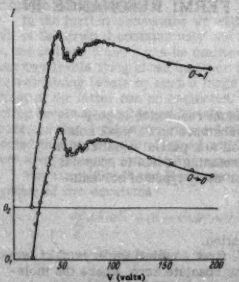

Fig. 4

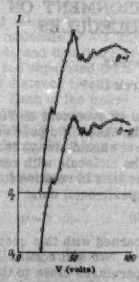

Fig. 5

Fig. 4. Behavior of the excitation functions of the (0 – 1) and (0 – 0) bands in the negative system N_2^+.
Fig. 5. Behavior of the excitation functions of the (0 – 1) and (0 – 0) bands of the negative system N_2^+ for an electron-beam energy spread of less than 1 ev.

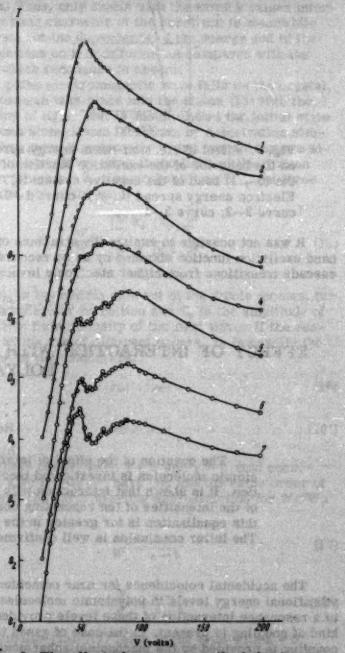

Fig. 6. The effect of pressure on the behavior of the excitation function of the (0 – 1) band of the negative system N_2^+. Nitrogen pressure (in mm Hg): curve 1—9×10^{-3}; curve 2—6.3×10^{-3}; curve 3—4.5×10^{-3}; curve 4—4×10^{-3}; curve 5—1.7×10^{-3}; curve 6—1×10^{-3}; curve 7—0.8×10^{-3}

and a fixed excitation electron current density (~10^{-3} amp/cm²) are shown in Fig. 6. From this figure it is clear that the structure of the excitation function for the (0 – 1) band was observed only when the pressure was lower than 4.5×10^{-3} mm Hg. The structure also disappeared if the monoenergetic character of the electron beam deteriorated even in the case of an insignificant nitrogen pressure, as can be seen in Fig. 7. The curves shown on this figure were obtained at a pressure of 10^{-3} mm Hg and electron current density of 10^{-3} amp/cm², but with different electron-beam energy spreads.

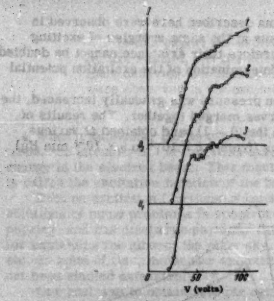

Fig. 7. Effect of electron-beam energy spread on the behavior of the excitation function of the (0 – 1) band of the negative system N_2^+. Electron energy spread (in ev): curve 1—3.5; curve 2—2; curve 3—1.

It was not possible to explain the structure of the band excitation function obtained by us by recourse to cascade transitions from higher electronic levels to the $B^2\Sigma$ level which is what happens for some mercury lines,[15, 16] since there are no such transitions to the $B^2\Sigma$ levels.

The appearance of maxima in the excitation functions is probably related to the elementary processes of dissociation and ionization which occur in molecular nitrogen when it is excited by an electron beam.

The author expresses his deep gratitude to S. E. Frish for discussions of the experimental results and valuable advice during the preparation of this manuscript, and also to I. P. Zapesochnii for guidance in this work.

REFERENCES

1. J. von Calker. Spectrochim. Acta 5, 476 (1953).
2. D. N. Radikov. Avtoref. diss. Tomsk, 1953.
3. A. E. Lindh. Z. Physik 67, 67 (1931).
4. L. S. Ornstein and G. O. Langstroth. Proc. Acad. Sci. Amst. 67, 384 (1933).
5. G. O. Langstroth. Proc. Roy. Soc. 143, 166 (1934).
6. O. Thieme. Z. Physik 78, 412 (1932).
7. F. P. Bundy. Phys. Rev. 52, 698 (1937).
8. R. Bernard. Compt. rend. 204, 488 (1937); Compt. rend. 205, 793 (1937).
9. D. T. Stewart. Proc. Phys. Soc. A69, 437 (1956).
10. S. M. Kishko and M. Iu. Kuchinka. Opt. i Spektr. 6, 580 (1959).
11. S. M. Kishko and I. P. Zapesochnii. Radiotekh. i Elektron. 3, 433 (1958).
12. S. M. Kishko and M. Iu. Kuchinka. Ukrain. Fiz. Zhurn. 4, 384 (1959).
13. I. P. Zapesochnii. Vestn. Leningrad Gosudarst. Univ. No. 11, 67 (1954).
14. G. Herzberg. "Molecular Spectra and the Structure of Diatomic Molecules." IL, Moscow, 1949.
15. S. E. Frish and I. P. Zapesochnii. Doklady Akad. Nauk SSSR 55, 971 (1954).
16. S. E. Frish and I. P. Zapesochnii. Izvest. Akad. Nauk. SSSR Ser. Fiz. 19, 5 (1955).

EFFECT OF INTERACTION WITH THE ENVIRONMENT ON FERMI RESONANCE IN POLYATOMIC MOLECULES

V. L. Strizhevsky

Received 18 March 1959

The question of the effect of interaction with the enrivonment on Fermi resonance in polyatomic molecules is investigated theoretically for the cases of a pure substance and a weak solution. It is shown that interaction with the environment should always lead to a partial equalization of the intensities of the resonating components. If the molecule with resonating levels is nonpolar, this equalization is far greater in the pure substance than in solution for many types of solvents. The latter conclusion is well confirmed from the experimental data.

The accidental coincidence (or near coincidence) of vibrational energy levels in polyatomic molecules leads to a resonance interaction of these levels provided some kind of coupling is present. In the case of gases this coupling is provided by the mechanical anharmonicity;[1] the interaction of levels which occurs in this case was investigated for the first time by Fermi.[1, 2] In addition to this interaction there exists in the condensed phases an intermolecular interaction which can also have an effect on Fermi resonance. It can be expected, generally speaking, that this effect will be more significant than the effect of mechanical anharmonicity, since the latter is usually very small.[1] The present investigation is concerned with this question.

We will consider first a molecular crystal at temperatures close to the absolute zero, where the molecules are held stationary in equilibrium positions formed by the lattice points of the crystal. Using the conventional designations of the theory of molecular crystals,[3] we will write the Hamiltonian of the crystal as follows:

$$H = \sum_{n\alpha} H_{n_\alpha} + \frac{1}{2} \sum_{n_\alpha, n'_{\alpha'}} V_{n_\alpha, n'_{\alpha'}} \equiv H_0 + V. \qquad (1)$$

Limiting our discussion to only those states of the crystal for which a single molecule is excited, we will

look for the correct wave function in the zeroth approximation in the form

$$\psi = (aN)^{-1/2} \sum_{n\alpha,f} a^f_{n\alpha} \chi^f_{n\alpha}; \quad \chi^f_{n\alpha} = \varphi^f_{n\alpha} \prod_{(m\beta \neq n\alpha)}{}' \varphi^0_{m\beta}. \tag{2}$$

Here the functions $\varphi^0_{n\alpha}$ and $\varphi^f_{n\alpha}$ refer to the ground state and fth excited states, respectively, of the molecule $n\alpha$ (all quantities referring to the free molecule are assumed to be known with the mechanical anharmonicity already taken into account). Substitution of (2) into the Schrödinger equation for stationary states leads to the following system of equations for the coefficients $a^f_{n\alpha}$

$$\sum_{f'} \sum_{m\beta}{}'' M^{ff'}_{n\alpha,\, m\beta}\, a^{f'}_{m\beta} - (E - \varepsilon^f)\, a^f_{n\alpha} = 0, \tag{3}$$

$$M^{ff'}_{n\alpha,\, m\beta} = \int \varphi^{f*}_{n\alpha} \varphi^{0*}_{m\beta} V_{n\alpha,\, m\beta}\, \varphi^0_{n\alpha} \varphi^{f'}_{m\beta}\, d\tau, \tag{4}$$

$$\varepsilon^f = E^f_0 + \sum_{n'\alpha'}{}' \left\{ E^0_0 + \int |\varphi^f_{n\alpha}|^2 V_{n\alpha,\, n'\alpha'} |\varphi^0_{n'\alpha'}|^2\, d\tau + \frac{1}{2} \sum_{m'\beta'}{}'' \int |\varphi^0_{n'\alpha'}|^2 V_{n'\alpha',\, m'\beta'} |\varphi^0_{m'\beta'}|^2\, d\tau \right\}, \tag{5}$$

where E^0_0 and E^f_0 are the energies of the ground and fth excited states of the free molecule,* and E is the total

*The single prime on the summation over $n'\alpha'$ in (5) means that terms with $n'\alpha' = n\alpha$ are to be omitted, and the double prime on the summation over $m'\beta'$ means that terms with $m'\beta' = n\alpha$ and $m'\beta' = n'\alpha'$ are to be omitted.

energy of the system. Expression (5) does not of course actially depend on $n\alpha$. For simplicity we will not write out the exchange terms. We will look for the solution of (3) in the form

$$a^f_{n\alpha} = B^f_\alpha e^{ikn}. \tag{6}$$

The coefficients B^f_α satisfy the system of equations

$$\sum_{\beta f'} L^{ff'}_{\alpha\beta} B^{f'}_\beta - (E - \varepsilon^f)\, B^f_\alpha = 0, \tag{7}$$

$$L^{ff'}_{\alpha\beta} = \sum_m{}'' M^{ff'}_{n\alpha,\, m\beta} e^{ik(m-n)}, \tag{8}$$

which do not depend on n

In the further discussion we will assume that the unit cell of the crystal contains only one molecule ($\sigma = 1$, that is, the indices α and β can be omitted), and that there are only two levels lying close together and separated from the remaining levels by such a large distance that the effect of the latter can be neglected. Each of the interacting levels is considered for simplicity as nondegenerate, so that f takes the values 1 and 2. It can be expected that the results obtained will be qualitatively correct even in more complicated cases.

The quantities B and E are then determined by the system of two equations

$$\sum_{f'} L^{ff'} B^{f'} - (E - \varepsilon^f)\, B^f = 0 \qquad (f = 1, 2), \tag{9}$$

the solution of which leads to the following relations:

$$\left.\begin{aligned} E_{+,-} &= E^0 \pm \frac{\chi}{2}, \quad E^0 = \frac{1}{2}(L^{11} + \varepsilon^1 + L^{22} + \varepsilon^2), \\ \chi &= \sqrt{\delta^2 + 4|L^{12}|^2}, \quad \delta = L^{11} + \varepsilon^1 - L^{22} - \varepsilon^2, \end{aligned}\right\} \tag{10}$$

$$B^1_+ = \left(\frac{\chi + \delta}{2\chi}\right)^{1/2}, \quad B^2_+ = \pm \left(\frac{\chi - \delta}{2\chi}\right)^{1/2}, \tag{11}$$

$$B^1_- = \left(\frac{\chi - \delta}{2\chi}\right)^{1/2}, \quad B^2_- = \mp \left(\frac{\chi + \delta}{2\chi}\right)^{1/2}, \tag{12}$$

in which in (11) and (12) the upper or lower signs are used according as the signs of δ and L^{12} are the same or different. The corresponding wave functions have the form

$$\psi_{+,-}(k) = N^{-1/2} \sum_{n,\, f=1,\, 2} B^f_{+,-}(k)\, e^{ikn} \chi^f_n. \tag{13}$$

The relations (10)–(12) have formally the same appearance as the corresponding expressions for resonance in gases;[1,2] however, the meaning of the quantities involved is somewhat different. "The distance between the unperturbed levels" in the theory for gases corresponds to the quantity δ, which, according to (5) and (10), can be written in the form

$$\delta(k) = E^1_0 - E^2_0 + L^{11} - L^{22} + \sum_{n'\alpha'}{}' \left\{ \int |\varphi^1_{n\alpha}|^2 V_{n\alpha,\, n'\alpha'} |\varphi^0_{n'\alpha'}|^2\, d\tau - \int |\varphi^2_{n\alpha}|^2 V_{n\alpha,\, n'\alpha'} |\varphi^0_{n'\alpha'}|^2\, d\tau \right\}. \tag{14}$$

The quantity δ here represents the energy difference of those levels which are formed as a result of the splitting of the molecular term into an exciton band, and which correspond to one and the same value of the wave vector k. Thus, only levels with the same k values interact. The band character of the spectrum is meanwhile preserved, but the dependence of the energy and of the wave functions on k is different as compared with the case in which resonance is absent.

If a plane electromagnetic wave falls on the crystal, transitions can take place into the states (13) with the absorption of light. If it is assumed that the initial state is a ground state, it can be shown, by a derivation similar to that given in reference 3, that transitions are allowed only into states lying at the limit of the exciton band, for which $k \approx 0$. The probabilities $W_{+,-}$ of these transitions are in the ratio

$$\frac{W_+}{W_-} = \frac{|\sum_f B^{f*}_+ (E_0 p_{f0})|^2}{|\sum_f B^{f*}_- (E_0 p_{f0})|^2}, \tag{15}$$

where p_{f0} is the matrix element of the dipole moment for the intramolecular transition and E_0 is the amplitude of the electric field intensity of the light wave. If the resonating terms are of different orders, as is usually the case, one of the inequalities,

$$|p_{10}| \gg |p_{20}| \tag{16}$$

or

$$|p_{20}| \gg |p_{10}|. \tag{16'}$$

must hold.

In these cases, when $\chi + \delta$ and $\chi - \delta$ (and consequently, also B^1 and B^2) have one and the same order of magnitude, the corresponding approximation for W_+/W_- gives

$$\frac{W_+}{W_-} = \frac{\chi + \delta}{\chi - \delta} \tag{17}$$

or

$$\frac{W_+}{W_-} = \frac{\chi - \delta}{\chi + \delta}. \tag{17'}$$

Formulas (15)–(17) refer to the case with $k \approx 0$. When $|\delta|$ is comparable with $2|L^{12}|$, $\chi + \delta$ and $\chi - \delta$ are already quantities of the same order, and the difference between them decreases the smaller $|\delta|$ is in comparison with $2|L^{12}|$.

Thus, in the transition from the gas to the condensed phase the intensities of the components of a resonance doublet always tend to become equalized, either partially or (for $\delta = 0$) completely. It is also significant that the

distance χ between the lines in the absorption spectrum, determined by expressions (10) and (14), does not necessarily increase as compared with $E_0^1 - E_0^2$; this differs from the case of gases, where equalization of the intensities of resonating components is always allied with an increase in the magnitude of purely resonance splitting.[1,2]

We will now consider the case of a molecule of the same substance placed in a foreign medium (weak solution). We will write the Hamiltonian of the system in the form

$$H = H_0 + \bar{H} + V, \tag{18}$$

where H_0 describes the internal motion of the molecule of the dissolved substance, $\bar{H}$ is the Hamiltonian of the solvent, and V is the potential energy of the interaction of the solute molecule with its environment. We will look for the wave function of the system in the form

$$\psi = \bar{\psi} \sum_{j=1,2} a_j \varphi^j, \tag{19}$$

where $\bar{\psi}$ is the wave function of the ground state of the solvent (quantities referring to the solvent molecules are designated with a bar).

In a way completely analogous to the foregoing we find

$$\left.\begin{aligned} E_{+,-} &= E'^0 \pm \frac{\chi'}{2}, \quad E'^0 = \frac{1}{2}(E_0^1 + E_0^2 + V_{11} + V_{22}) + \bar{E}, \\ \chi' &= \sqrt{\delta'^2 + 4|V_{12}|^2}, \quad \delta' = E_0^1 - E_0^2 + V_{11} - V_{22}, \end{aligned}\right\} \tag{20}$$

$$V_{jj'} = \int \bar{\psi}^* \varphi^{j*} V \bar{\psi} \varphi^{j'} d\tau \quad (j', j = 1, 2), \tag{21}$$

where $\bar{E}$ is the energy of the ground state of the solvent. Formulas similar to (11)-(17) also hold. Thus, in this case also the interaction with the medium leads to an intensification of the resonance phenomena.

It is interesting to compare the effect of the interaction with the medium on the resonance for a pure substance and for a solution. We will do this assuming that the molecule with the resonating levels is nonpolar. From (17) and (17′) it is evident that the degree of equalization of the intensities is the greater, the more χ differs from δ, or according to (10), the greater the quantity $2|L^{12}|$ is in comparison with δ (or $2|V_{12}|$ in comparison with δ'). The potential energy of the interaction of two molecules i and k (V^{ik}) can be developed in a series in inverse powers of the distance between the molecules and can be confined to the terms which give the dipole-dipole interaction

$$V^{ik} = R_{ik}^{-3}[\hat{p}_i \hat{p}_k - 3(\hat{p}_i e_{ik})(\hat{p}_k e_{ik})]. \tag{22}$$

Here $\hat{p}_i$ and $\hat{p}_k$ are the dipole moment operators of the molecules, R is the distance between the molecules, and e_{ik} is the unit vector along the line joining the molecules. As is evident from (21), V_{12} is a sum of terms proportional to p_{12}, that is,

$$p_{12} = \int \varphi^{1*} \hat{p} \varphi^2 d\tau, \tag{23}$$

where $\hat{p}$ is the dipole moment operator of the molecule in which the resonance occurs, whereas L^{12}, according to (8) and (4), is determined by a sum of terms proportional to p_{01} and p_{02}. The latter quantities are ordinarily much larger than P_{12}. For this reason one can expect that in the majority of cases $|V_{12}| < |L^{12}|$.

In the same way the quantities L^{11}, L^{22} are greater in absolute magnitude than the values of V_{11}, V_{22} (we will show this in greater detail with a concrete example which will be discussed below). Hence equalization of the intensities of the resonating components in the case of weak solutions should occur to a much smaller degree than in the case of the pure substance. It is difficult to predict the relative size of the splitting in the general case.

We have compared the theory developed here with the experimental data given in reference 4, in which the resonance of the vibrational terms $\nu_1 + \nu_4$ and ν_3 in the CCl_4 molecule was studied in the pure substance and in solution in benzene, toluene, dioxane and methyl acetate. Obviously, a comparison of the theory with experiment can be only qualitative since the experiments described in reference 4 were carried out at room temperature and the theory has been developed for low temperatures. We will make an estimate of the quantities $|p_{01}|$, $|p_{02}|$, etc., for this case. Since $\nu_3 > \nu_1 + \nu_4$, the states "1" and "2" will be taken to refer to the states with energies $h\nu_3$ and $h(\nu_1 + \nu_4)$, respectively (the electronic state is assumed to be the ground state). The dipole moment of the molecule averaged over the electronic coordinates can be developed in a series in powers of the normal coordinates

$$p = \sum_i a_i Q_i + \sum_{i,j} a_{ij} Q_i Q_j + \sum_{ijk} a_{ijk} Q_i Q_j Q_k + \dots \tag{24}$$

We note that no constant term is present, as a consequence of the nearly spherical symmetry of the CCl_4 molecule. Using the general formulas given in references 1 and 2, the wave functions φ^1 and φ^2 of the free molecule taking the anharmonicity into account can be written as follows:

$$\left.\begin{aligned} \varphi^1 &= (2x'')^{-1/2}[(x'' + \delta'')^{1/2} u_{\nu_3}^1 u_{\nu_1}^0 u_{\nu_4}^0 \pm (x'' - \delta'')^{1/2} u_{\nu_3}^0 u_{\nu_1}^1 u_{\nu_4}^1], \\ \varphi^2 &= (2x'')^{-1/2}[(x'' - \delta'')^{1/2} u_{\nu_3}^1 u_{\nu_1}^0 u_{\nu_4}^0 \mp (x'' + \delta'')^{1/2} u_{\nu_3}^0 u_{\nu_1}^1 u_{\nu_4}^1], \\ x'' &= \sqrt{\delta''^2 + 4|(H')_{011}^{100}|^2}, \end{aligned}\right\} \tag{25}$$

where δ'' is the separation of the unperturbed anharmonic levels; $(H')_{011}^{100}$ is the matrix element of the anharmonic terms in the potential energy of the nuclear motion between the states $u_{\nu_3}^1 u_{\nu_1}^0 u_{\nu_4}^0$ and $u_{\nu_3}^0 u_{\nu_1}^1 u_{\nu_4}^1$; u^1 and u^0 are the wave functions of the excited and normal states of the linear harmonic oscillators with the frequencies ν_3, ν_1 and ν_4. The choice of signs in (25) depends on whether δ'' and $(H')_{011}^{100}$ have the same or different signs; this is unimportant for our purpose. With the help of (24) and (25) and using the well-known selection rules for the harmonic oscillator, one can convince oneself that the quantities p_{01} and p_{02} are determined by terms of the first order of smallness in Q in the series expansion (24), and the quantities p_{13}, p_{11}, and p_{22} by terms of the second order of smallness. A comparison of the intensities of lines of different orders, according to the data in reference 5, shows that terms of different order of smallness in Q differ in order of magnitude; therefore $|p_{11}|$, $|p_{22}|$, $|p_{12}| \ll |p_{01}|$, $|p_{02}|$, in agreement with what was stated above. Since we do not know the values of δ'' and $(H')_{011}^{100}$, we will estimate the magnitudes of $|p_{01}|$ and $|p_{02}|$ from the data given in reference 5 on the integrated intensities of the lines ν_3 and $\nu_1 + \nu_4$ in the gaseous state, using the usual formulas for the absorption of light by atomic systems. This estimate leads to the following values for $|p_{01}|$ and $|p_{02}|$:

$$|p_{01}| = 0.22D, \quad |p_{02}| = 0.13D.$$

These are of the same order of magnitude as the values, entering into (21), of the dipole moments of the solvent molecules averaged over the ground state

$$\bar{p} = \int \bar{\psi} \hat{p} \bar{\psi} d\tau, \tag{26}$$

The values of these were quoted in reference 4, except

for benzene which has of course no dipole moment. Since the quantities $V_{f'f}(f', f = 1,2)$ contain terms proportional to $\overline{pp}_{11}$, $\overline{pp}_{22}$ and $\overline{pp}_{12}$, and $L^{ff'}$ contains terms proportional to p_{0f}, $p_{0f'}$ (f, f' = 1,2), then, as is evident from (4) and (8), the inequality, $|L^{ff'}| \gg |V_{ff'}|$, is fulfilled independent of the type of solvent. Thus, one must expect that the degree of equalization of the intensities of the resonating components in the pure substance will be much greater than in any of the four solutions studied. This conclusion is well confirmed by the experimental data.[4]

Generalizing the discussions given above, one can make the following deduction; equalization of the intensities of the resonating components in a solution will be the smaller in comparison with the pure substance the better the relations

$$|p_{01}|, |p_{02}| \geqslant |\beta|, \tag{27}$$

$$|p_{01}|, |p_{02}| \gg |p_{11}|, |p_{22}|, |p_{12}|. \tag{27'}$$

are fulfilled.

It is easy to convince oneself that expression (27′) does not necessarily have to be fulfilled for polar molecules; in this case a term of zeroth order in Q appears in the series expansion (24) and this changes the course of the discussion. Moreover, it was noted in reference 6 that if a Fermi resonance occurs for lines of any one order, then it occurs also for lines of higher orders. In this case condition (27) as well as condition (27′) can be violated. The latter relation is violated because of the general weakening of the intensities of resonating lines in going to higher orders. For the case of CCl_4 the existence of such weakening was confirmed by measurements[7] for the resonance of the combination tones $\nu_1 + \nu_3$ and $\nu_3 + (\nu_1 + \nu_4)$. It might be expected that the effect of the solvent on the resonance in this last case would be stronger than in the case of the resonance of the frequencies ν_3 and $\nu_1 + \nu_4$; however, measurements which would show this were not carried out.

In conclusion the author expresses his deep gratitude to M. P. Lisitsa, on whose suggestion the present research was carried out, for his interest in the work, and discussions in connection with it.

REFERENCES

1. M. V. Vol'kenshtein, M. A. El'iashevich, and B. I. Stepanov. "Kolebaniya molekul." (Vibrations of Molecules), Vol. I, Gosudarst. Izd. Tekh.-Teoret. Lit., 1949.
2. E. Fermi. Z. Physik 71, 250 (1931).
3. A. S. Davydov. "Teoriya pogloshcheniya cveta v molekulyarnikh kristallakh." (Theory of Light Absorption in Molecular Crystals), Izd. Akad. Nauk SSSR, 1951.
4. M. P. Lisitsa and L. A. Ovander. Opt. i Spektr. 7, 632 (1959).
5. M. P. Lisitsa and V. N. Malinko. Opt. i Spektr. 4, 456 (1958).
6. M. P. Lisitsa and V. L. Strizhevskii. Opt. i Spektr. 7, 478 (1959).
7. M. P. Lisitsa and V. N. Malinko. Ukr. Fiz. Zhur. 3, 482 (1959).

ON THE THEORY OF THE USE OF DEPENDENT COORDINATES IN THE PROBLEM OF MOLECULAR VIBRATIONS

I. V. Rigina and I. N. Godnev

Received 11 May 1959

It is shown that a consideration of the problem of molecular vibrations with the help of the Lagrangian equations with included restraints leads to equations which are more general than the equations of Gold, Dowling, and Meister, and which appear to be useful for the determination of the form of the matrices used in the solution of the problem in dependent coordinates.

In a recently published investigation by Gold, Dowling, and Meister[1] the method of a transformation from independent to dependent coordinates was used in the calculation of rotation-vibrational spectra of polyatomic molecules, giving the amplitude equations with singular matrices. However, as will be shown below, the use of these equations does not appear to be obligatory, and there exist other, more general equations which result from the application of the Lagrangian equations with included restraints to the problem (cf. our previous publication[2]). These equations appear to be useful for the consideration of the general problem of molecular vibrations in dependent coordinates.

As in reference 2, let $q_1, q_2, \ldots, q_n$ represent natural coordinates obeying the condition

$$a_1q_1 + a_2q_2 + \ldots + a_nq_n = aq = 0; \tag{1}$$

and let T be one of the matrices by means of which the kinetic energy can be written down in these coordinates, U the corresponding matrix for the potential energy,*

*In using dependent coordinates the kinetic and potential energies can be written down from the mathematical point of view by means of a multiplicity of matrices T′, T″, T‴, ..., U′, U″, U‴, ... which give T_0 and U_0 excluding q_n. This arbitrariness is partly restricted by physical considerations, for example, symmetry requirements, etc.

$Q_1, Q_2, \ldots Q_{n-1}$ independent coordinates which are the same as the first n − 1 coordinates q, T_0 and U_0 the matrices of the kinetic and potential energies in the coordinates, Q, and, finally, $A_0 = T_0^{-1}$.*

*The matrices of the kinetic and potential energies are assumed to be symmetrical ($t_{ik} = t_{ki}$).

With the above choice of the independent coordinates we have

$$q = NQ, \tag{2}$$

where q and Q are column matrices and

$$N = \left\| \begin{array}{cccc} 1 & 0 & \ldots & 0 \\ 0 & 1 & \ldots & 0 \\ \ldots & \ldots & \ldots & \ldots \\ 0 & 0 & \ldots & 1 \\ -\frac{a_1}{a_n} & -\frac{a_2}{a_n} & \ldots & -\frac{a_{n-1}}{a_n} \end{array} \right\|_{n-1}. \tag{3}$$

The method of Gold, Dowling, and Meister[1] consists in applying the transformations

$$q = LR \tag{4}$$

and

$$R = Iq, \tag{5}$$

where the R's are independent coordinates different from Q, and L is a rectangular matrix* which satisfies the relations

*This matrix is designated in reference 1 as $\tilde{u}$. The specific choice of this matrix is due to the fact that $R \neq Q$.

$$LI = E_{n-1} \tag{6}$$

and

$$q = LIq, \tag{7}$$

the latter of which defines the interdependence between the coordinates. The transition from the coordinates R to the coordinates q gives the expanded amplitude equation*

$$(A_r U_r - \lambda E)\, l = 0, \tag{8}$$

*Along with Eq. (8) the amplitude equation, $(U_r - \lambda T_r)l = 0$, is also introduced in reference 1, together with the corresponding secular equation, where $T_r = LT_0\tilde{L}$. However this amplitude equation as such has no secular equation (cf. the criteria for the existence of the latter in the monograph[3] and therefore has solutions which depend on arbitrary functions.

where l is the amplitude vector, and the matrices

$$A_r = LA_0\tilde{L} \tag{9}$$

and

$$U_r = LU_0\tilde{L} \tag{10}$$

are singular.

We will show that, in addition to the above equation of Gold, Dowling, and Meister, there exist other, more general, equations which arise from the Lagrangian equations with included constraints[4, 5]

$$T\ddot{q} + Uq = a\alpha, \tag{11}$$

where α is the Lagrangian parameter.

The form of the equations obtained from (11) depends on the method of eliminating α. If we eliminate α by relation (1) differentiated twice, we obtain[2] the well-known equation[6, 7]

$$\ddot{q} + AUq = 0, \tag{12}$$

where*

*In using dependent coordinates the matrix T can always be chosen to be nonsingular.

$$A = T^{-1} - \frac{T^{-1}a\delta T^{-1}}{\delta T^{-1}a} = MA_0\tilde{M} \tag{13}$$

is the matrix of the kinematic coefficients in the dependent coordinates and M is the rectangular matrix (3).

Equation (11) assumes a different form if α is eliminated directly by means of (1). Substituting in (1) the value of q obtained from (11), we have

$$\alpha = \frac{\delta U^{-1}T}{\delta U^{-1}a}\,\ddot{q}. \tag{14}$$

It follows now from (11) and (14) that

$$\left(E - \frac{a\delta U^{-1}}{\delta U^{-1}a}\right)T\ddot{q} + Uq = 0, \tag{15}$$

from which

$$\left(U^{-1} - \frac{U^{-1}a\delta U^{-1}}{\delta U^{-1}a}\right)T\ddot{q} + q = 0 \tag{16}$$

or

$$U^*T\ddot{q} + q = 0, \tag{17}$$

where

$$U^* = U^{-1} - \frac{U^{-1}a\delta U^{-1}}{\delta U^{-1}a}. \tag{18}$$

The matrix U* given by (18) has the same structure as A (cf. formula 13), and consequently can be transformed to the form

$$U^* = MU_0^{-1}\tilde{M}. \tag{19}$$

Equation (17) obtained above allows one to introduce the matrix U* into the argument in a natural way, and this matrix can be used in determining the action coefficients in dependent coordinates (cf. reference 8). This permits an extension of the proof of the invariability of the action coefficients, given by Mayants,[8] to the case of dependent coordinates.*

It follows from formula (18) that the coordinate transformation $q = Bq'$ will transform the matrix U according to the formula $U^{*\prime} = B^{-1}U^*\tilde{B}^{-1}$. The demonstration of this is necessary[9] for a discussion of the invariability.

We will note some properties of Eqs. (12) and (17). First of all we will show that the secular equations,*

*The existence of these secular equations follows from the criterion derived in reference 3.

$$|AU - \lambda E| = 0 \tag{20}$$

and

$$\left|U^*T - \frac{1}{\lambda}E\right| = 0 \tag{21}$$

can be reduced to the forms (cf. Appendix 1),

$$\lambda \cdot |A_0U_0 - \lambda E| = 0 \tag{22}$$

and

$$\frac{1}{\lambda} \cdot \left|U_0^{-1}T_0 - \frac{1}{\lambda}E\right| = 0, \tag{23}$$

respectively, from which it follows that one of the roots (λ or $1/\lambda$) is equal to zero, and the remaining $n - 1$ roots coincide with the roots of the secular equation corresponding to the independent coordinates.

It can also be shown (cf. Appendix 2) that the solution of Eqs. (12) and (17), q^1, corresponding to the root λ_1 (the q^{1}'s are column matrices with elements $q_1^1, q_2^1, \ldots q_n^1$), can be expressed in terms of the corresponding solution, Q^1, of the equations in independent coordinates by means of the relation

$$q^1 = MQ^1, \tag{24}$$

where M is matrix (3).

From what has been said it follows that the q^1 will depend only on the conditions of the constraint and on the solutions of the problem in independent coordinates. Therefore the solutions of Eq. (12) will be the same for all those matrixes U (singular and nonsingular) which give the matrix U_0 when the redundant coordinate q_n is eliminated, and the solutions of Eq. (17) will be the same for all those matrices T which give the matrix T_0 when q_n is eliminated.

Thus, along with Eq. (12) there exists an equation

$$\ddot{q} + AU_{\text{sing.}}q = 0. \tag{25}$$

Among the multiplicity of singular matrices, $U_{\text{sing.}}$, by means of which Eq. (25) can be written, a $U_{\text{sing.}}$ can be

chosen so that

$$U_{\text{sing.}} = U_r = LU_{0r}L, \tag{26}$$

where U_{0r} is the matrix of the potential energy in the independent coordinates R. Substituting (26) in (25) we obtain

$$\ddot{q} + AU_r q = 0, \tag{27}$$

from which the amplitude equation (8) of Gold, Dowling, and Meister containing the singular matrix U_r ensues.

However, the use of such a singular matrix does not seem to be obligatory. In particular it must be emphasized that the calculation of rotational distortion constants can be carried out regardless of the choice of U. In fact, as has been shown in reference 1, for the calculation of these constants it is necessary to find the matrix $LU_{0r}^{-1}L$. It is easy to convince oneself by a transformation from the coordinates R to the coordinates Q, that this matrix becomes

$$LU_{0r}^{-1}L = MU_0^{-1}\tilde{M} = U^*, \tag{28}$$

It follows from this that the matrix is independent of the choice of U.

We note in conclusion that the results obtained above can be used to prove the rules for eliminating the redundant coordinate in Eqs. (12) and (17). The first of these equations is very convenient for the solution of practical problems.[7] The elimination rule for it is well-known.[7,9] The corresponding rule for the second equation, which is less convenient since it requires the calculation of the kinetic energy matrix T,[7,10] * follows

*There are possible cases for which the direct calculation of T proves convenient (cf. reference 11).

directly from formula (19) and the transformation (2). Actually, when Eq. (17) is transforme . to the independent coordinates Q it takes the form,

$$U_0^{-1}T_0\ddot{Q} + Q = 0, \tag{29}$$

Here the matrix U_0^{-1} is obtained from U^* by deleting the last row and the last column, as follows from the similar rule for obtaining A (cf. references 2, 7, 9) and from formula (19). The matrix T can be obtained from the formula,

$$T_0 = \tilde{M}TM, \tag{30}$$

which represents the transformation of the kinetic energy matrix T by means of (2) to the variables Q. Thus, in order to go over to the independent coordinates in Eq. (17), it is necessary to delete in matrix U^* the row and column which correspond to the redundant coordinate, and to apply to the matrix T the same rule which is used in the method of El'yashevich[7] for obtaining the matrix U_0 from the matrix U.

The rules given above for obtaining A_0 and U_0^{-1} from the matrices A and U^* by deletion make convenient the use of the secular equation

$$\left| U_0^{-1}\lambda - A_0 \right| = 0, \tag{31}$$

However, in contrast to the secular equations (20) and (21) considered above, the existence of which is confirmed by the criterion given in reference 3, it is impossible to juxtapose with Eq. (31) an expanded secular equation of the form

$$| U^*\lambda - A | = 0. \tag{32}$$

In reality the equality in (32) is an identity, just as in the case of the "secular" determinant of Gold, Dowling, and Meister mentioned above.

APPENDIX 1

To prove the transformation of the secular equations (20) and (21) to the form (22) and (23), we multiply (20) and (21) on the left with the determinant | C | of the non-singular matrix*

*This matrix was used by Mayants.[8]

$$C = \begin{pmatrix} 1 & 0 & \dots & 0 \\ 0 & 1 & \dots & 0 \\ \dots & \dots & \dots & \dots \\ a_1 & a_2 & \dots & a_n \end{pmatrix}, \tag{33}$$

and on the right with $| C^{-1} |$.

We obtain

$$|C| \cdot |AU - \lambda E| \cdot |C^{-1}| = |CA\tilde{C}\tilde{C}^{-1}UC^{-1} - \lambda E| = 0, \tag{34}$$

$$|C| \cdot \left| U^*T - \frac{1}{\lambda}E \right| \cdot |C^{-1}| = \left| CU^*\tilde{C}\tilde{C}^{-1}TC^{-1} - \frac{1}{\lambda}E \right| = 0, \tag{35}$$

Taking into account the linear dependence between the rows and columns in the matrices A and U^*, we have

$$\begin{vmatrix} A_0U_0 - \lambda E_{n-1} & (AU)'_{n-1} \\ O_1^{n-1} & -\lambda \end{vmatrix} = 0 \tag{36}$$

and

$$\begin{vmatrix} U_0^{-1}T_0 - \frac{1}{\lambda}E_{n-1} & (U^*T)'_{n-1} \\ O_1^{n-1} & -\frac{1}{\lambda} \end{vmatrix} = 0. \tag{37}$$

Developing (36) and (37) in terms of the elements of the last row gives Eqs. (22) and (23).

APPENDIX 2

Let the column matrix Q^1 be one of the solutions of the equation in independent coordinates,

$$\ddot{Q} + A_0U_0Q = 0, \tag{38}$$

and λ_1 the square of the frequency for this solution. We have then

$$-\lambda_1Q^1 + A_0U_0Q^1 = 0. \tag{39}$$

Multiplying (39) on the left with M and taking into account (13) and the equation

$$U_0 = \tilde{M}UM, \tag{40}$$

which arises from the transformation of U to the independent coordinates by means of (2), we obtain

$$-\lambda_1MQ^1 + AUMQ^1 = 0. \tag{41}$$

A comparison of (41) with the expression,

$$-\lambda_1q^1 + AUq^1 = 0, \tag{42}$$

which is obtained as a result of the substitution in Eq. (12) of the corresponding solution q^1, gives relation (24).

In a similar way it can be shown that (24) represents also a solution of Eq. (17).

REFERENCES

1. R. Gold, J. M. Dowling, and A. G. Meister. J. Mol. Spectroscopy **2**, 9 (1958).
2. I. N. Godnev and I. V. Orlova. Opt. i Spektr. **6**, 380 (1959).

3. B. B. Bulgakov. "Kolebaniya." (Vibrations), Gosudarst. Izd. Tekh.-Teoret. Lit., Moscow, 1954.
4. L. Nordheim. Handb. d. Phys. 5, 57 (1927).
5. L. G. Loitsyanskii and A. I. Lur'e. "Kurs teoreticheskoi mekhaniki" Vol. 2, Gosudarst. Izd. Tekh-Teoret. Lit., Moscow, 1954.
6. M. A. El'yashevich. Doklady Akad. Nauk SSSR 28, 605 (1940); Zhur. Fiz. Khim. 15, 847 (1941).
7. M. V. Vol'kenshtein, M. A. El'yashevich, and B. I. Stepanov. "Kolebaniya molekul." (Vibrations of Molecules), Vol. 1, Gosudarst. Izd. Tekh.-Teoret. Lit., Moscow, 1949.
8. L. S. Mayants. Trudy Fiz. Inst. Akad. Nauk 5, 63 (1950).
9. L. S. Mayants. Doklady Akad. Nauk SSSR 89, 423 (1953).
10. L. S. Mayants. Doklady Akad. Nauk SSSR 32, 120 (1941).
11. W. J. Taylor and K. S. Pitzer. J. Research Natl. Bur. Standards 38, 1 (1947).

POLARIZATION OF HARMONIC OSCILLATOR LUMINESCENCE

V. P. Gribkovskii and B. I. Stepanov

Received 12 May 1959

A quantum mechanical calculation has been made of the polarization of luminescence from a system of particles with two energy levels and from an assemblage of harmonic oscillators. The value of the polarization of harmonic oscillator luminescence is equal to $\frac{1}{3}$; it is independent of temperature and intensity of the exciting radiation, and also it agrees completely with the results of a classical calculation of the polarization of radiation from an assemblage of dipoles.

According to reference 1, the value of the efficiency of absorption and luminescence and also the duration of the afterglow of a harmonic oscillator agree completely with each other whether calculated by classical or quantum methods. In this paper a quantum calculation of the polarization of luminescence from an assembly of harmonic oscillators is made. The results thereof are identical with the results of a classical calculation. At the same time the polarization of luminescence from a system of particles with two energy levels, which is in general comparable to a classical dipole, is smaller than the polarization of luminescence of harmonic oscillators and depends on the intensity of the exciting radiation and the temperature of the medium. A particle with two energy levels can be considered equivalent to a classical dipole only for small incident radiation intensities and at low temperatures.

1. Let us start by considering the luminescence of particles with two energy levels. In accordance with what Vavilov found, an accurate calculation requires that one take into account the thermal emission noise.[2,3] Assume that the particles have a random spatial orientation and that they cannot change the directions of their dipole moments. The exciting light flux propagates along the x-axis, the electric vector is oriented along the z-axis, and luminescence is observed along the y-axis. The luminescence intensity for electric vectors, oriented along the z- and x-axes in the same general case is given by*

*The luminescence intensity is computed on the basis of a unit solid angle.

$$W_z = h\nu \int_{\Omega} \{ n_2(\Omega) [A_z(\Omega) + B_z(\Omega) u_1] - n_1(\Omega) B_z(\Omega) u_1 \} d\Omega, \quad (1)$$

$$W_x = h\nu \int_{\Omega} \{ n_2(\Omega) [A_x(\Omega) + B_x(\Omega) u_1] - n_1(\Omega) B_x(\Omega) u_1 \} d\Omega. \quad (2)$$

Here $n_2(\Omega)$ and $n_1(\Omega)$ are the numbers of excited and non-excited particles with dipole moments located within the unit solid angle Ω; $u_1 = (1/8\pi)u$ is the quantum radiation density, calculated for unit solid angle and a single polarization; $A_z(\Omega)$ and $A_x(\Omega)$ are the probabilities of spontaneous emission of a light photon directed along the y-axis and polarized along the z- and x-axes respectively; $B_z(\Omega)$ and $B_x(\Omega)$ are the Einstein coefficients of forced emission* (absorption) of a light quantum of the indicated

*For large incident light intensities and high temperatures, the forced emission essentially acts to depolarize the luminescence and it need not be taken into account.

polarization. The angular dependence of the Einstein differential coefficients (calculated per unit solid angle) in spherical coordinates is determined by the quantum theory of light emission[4] in the form

$$\left.\begin{aligned} A_z(\Omega) &= \frac{3}{8\pi} A_0 \cos^2\vartheta, \\ A_x(\Omega) &= \frac{3}{8\pi} A_0 \sin^2\vartheta \cos^2\varphi, \\ B_z(\Omega) &= 3B_0 \cos^2\vartheta, \\ B_x(\Omega) &= 3B_0 \sin^2\vartheta \cos^2\varphi, \end{aligned}\right\} \quad (3)$$

where A_0 and B_0 are the Einstein integral coefficients. Equations (3) are valid only for dipole emission.

In the conditions of stationary illumination, the number of particle transitions from level (2) to level (1) is equal to the number of inverse transitions. This allows one to determine the values of $n_2(\Omega)$ and $n_1(\Omega)$. The particle balance equations have the form[2]

$$n_2(\Omega) [A_0 + B_0 u + d_{21} + B_x(\Omega) s\Delta\Omega'] = n_1(\Omega) [B_0 u + d_{12} + B_x(\Omega) s\Delta\Omega'], \quad (4)$$

where s is the exciting current density calculated per unit solid angle; $\Delta\Omega'$ is the solid angle of the incident flux;* d_{21} and d_{12} are the probabilities of nonoptical

*In the calculation, it is assumed that $\Delta\Omega'$ is small and it can be considered that all the light is directed along the x-axis.

transitions which are connected by the relation;[2,3]

$$d_{12} = d_{21} e^{-\frac{h\nu}{kT}}.$$

By taking into account that for any direction

$$n_2(\Omega) + n_1(\Omega) = \frac{1}{4\pi} n, \quad (5)$$

where $(1/4\pi)n$ is generally independent of direction and

of the number of particles with dipole moments in a unit solid angle, from Eqs. (4) and (5) we obtain

$$n_2(\Omega) = \frac{n}{4\pi} \frac{B_0 u + d_{21} e^{-\frac{h\nu}{kT}} + 3B_0 s\Delta\Omega' \cos^2\theta}{\left[A_0 + 2B_0 u + d_{21}\left(1 + e^{-\frac{h\nu}{kT}}\right)\right](1 + b\cos^2\theta)}, \quad (6)$$

$$n_1(\Omega) = \frac{n}{4\pi} \frac{A_0 + B_0 u + d_{21} + 3B_0 s\Delta\Omega' \cos^2\theta}{\left[A_0 + 2B_0 u + d_{21}\left(1 + e^{-\frac{h\nu}{kT}}\right)\right](1 + b\cos^2\theta)}, \quad (7)$$

where

$$b = \frac{6B_0 s\Delta\Omega'}{A_0 + 2B_0 u + d_{21}\left(1 + e^{-\frac{h\nu}{kT}}\right)}. \quad (8)$$

is a parameter which is proportional to the intensity of exciting radiation and which is a function of the transition probability.

In spite of the initial random angular distribution of the particles, there is a completely determined orientation of the dipole moments in the excited state, which is associated with the anisotropy of the exciting radiation and depends on the intensity and on the temperature of the medium. For relatively small $s\Delta\Omega'$ and $T = 0$, the angular dependence of $n_2(\Omega)$ is determined by the factor $\cos^2\theta$. For the most part, those particles end up in the excited state for which the dipole moment is oriented along the electric vector of the incident radiation. For sufficiently large light intensities (when $B_0 s\Delta\Omega'$ is commensurable with $A_0 + d_{21}$), the orientation of the excited particles becomes less well defined and in the limit for $s\Delta\Omega' \to \infty$ it is completely absent. The effect of temperature has a similar character. For small temperatures the effect of thermal emission noise is very slight, and it can be neglected. If u is commensurable with $s\Delta\Omega'$, the thermal noise decreases the orientation of the excited particles. In the limit as $T \to \infty$, the excited molecules are randomly distributed for any $s\Delta\Omega'$.

By substituting (6) and (7) into (1) and (2), taking (3) into account and completing the integration over angle, it is easy to obtain a final expression for W_z and W_x, determined by the constants A_0 and d_{21}, the intensity of the exciting radiation, and the temperature.

$$W_z = \frac{9}{8\pi} \frac{nA_0 B_0 s\Delta\Omega' h\nu}{A_0 + 2B_0 u + d_{21}\left(1 + e^{-\frac{h\nu}{kT}}\right)} \left(\frac{1}{3b} - \frac{1}{b^2} + \frac{1}{b^{3/2}} \arctan b^{1/2}\right), \quad (9)$$

$$W_x = \frac{9}{8\pi} \frac{nA_0 B_0 s\Delta\Omega' h\nu}{A_0 + 2B_0 u + d_{21}\left(1 + e^{-\frac{h\nu}{kT}}\right)} \left[\frac{1}{3b} + \frac{1}{2b^2} - \frac{1}{2}\left(\frac{1}{b^{5/2}} + \frac{1}{b^{3/2}}\right)\arctan b^{1/2}\right]. \quad (10)$$

By definition, the polarization of luminescence is equal to

$$P = \frac{W_z - W_x}{W_z + W_x}. \quad (11)$$

By substituting the values of W_z and W_x into the above, we obtain

$$P = \frac{(3+b)\arctan b^{1/2} - 3b^{1/2}}{\frac{4}{3}b^{3/2} + (1-b)\arctan b^{1/2} - b^{1/2}}. \quad (12)$$

As is evident from Eqs. (12) and (8), the polarization of luminescence from a system of particles with two energy levels is a complex function of temperature. For sufficiently large temperatures ($u \to \infty$), it reduces to the form

$$P = \frac{1}{2} - \frac{9}{28}\left(\frac{s\Delta\Omega'}{u}\right) + \ldots \quad (13)$$

In this case the polarization of the luminescence converges toward a limiting value equal to ½. The small deviation from ½ is determined by the ratio $s\Delta\Omega'/u$, which tends toward zero as $T \to \infty$.

In the majority of practically important cases the thermal emission noise is insignificant, and it can be neglected. Then Eqs. (9) and (10) simplify to the following

$$W_z = \frac{9}{8\pi} n\gamma B_0 s\Delta\Omega' h\nu \left[\frac{1}{3b_0} - \frac{1}{b_0^2} + \frac{1}{b_0^{3/2}} \arctan b_0^{1/2}\right], \quad (14)$$

$$W_x = \frac{9}{8\pi} n\gamma B_0 s\Delta\Omega' h\nu \left[\frac{1}{3b_0} + \frac{1}{2b_0^2} - \frac{1}{2}\left(\frac{1}{b_0^{5/2}} + \frac{1}{b_0^{3/2}}\right)\arctan b_0^{1/2}\right], \quad (15)$$

where

$$b_0 = b\,(T=0) = \frac{6B_0}{A_0}\gamma s\Delta\Omega' = \frac{3}{4\pi}\frac{c^3}{h\nu^3}\gamma s\Delta\Omega', \quad (16)$$

and

$$\gamma = \frac{A_0}{A_0 + d_{21}} \quad (17)$$

is the quantum fluorescence yield.

The figure shows how W_z and W_x depend on the parameter b_0 (and, consequently, on the intensity of exciting radiation). As is evident from the figure, both functions increase with increasing b_0, at which time the value of W_z always dominates the value of W_x. The ratio W_z/W_x decreases as b_0 increases, and in the limit it approaches unity.

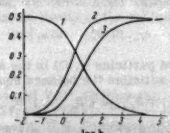

Dependence of different spectral characteristics (in arbitrary units) on the parameter b_0. Curve 1—polarization of luminescence P; curve 2—intensity of luminescence $8\pi/nA_0 h\nu W_z$; curve 3—intensity of luminescence $8\pi/nA_0 h\nu W_x$.

The value of the polarization of luminescence at $T = 0$ is expressed by Eq. (12), in which one must replace the parameter b by b_0 from (16). According to Eqs. (12) and (16), the polarization of the luminescence depends on the intensity of the exciting light, on the quantum yield of luminescence, and on the frequency.

It should be noted that for $\gamma = 1$ ($d_{21} = 0$) the accumulation of particles in the second level and, consequently, the depolarization of luminescence do not depend on the duration of the excited state. The dependence of $P_{T=0}$ on τ for transitions from one system to another can be coupled only in the presence of a probability for nonradiative transitions.

The dependence of $P_{T=0}$ on b_0 is also shown in the figure. In the limit of small densities of incident radiation or small quantum yield, $P = ½$. This case usually occurs in reality. In the other set of cases ($b_0 \to \infty$), the polarization of the luminescence tends toward zero, which is associated with the absence of anisotropy in the distribution of dipole moments of the excited particles. This case can occur, in particular, at low frequencies (for the infrared and radiowave regions of the spectrum).

For $b_0 = 1$, it follows from Eq. (12) that P = 42.5%. If $b_0 < 1$ then Eq. (12) can be expanded into a series.

$$P_{T=0} = \frac{\sum_{k=0}^{\infty} (-1)^k \frac{k+1}{(2k+5)(2k+3)} b_0^k}{\sum_{k=0}^{\infty} (-1)^k \frac{k+2}{(2k+5)(2k+3)} b_0^k} = \frac{1}{2} - \frac{3}{28} b_0 + \cdots \quad (18)$$

Significant departures of the polarization of luminescence from the value P = ½ can be observed only at those intensities of the exciting light for which $B_{\varphi} s \Delta\Omega'$ becomes commensurable with A_0. In this case, there occurs a considerable accumulation of particles in the second level and an increase in their number in the first level which causes a corresponding violation of Buger's Law. A connection between the depolarization of luminescence and a decrease in the absorption coefficient is particularly characteristic of a system of particles with three energy levels (it will be considered at length in a subsequent paper).

2. Let us now consider the polarization of luminescence from an assembly of harmonic oscillators. In the same general case, the luminescence intensity for the electric vector directed along the z- and x-axes appearing during transitions of oscillators from the level ν to the level ν − 1 is expressed by the equation

$$W^z_{\nu,\nu-1} = h\nu \int_{\Omega} \left\{ n_{\nu}(\Omega) \left[A^z_{\nu,\nu-1}(\Omega) + B^z_{\nu,\nu-1}(\Omega) u_1 \right] - n_{\nu-1}(\Omega) B^z_{\nu-1,\nu}(\Omega) u_1 \right\} d\Omega, \quad (19)$$

$$W^x_{\nu,\nu-1} = h\nu \int_{\Omega} \left\{ n_{\nu}(\Omega) \left[A^x_{\nu,\nu-1}(\Omega) + B^x_{\nu,\nu-1}(\Omega) u_1 \right] - n_{\nu-1}(\Omega) B^x_{\nu-1,\nu}(\Omega) u_1 \right\} d\Omega. \quad (20)$$

The number of particles $n_{\nu}(\Omega)$ in the stationary illumination region satisfies the balance equation

$$-n_{\nu}(\Omega)\left[A_{\nu,\nu-1} + B_{\nu,\nu-1}u + B_{\nu,\nu+1}u + B^z_{\nu,\nu-1}(\Omega)\, s\Delta\Omega' + B^x_{\nu,\nu+1}(\Omega)\, s\Delta\Omega'\right] + n_{\nu+1}(\Omega)\left[A_{\nu+1,\nu} + B_{\nu+1,\nu}u + B^x_{\nu+1,\nu}(\Omega)\, s\Delta\Omega'\right] + n_{\nu-1}(\Omega)\left[B_{\nu-1,\nu}u + B^x_{\nu-1,\nu}(\Omega)\, s\Delta\Omega'\right] = 0, \quad (21)$$

where, according to

$$\left.\begin{aligned} A^x_{\nu,\nu-1}(\Omega) &= \frac{3}{8\pi} A_{\nu,\nu-1}\cos^2\theta = \frac{3}{8\pi} \nu A_0 \cos^2\theta, \\ A^z_{\nu,\nu-1}(\Omega) &= \frac{3}{8\pi} A_{\nu,\nu-1}\sin^2\theta\cos^2\varphi = \frac{3}{8\pi} \nu A_0 \sin^2\theta\cos^2\varphi, \\ B^x_{\nu,\nu-1}(\Omega) &= 3B_{\nu,\nu-1}\cos^2\theta = 3\nu B_0\cos^2\theta, \\ B^z_{\nu,\nu-1}(\Omega) &= 3B_{\nu,\nu-1}\sin^2\theta\cos^2\varphi = 3\nu B_0\sin^2\theta\cos^2\varphi, \\ B_0 &= \frac{\pi c^3}{3mh\nu}, \quad A_0 = \frac{8\pi^2 e^2 s^2}{3mc^2}. \end{aligned}\right\} \quad (22)$$

In the calculation we assumed that the oscillators do not interact with the medium and therefore nonoptical transitions do not occur. By solving Eq. (21), while taking (22) into account, and keeping in mind conservation of the number of particles

$$\sum_{\nu=0}^{\infty} n_{\nu}(\Omega) = \frac{1}{4\pi} n, \quad (23)$$

we obtain

$$n_{\nu}(\Omega) = \frac{n}{4\pi} \frac{A_0}{A_0 + B_0 u + 3B_0 s\Delta\Omega' \cos^2\theta} \left[\frac{B_0 u + 3B_0 s\Delta\Omega' \cos^2\theta}{A_0 + B_0 u + 3B_0 s\Delta\Omega' \cos^2\theta} \right]^{\nu} \quad (24)$$

By substituting Eq. (24) into (19) and (20), summing over ν and integrating over θ and φ it is easy to arrive at the simple expression

$$W^z = \sum_{\nu=1}^{\infty} W^z_{\nu,\nu-1} = \frac{9}{8\pi} n B_0 s\Delta\Omega' h\nu \frac{1}{5}, \quad (25)$$

$$W^x = \sum_{\nu=1}^{\infty} W^x_{\nu,\nu-1} = \frac{9}{8\pi} n B_0 s\Delta\Omega' h\nu \frac{1}{15}. \quad (26)$$

The intensities W^z and W^x do not depend on temperature and Buger's law is strictly fulfilled. From Eqs. (25) and (26), it follows that the polarization of luminescence of an assembly of harmonic oscillators is equal to ⅓. This value is satisfied for any densities of exciting radiation, any temperatures of the medium, and it agrees completely with the value of polarization obtained for an assembly of dipoles by a classical calculation.[5,6] Only a quantum harmonic oscillator is completely equivalent to the classical dipole. A quantum system of particles with two energy levels can be approximated by a classical dipole only at low temperatures and for such intensities of the exciting radiation which exclude a significant accumulation of particles in the excited state.

The polarization of luminescence for an assembly of harmonic oscillators is equal to ½ only for the total radiation appearing during transitions from all energy levels. The polarization of separate lines appearing during transitions from level ν to ν − 1 depends on the number of levels, on the intensity of the radiation, and on the temperature which results from the strong dependence of $n_{\nu}(\Omega)$ on θ and φ. According to Eq. (24), the orientation of the excited particles is greatest for large values of ν.

In order to investigate the dependence of $P_{\nu,\nu-1}$ on the intensity of the exciting light, we first put in Eqs. (19), (20), and (24) u = 0 which corresponds to T = 0. Then the expression for the luminescence intensity is transformed into

$$W^z_{\nu,\nu-1} = h\nu \int_{\Omega} n_{\nu}(\Omega) A^z_{\nu,\nu-1}(\Omega)\, d\Omega = -\frac{3}{16\pi} \nu A_0 b_1^{\nu} \frac{1}{b_1^{1/2}} \int_{b_1^{1/2}}^{-b_1^{1/2}} \frac{z^{2(\nu+1)}\, dz}{(1+z^2)^{\nu+1}}, \quad (27)$$

$$W^x_{\nu,\nu-1} = h\nu \int_{\Omega} n_{\nu}(\Omega) A^x_{\nu,\nu-1}(\Omega)\, d\Omega = \frac{3}{32\pi} \nu A_0 b_1^{\nu} \left(-\frac{1}{b_1^{1/2}} \int_{b_1^{1/2}}^{-b_1^{1/2}} \frac{z^{2\nu} dz}{(1+z^2)^{\nu+1}} + \frac{1}{b_1^{1/2}} \int_{b_1^{1/2}}^{-b_1^{1/2}} \frac{z^{2(\nu+1)} dz}{(1+z^2)^{\nu+1}} \right), \quad (28)$$

where the following symbols were used:

$$b_1 = \frac{3B_0 s\Delta\Omega'}{A_0}, \qquad z = b_1^{1/2} \cos\theta.$$

The integrals, which enter into Eqs. (27) and (28), can be evaluated accurately for any given ν. For large ν, however, the integration leads to an unwieldy result. We shall therefore derive the polarization of separate lines for some frequently encountered cases. By performing the integration in Eqs. (27) and (28) for ν equal to 1 and 2 we obtain the polarization for the first two lines with the help of (11):

$$P_{10} = \frac{7b_1^{-1/2} + 9b_1^{-3/2} - (b^{-1}+1)(1+9b_1^{-1})\arctan b_1^{1/2}}{b_1^{-1/2} + 3b_1^{-3/2} + (b_1^{-1}+1)(1-3b_1^{-1})\arctan b_1^{1/2}}, \quad (29)$$

$$P_{21}=\frac{29b_1^{-1/3}+78b_1^{-2/3}+45b_1^{-3/3}-(b^{-1}+1)^3(45b_1^{-1}+3)\arctan b_1^{1/3}}{3b_1^{-1/3}+22b_1^{-2/3}+15b_1^{-3/3}+(b_1^{-1}+1)^3(3-15b_1^{-1})\arctan b_1^{1/3}}. \quad (30)$$

Equations (29) and (30) give an accurate value for the polarization of the first and second lines for u = 0 and any intensities $s\Delta\Omega'$. When $s\Delta\Omega' \to 0$ ($b_1 \to 0$) with the help of an expansion of the arc tan $b_1^{1/3}$ into a power series in b_1, we obtain an approximate value of the polarization:

$$P_{10}=\frac{1}{2}-\frac{3}{14}b_1+\ldots, \quad (31)$$

$$P_{21}=\frac{2}{3}-\frac{5}{27}b_1+\ldots \quad (32)$$

For $s\Delta\Omega' \to \infty$ ($b_1 \to \infty$) all the terms in Eqs. (29) and (30) with negative powers disappear, and the polarization of both lines tends toward unity (already for $b_1 = 10^4$, $P_{10} = -0.95$; $P_{21} = -0.93$). This means that in the radiation of the first and second lines only the x-component is represented. Thus for an infinite increase in the density of the exciting radiation, i.e., $s\Delta\Omega'$ from 0 to ∞, the polarization of the lines changes from $1/3$ and $2/5$ to -1.

In order to obtain the limiting value of the polarization, all the lines for $b_1 \to 0$ will be expanded into a power series in x^2 in the integrands in Eqs. (27) and (28). By performing the integration and limiting ourselves to the first two terms in the expansion, we will have

$$W^x_{v,\,v-1}=\frac{3}{8\pi}\nu n A_{ij}\hbar\omega_1^3\left[\frac{1}{2v+3}-\frac{v+1}{2v+5}b_1+\ldots\right], \quad (33)$$

$$W^z_{v,\,v-1}=\frac{3}{8\pi}\nu n A_{ij}\hbar\omega_1^3\left[\frac{1}{(2v+1)(2v+3)}-\frac{v+1}{(2v+3)(2v+5)}b_1+\ldots\right], \quad (34)$$

which corresponds to the polarization

$$P_{v,\,v-1}=\frac{v}{v+1}-\frac{2v+1}{(v+1)(2v+5)}b_1+\ldots \quad (35)$$

The limiting value of $P_{v,\,v-1}$ for negligibly small values of $s\Delta\Omega'$ for the series of subsequent lines is equal to: $1/3$, $3/5$, $5/7$, $7/9$, ... 1.

The obtained values of polarization of the separate lines do not disagree with the fact, that the polarization of the total luminescence is equal to $1/2$ for any density of exciting radiation. This becomes clear if the polarization of the total radiation P is expressed in terms of the polarization of separate lines $P_{v,\,v-1}$:

$$P=\frac{\sum_{v=1}^{\infty}W^x_{v,\,v-1}-\sum_{v=1}^{\infty}W^z_{v,\,v-1}}{\sum_{v=1}^{\infty}W^x_{v,\,v-1}+\sum_{v=1}^{\infty}W^z_{v,\,v-1}}=\frac{P_{10}+\sum_{v=2}^{\infty}a_vP_{v,\,v-1}}{1+\sum_{v=2}^{\infty}a_v}, \quad (36)$$

where

$$a_v=\frac{W^x_{v,\,v-1}+W^z_{v,\,v-1}}{W^x_{10}+W^z_{10}}$$

gives the ratio of the intensity of luminescence emitted during the transitions $v \to v-1$ to the intensity of luminescence of the first line. As is seen from Eqs. (33), (34), and (36) all a_v, starting with a_2, tend toward zero for $b \to 0$, and the polarization of the total luminescence in the limit agrees with $P_{10} = 1/2$. For large b_1, the negative polarization of the first line is compensated by the positive polarization of the lines appearing as a result of transitions between higher energy levels, since the specific weight of the line with a large value of v increases in the total luminescence with increasing b_1.

The dependence of $P_{v,\,v-1}$ on the density of the Planck radiation is fundamentally different from the dependence of polarization on $s\Delta\Omega'$. Calculations showed that when the density of the exciting light is negligibly small in comparison to the intensity of the Planck radiation $s\Delta\Omega' \ll u$, the polarization of all the lines $P_{v,\,v-1}$ approaches $1/2$.

It should be noted that the polarization of different lines of a strongly harmonic oscillator are in the main not observed since the lines are all exactly equal in frequency and fall on top of each other. For a weakly anharmonic oscillator, however, for which the results described above are qualitatively applicable, the levels move apart, i.e., different transitions correspond to different frequencies. In this case the polarization of different lines can be measured experimentally. If the frequencies of different transitions are close to each other and all the lines overlap, then under certain specific conditions the differences in polarizations ought to be detectable within the limits of the contours of the line.

REFERENCES

1. B. I. Stepanov and V. P. Gribkovskii. Doklady Akad. Nauk SSSR 121, 446 (1958); V. P. Gribkovskii, B. I. Stepanov, and P. A. Apanasevich. Trudy Inst. Fiz. Mat. Akad. Nauk, Byeloruss. SSR 3, 131 (1959).
2. B. I. Stepanov. Doklady Akad. Nauk SSSR 99, 971 (1954).
3. B. I. Stepanov. "Luminescence of Complex Molecules." Izd. Akad. Nauk Byeloruss. SSR, Minsk, 1956.
4. D. I. Blokhintsev. "Fundamentals of Quantum Mechanics." GITTL, Moscow, 1949.
5. P. P. Feofilov. Uspekhi Fiz. Nauk 36, 417 (1948).
6. S. I. Vavilov and V. L. Levshin. Z. Physik 16, 136 (1923).

THEORY OF THE INTENSITIES OF INFRARED SPECTRA OF MOLECULES VI. BF_3, NF_3, SiF_4, and SF_6

L. M. Sverdlov

Received 13 May 1959

A calculation of the electro-optical parameters of the molecules BF_3, NF_3, SiF_4, and SF_6 has been carried out in a first approximation valence-optical scheme using the absolute integrated intensities of the infrared spectra of the molecules. A regular increase of the dipole moment of the X—F bond with increasing difference of the electronegativities of the X and F atoms was established.

1. The calculation of the intensities and the electro-optical parameters of fluoro-compounds has a special interest since the infrared spectra of these compounds have strong absorption bands.

As a continuation of calculations made previously[1] (for the CF_4 and C_2F_6 molecules) in the present investigation a calculation of the electro-optical parameters is carried out for the molecules BF_3, NF_3, SiF_4, and SF_6 in a first approximation valence-optical scheme.

The absolute integrated intensities of the infrared bands of the BF_3 and NF_3 molecules have been measured by McKean[2] and Schatz and Levin,[3] respectively. They also calculated the electro-optical parameters, μ_{XY} and $\partial\mu_{XY}/\partial q$, in the zeroth order valence-optical scheme; in this, however, they encountered the usual difficulties, that is, they found that the parameters have different values for different symmetry species. The integrated intensities for SiF_4 and SF_6 were determined in an investigation of Schatz and Hornig.[4] The experimental values of $\partial P/\partial Q$ reported[2-4] for BF_3, NF_3, SiF_4, and SF_6 are given in Table 1.

Table 1. Experimental Values of $\partial P/\partial Q_i$ for BF_3, NF_3, SiF_4, and SF_6 (in units CGSE/cm. $gm^{1/2}$)

BF_3				NF_3							
Symmetry	Frequency (cm^{-1})		$\frac{\partial P}{\partial Q_i}$	Symmetry	Frequency (cm^{-1})		$\frac{\partial P}{\partial Q_i}$	Symmetry	Frequency (cm^{-1})		$\frac{\partial P}{\partial Q_i}$
A_2''	ω_2	730.17	102.2	A_1	ν_1(N—F)	1032	71.91	E	ν_3(N—F)	906	186.43
E'	ω_3(B—F)	1549.6	227.4	A_1	ν_2(FNF)	642	16.4	E	ν_4(FNF)	492	10.88
E'	ω_4(FBF)	509.2	38.95								

SiF_4				SF_6			
Symmetry	Frequency (cm^{-1})		$\frac{\partial P}{\partial Q_i}$	Symmetry	Frequency (cm^{-1})		$\frac{\partial P}{\partial Q_i}$
F_2	ν_3(Si—F)	1031	167.6	F_{1u}	ν_3(SF)	947	226.1
F_2	ν_4(FSiF)	391	73.45	F_{1u}	ν_4(FSF)	615	54.62

2. For the calculation we will introduce the natural vibrational coordinates q and α (Figs. 1 and 2) and the valence-optical coordinates $\beta_{\alpha\xi}$, $\beta_{\alpha\eta}$, $\beta_{\alpha\zeta}$ giving the angle changes between the bonds and the coordinate axes. For NF_3 and BF_3 calculations we will introduce in addition the independent coordinates, φ, for the angle changes between the X—F bonds and the ζ-axis, and ψ, for the rotation of the X—F bonds around the ζ-axis. The molecules BF_3, NF_3, SiF_4, and SF_6 belong to the symmetry groups D_{3h}, C_{3v}, T_d, and O_h, respectively. The vibrations active in the infrared have the symmetry species A_2'' and E' for BF_3, A_1 and E for NF_3, F_2 for SiF_4, and F_{1u} for SF_6.

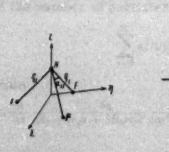

Fig. 1

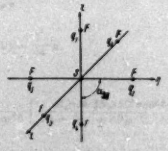

Fig. 2

The symmetry coordinates S_k^{Σ} are as follows:

BF_3: $q^{A_2''} = \frac{1}{\sqrt{3}}(q_1+q_2+q_3)$; $q^{E'I} = \frac{1}{\sqrt{6}}(2q_1-q_2-q_3)$;

$\alpha^{E'I} = \frac{1}{\sqrt{6}}(2\alpha_{23}-\alpha_{12}-\alpha_{13})$; $\psi^{E'I} = \frac{1}{\sqrt{2}}(\psi_2-\psi_3)$

SF_6: $q^{F_{1u}III} = \frac{1}{\sqrt{2}}(q_1-q_4)$; $\alpha^{F_{1u}III} =$

$\frac{1}{\sqrt{8}}(\alpha_{12}+\alpha_{34}+\alpha_{45}+\alpha_{36}-\alpha_{13}-\alpha_{15}-\alpha_{23}-\alpha_{26})$

The symmetry coordinates are expressed in terms of the normal coordinates $Q_i(S_k^{\Sigma} = \sum_i L_{ki}Q_i)$ as follows:

BF_3: $q^{A_2''} = E_4Q_2$; $q^{E'I} = \sum_{i=3}^{4} C_{qi}Q_i$; $\alpha^{E'I} = \sum_{i=3}^{4} D_{\alpha i}Q_i$; $\psi^{E'I} = \sum_{i=3}^{4} F_iQ_i$,

in which $F_1 = -(1/\sqrt{3})D_{\alpha 1}$.

SF_6: $q^{F_{1u}III} = \sum_{i=3}^{6} C_{qi}Q_i$; $\alpha^{F_{1u}III} = \sum_{i=3}^{6} D_{\alpha i}Q_i$

The corresponding formulas for NF_3 and SiF_4, as well as the formulas relating the valence-optical coordinates $\beta_{\alpha i}$ with φ and ψ, are given in references 5 and 6, in which calculations for ammonia (NH_3) and methane (CH_4) were carried out.

The derivatives of the dipole moment with respect to the symmetry coordinates, $\partial P/S_k^{\Sigma}$, in the first approximation valence-optical scheme have the form:

$$BF_3: \quad \frac{\partial P_\zeta}{\partial q^{A_2''}} = \left[-\sqrt{3}\,\frac{\mu_{BF}}{r_{BF}}\right] = E_2^{-1}\,\frac{\partial P_\zeta}{\partial Q_2^{A_2''}}. \tag{1a}$$

$$\left.\begin{aligned} \frac{\partial P}{\partial q^{E'II}} &= \sqrt{\frac{3}{2}\left[\left(\frac{\partial\mu_{BF}^{(1)}}{\partial q_1}-\frac{\partial\mu_{BF}^{(2)}}{\partial q_1}\right)^2+\left(\mu_{BF}\frac{\partial\gamma_1}{\partial q_1}-\mu_{BF}\frac{\partial\gamma_1}{\partial q_1}\right)^2\right]} = \\ &= \pm\left[\sum_{i=3}^{4} L_{2i}^{-1}\frac{\partial P}{\partial Q_i}\right]. \\ \frac{\partial P}{\partial \psi^{E'II}} &= \sqrt{\left[\frac{3}{2}\left(\frac{\mu_{BF}}{r_{BF}}\right)^2+6\left(\frac{1}{r_{BF}}\frac{\partial\gamma_{BF}^{(1)}}{\partial\gamma_1}-\frac{1}{r_{BF}}\frac{\partial\gamma_{BF}^{(2)}}{\partial\gamma_1}\right)^2\right]} = \\ &= \pm\left[\sum_{i=3}^{4} L_{2i}^{-1}\frac{\partial P}{\partial Q_i}\right]. \end{aligned}\right\} \tag{1b}$$

SF_6: $\frac{\partial P_\zeta}{\partial q^{F_{III}}_{III}} = \left[\sqrt{2}\left(\frac{\partial r^{(1)}_{SF}}{\partial q_1} - \frac{\partial r^{(2)}_{SF}}{\partial q_1}\right)\right] = \sum_{l=1}^{4} L^{-1}_{1l}\frac{\partial P_\zeta}{\partial Q_l}$, (2a)

$$\frac{\partial P_\zeta}{\partial \alpha^{F_{III}}_{III}} = \left[-\sqrt{2}\,\frac{\mu_{SF}}{r_{SF}}\right] = \sum_{l=1}^{4} L^{-1}_{2l}\frac{\partial P_\zeta}{\partial Q_l}. \quad (2b)$$

NF_3:

$$\left.\begin{aligned}
&\frac{\partial P_\zeta}{\partial q^{F_1}_{I}} = \left[-x\sqrt{3}\left(\frac{\partial r^{(1)}_{NF}}{\partial q_1} + 2\frac{\partial r^{(2)}_{NF}}{\partial q_1}\right) - 2\sin\frac{\theta}{2}\right.\\
&\left.\mu_{NF}\left(\frac{\partial \gamma_1}{\partial q_1} + 2\frac{\partial \gamma_2}{\partial q_1}\right)\right] = \sum_{l=1}^{3} L^{-1}_{1l}\frac{\partial P_\zeta}{\partial Q_l},\\
&\frac{\partial P_\zeta}{\partial q^{F_2}_{I}} = \left[-2\sin\frac{\theta}{2}\cdot\frac{\mu_{NF}}{r_{NF}} - 2x\sqrt{3}\left(\frac{\partial r^{(1)}_{NF}}{\partial q_1} + 2\frac{\partial r^{(2)}_{NF}}{\partial q_1}\right)\frac{1}{r_{NF}}\right]\\
&\qquad = \sum_{l=1}^{3} L^{-1}_{1l}\frac{\partial P_\zeta}{\partial Q_l}.
\end{aligned}\right\} \quad (3a)$$

$$\frac{\partial P_\eta}{\partial q^{F_{III}}_{III}} = \left[\sqrt{2}\sin\frac{\theta}{2}\left(\frac{\partial r^{(1)}_{NF}}{\partial q_1} - \frac{\partial r^{(2)}_{NF}}{\partial q_1}\right) - x\sqrt{\frac{3}{2}}\,\mu_{NF}\left(\frac{\partial \gamma_1}{\partial q_1} - \frac{\partial \gamma_2}{\partial q_1}\right)\right]$$
$$= \sum_{l=1}^{4} L^{-1}_{1l}\left[\frac{\partial P_\eta}{\partial Q_l} + \frac{\sqrt{2}}{3x}\sin\frac{\theta}{2}\cdot\frac{\mu_{NF_3}}{r_{NF}}\cdot F_l\right] \quad (3b)^*$$

$$\frac{\partial P_\eta}{\partial q^{F_{III}}_{III}} = \left[-x\sqrt{\frac{3}{2}}\,\frac{\mu_{NF}}{r_{NF}} + 2\sqrt{2}\sin\frac{\theta}{2}\left(\frac{\partial r^{(1)}_{NF}}{\partial q_1} - \frac{\partial r^{(2)}_{NF}}{\partial q_1}\right)\frac{1}{r_{NF}}\right]$$
$$= \sum_{l=1}^{4} L^{-1}_{2l}\left[\frac{\partial P_\eta}{\partial Q_l} + \frac{\sqrt{2}}{3x}\sin\frac{\theta}{2}\cdot\frac{\mu_{NF_3}}{r_{NF}}\cdot F_l\right];$$

*$\partial P_\xi/\partial Q^{F_{III}}_{l} = \partial P_\zeta/\partial Q^{F_{III}}_{l} = 0$. In addition, it is assumed that $\partial\mu/\partial\psi = \partial\psi/\partial q = 0$, as in reference 5.

SiF_4: $\frac{\partial P_\zeta}{\partial q^{F_{III}}_{III}} = \left[\frac{2}{\sqrt{3}}\left(\frac{\partial r^{(1)}_{SiF}}{\partial q_1} - \frac{\partial r^{(2)}_{SiF}}{\partial q_1}\right)\right] = \sum_{l=1}^{4} L^{-1}_{1l}\frac{\partial P_\zeta}{\partial Q_l}$,

$$\frac{\partial P_\zeta}{\partial \alpha^{F_{III}}_{III}} = \left[-\frac{2}{\sqrt{3}}\,\frac{\mu_{SiF}}{r_{SiF}}\right] = \sum_{l=1}^{4} L^{-1}_{2l}\frac{\partial P_\zeta}{\partial Q_l} \quad (4)$$

In formulas (3) the following abbreviations have been introduced:

$$\theta = \sphericalangle FNF; \qquad x = \sqrt{1 - \frac{4}{3}\sin^2\frac{\theta}{2}}$$

3. The mechanical problem of evaluating the coefficients L_{kl} for the various molecules was solved. In the calculations the following geometrical parameters were used:

NF_3: $\theta = 102°9';^7$ $r_{NF} = 1.371$ A.

BF_3: $r_{BF} = 1.295$ A.[8]

SF_6: $r_{SF} = 1.57$ A.[9]

SiF_4: $r_{SiF} = 1.54$ A.[9, 10]

Force constants for BF_3 and NF_3 were taken from references 2 and 11. For SiF_4 and SF_6 they were calculated in the present investigation (Table 2). The secular equations were solved by the iteration method of Mayants.[12] The calculated coefficients L_{kl} were used to determine the coefficients L^{-1}_{kl} (Table 3).

Formulas (1)-(4) with the data of Tables 1 and 3 were used to evaluate the derivatives of the dipole moment

Table 2. Symmetrized Matrices of the Force Coefficients for BF_3, NF_3, SiF_4, SF_6 (in units 10^5 cm^{-2})

BF_3			NF_3					
E'	q	α	A_1	q	α	E	q	α
q	12.2808	−0.479	q	9.6874	0.929	q	6.2544	−0.8051
α	−0.479	1.0084	α	0.929	2.2901	α	−0.8051	1.4527

SiF_4			SF_6		
F_2	q	α	F_{1u}	q	α
q	9.9083	0.0707	q	6.7082	−1.0791
α	0.0707	0.7975	α	−1.0791	2.1737

Table 3. Matrices of the Coefficients L^{-1}_{kl} for BF_3, NF_3, SiF_4, and SF_6 (in units 10^{-12} $gm^{1/2}$)

BF_3			NF_3					
E'	q	φ	A_1	q	γ	E	q	γ
Q_2	2.6988	−0.3547	Q_1	2.9479	1.3044	Q_3	4.5548	3.6547
Q_4	−3.3228	−4.2662	Q_2	4.442	−3.0523	Q_4	13.0314	43.7982
$E^{-1}_2 = 2.2598$						$F_3 = -0.218$		
						$F_4 = -0.2044$		

SiF_4			SF_6		
F_2	q	α	F_{1u}	q	α
Q_2	3.7501	−0.3099	Q_2	2.1104	1.2013
Q_4	3.13	2.8289	Q_4	−4.3451	2.4734

with respect to the symmetry coordinates for various combinations of signs of the $\partial P/\partial Q_l$ (Table 4). Combining the derivatives $\partial P/\partial S^{(k)}_\kappa$ for the different symmetry species we obtain expressions for the electro-

Table 4. Derivatives of the Dipole Moment with Respect to the Symmetry Coordinates, $\partial P/\partial S^{(k)}_\kappa$ (in units D/A) for BF_3, NF_3, SiF_4, and SF_6

NF_3								BF_3		
A_1	Signs of $\frac{\partial P}{\partial Q_{1,2}}$		E	Signs of $\frac{\partial P}{\partial Q_{3,4}}$				E'	Signs of $\frac{\partial P}{\partial Q_{3,4}}$	
	++	+−		++	+−	−+	−−		++	+−
$\frac{\partial P}{\partial q^{A_1}_{I}}$	2.8482	1.3914	$\frac{\partial P}{\partial q^{E}_{I}}$	9.3892	6.5527	−7.594	−10.4304	$\frac{\partial P}{\partial q_1}$	±4.8429	±7.4314
$\frac{\partial P}{\partial \alpha^{A_1}_{I}}$	0.4375	1.4385	$\frac{\partial P}{\partial \alpha^{E}_{I}}$	10.1919	0.6588	−3.435	−12.9681	$\frac{\partial P}{\partial \gamma_1}$	∓2.4683	±0.855

SiF_4			SF_6		
F_2	Signs of $\frac{\partial P}{\partial Q_{3,4}}$		F_{1u}	Signs of $\frac{\partial P}{\partial Q_{3,4}}$	
	−−	+−		++	−+
$\frac{\partial P}{\partial q_1}$	−8.5767	3.9788	$\frac{\partial P}{\partial q_1}$	2.3983	−7.1448
$\frac{\partial P}{\partial \alpha_1}$	−1.5576	−2.5951	$\frac{\partial P}{\partial \alpha_1}$	4.0671	−1.3852

optical parameters (Table 5). For the selection of the correct values of the electro-optical parameters, criteria previously formulated[5] were used: firstly, $|\partial\mu^{(1)}/\partial q_1| \gg |\partial\mu^{(2)}/\partial q_1|$, $|\partial\mu^{(1)}/\partial\varphi_1| \gg |\partial\mu^{(2)}/\partial\varphi_1|$; secondly, the $|\partial\mu/\partial\varphi|$ should have maximal values; thirdly, $\partial\mu^{(1)}/\partial q_1$ and the bond dipole moment μ should have different signs.

For NF_3 the criteria given are best satisfied by the third variant: $+\partial P/\partial Q^{A_1}_1$, $+\partial P/\partial Q^{A_1}_2$, $-\partial P/\partial Q^{E}_3$, $+\partial P/\partial Q^{E}_4$. For SiF_4 it is necessary to choose the first variant:

Table 5. Electro-Optical Parameters of NF_3 (in units D/A) for Various Combinations of Signs of $\partial P/\partial Q_{1,2}$ and $\partial P/\partial Q_{3,4}$

Signs of $\frac{\partial P}{\partial Q_m}$	++	++	++	++	+−	+−	+−	+−
Signs of $\frac{\partial P}{\partial Q_n}$	++	+−	−+	−−	++	+−	−+	−−
$\left[\frac{\partial \mu_{NF}^{(1)}}{\partial q_1}\right]$	4.4426	2.7238	−5.8491	−7.568	5.0805	3.3617	−5.2112	−6.9301
$\left[\frac{\partial \mu_{NF}^{(2)}}{\partial q_1}\right]$	−4.0921	−3.2326	1.0538	1.9132	−3.4542	−2.5947	1.6917	2.5511
$\left[\frac{1}{r_{NF}}\frac{\partial \mu_{NF}^{(1)}}{\partial q_1}\right]$	2.9694	0.0809	−1.1595	−4.0481	2.7502	−0.1383	−1.3787	−4.2872
$\left[\frac{1}{r_{NF}}\frac{\partial \mu_{NF}^{(2)}}{\partial q_1}\right]$	−1.6945	−0.2502	0.37	1.8142	−1.9137	−0.4694	0.1508	1.5951
Signs of $\frac{\partial P}{\partial Q_m}$	−−	−−	−−	−−	−+	−+	−+	−+
Signs of $\frac{\partial P}{\partial Q_n}$	++	+−	−+	−−	++	+−	−+	−−
$\left[\frac{\partial \mu_{NF}^{(1)}}{\partial q_1}\right]$	6.937	5.2181	−3.3548	−5.0736	6.290	4.5802	−3.9927	−5.7115
$\left[\frac{\partial \mu_{NF}^{(2)}}{\partial q_1}\right]$	−1.5977	−0.7383	3.5481	4.4078	−2.2356	−1.3762	2.9102	3.7697
$\left[\frac{1}{r_{NF}}\frac{\partial \mu_{NF}^{(1)}}{\partial q_1}\right]$	3.1609	0.2734	−0.968	−3.8565	3.3801	0.4915	−0.7488	−3.6373
$\left[\frac{1}{r_{NF}}\frac{\partial \mu_{NF}^{(2)}}{\partial q_1}\right]$	−1.5029	−0.0587	0.5615	2.0058	−1.2838	0.1605	0.7807	2.2249

$-\partial P/\partial Q_3$, $-\partial P/\partial Q_4$; and for SF_6, the second variant: $-\partial P/\partial Q_3$, $+\partial P/\partial Q_4$. For BF_3 the first variant $+\partial P/\partial Q_3$, $+\partial P/\partial Q_4$ has a physical significance, since only thus does the value of $\partial P/\partial \psi$ agree with the value, $\mu_{XF}\, r_{NF} = 1.3334$ D/A, which is determined from the intensity of the vibration of A_2'' species.

Since the electronegativity of the fluorine atom is greater than that of the nitrogen, sulphur, boron, and silicon atoms, it must be assumed that the negative end of the dipole X—F (where X = N, S, B, Si) is located on the fluorine atom. This corresponds to the positive sign for μ_{XF}. For most of the electro-optical parameters the signs were determined in this way; they are given in Table 6.

4. A comparison of the electro-optical parameters μ_{XF}, μ_{XF}/r_{XF} and $[(\partial\mu_{XF}^{(1)}/\partial q_1) - (\partial\mu_{XF}^{(2)}/\partial q_1)]$ of the compounds studied leads to the following conclusions.

The dipole moment of the X—F bond increases in a regular way with increasing difference in the electronegativities, Δ_{XF}, of the X and F atoms:

$$\mu_{SiF} > \mu_{BF} > \mu_{SF} > \mu_{NF}$$

The same is true also for μ_{XF}/r_{XF}. However, μ_{XF} and Δ_{XF} are not directly proportional. This can be explained by the fact that the bond dipole moment depends not only on the difference in the electronegatives of the atoms forming the bond, but also on their valence state (i.e., the type of hybridization of the wave functions) and on the influence of neighboring bonds. It is interesting to compare the CF_4[1] and SF_6 molecules in this connection. In spite of the fact that $\Delta_{SF} = \Delta_{CF}$, the dipole moment of the S—F bond is greater than that of the C—F bond. This is evidently related to the fact that the nature of the hybridization of the wave functions of C and S is different; in the one case sp_3 hybridization is present, and in the other spd hybridization.

In addition, it must be noted that the regular variation indicated above is not observed for $[(\partial\mu_{XF}^{(1)}/\partial q_1) - (\partial\mu^{(2)}/\partial q_1)]$. Apparently, the valence state of the central atom X and the influence of the neighboring bonds play a role here which is just as important as the difference in electronegativities, Δ_{XF}. At the same time a high value of the derivative of the dipole moment with respect to the bond length is characteristic for the stretching vibrations of all the X—F bonds; this is shown by the high intensity of the infrared absorption bands.

REFERENCES

1. L. M. Sverdlov. Opt. i Spektr. **7**, 600 (1959).
2. D. C. McKean. J. Chem. Phys. **24**, 1002 (1956).
3. P. N. Schatz and I. W. Levin. J. Chem. Phys. **29**, 475 (1958).
4. P. N. Schatz and D. F. Hornig. J. Chem. Phys. **21**, 1516 (1953).
5. L. M. Sverdlov. Opt. i Spektr. **7**, 152 (1959).
6. L. M. Sverdlov. Opt. i Spektr. **7**, 21 (1959).
7. V. Gordy, V. Smit, and R. Trambarulo. "Radio-

Table 6. Electro-Optical Parameters of BF_3, NF_3, SiF_4, and SF_6 (in units D/A)

NF_3		BF_3		SiF_4	
μ_{NF} (in D units)	0.1775	μ_{BF} (in D units)	1.7268	μ_{SiF} (in D units)	2.0773
$\frac{\mu_{NF}}{r_{NF}}$	2.1294	$\frac{\mu_{BF}}{r_{BF}}$	1.3334	$\frac{\mu_{SiF}}{r_{SiF}}$	1.3489
$\left[\frac{\partial \mu_{NF}^{(1)}}{\partial q_1} + \frac{\mu_{NF}}{x\sqrt{3}\sin\frac{\varphi}{2}}\left(-\cos\frac{\vartheta}{2}\cdot\frac{\partial \vartheta_1}{\partial q_1} + \frac{\partial \gamma_1}{\partial q_1}\right)\right]$	−5.8491	$\left(\frac{\partial \mu_{BF}^{(1)}}{\partial q_1} - \frac{\partial \mu_{BF}^{(2)}}{\partial q_1}\right)\sqrt{1+a^2}$*	−3.9542	$\left(\frac{\partial \mu_{SiF}^{(1)}}{\partial q_1} - \frac{\partial \mu_{SiF}^{(2)}}{\partial q_1}\right)$	−7.4276
$\left\{\frac{\partial \mu_{NF}^{(2)}}{\partial q_1} + \frac{\mu_{NF}}{2x\sqrt{3}\sin\frac{\varphi}{2}}\left[\frac{\partial \gamma_1}{\partial q_1} - \left(\cos^2\frac{\vartheta}{2} - 3\sin^2\frac{\vartheta}{2}\right)\frac{\partial \vartheta_1}{\partial q_1}\right]\right\}$	1.0538			SF_6	
				μ_{SF} (in D units)	1.5155
$\frac{1}{r_{NF}}\frac{\partial \mu_{NF}^{(1)}}{\partial q_1}$	−1.1595			$\frac{\mu_{SF}}{r_{SF}}$	0.9853
$\frac{1}{r_{NF}}\frac{\partial \mu_{NF}^{(2)}}{\partial q_1}$	0.37	$\frac{1}{r_{BF}}\left(\frac{\partial \mu_{BF}^{(1)}}{\partial q_1} - \frac{\partial \mu_{BF}^{(2)}}{\partial q_1}\right)$	±0.7556	$\left(\frac{\partial \mu_{SF}^{(1)}}{\partial q_1} - \frac{\partial \mu_{SF}^{(2)}}{\partial q_1}\right)$	−5.0521

* $a = -\dfrac{\mu_{BF}\frac{\partial \gamma_1}{\partial q_1} - \mu_{BF}\frac{\partial \vartheta_1}{\partial q_1}}{\frac{\partial \mu_{BF}^{(1)}}{\partial q_1} - \frac{\partial \mu_{BF}^{(2)}}{\partial q_1}}$

spektroskopiya." (Radio-Spectroscopy), Gosudarst. Izd. Tekh.-Teoret. Lit., Moscow, 1955.
8. A. H. Nielsen. J. Chem. Phys. 22, 659 (1954).
9. L. O. Brockway. Revs. Modern Phys. 8, 231 (1936).
10. P. W. Allen and L. E. Sutton, Acta Cryst. 3, 46 (1950).
11. P. N. Schatz. J. Chem. Phys. 29, 481 (1958).
12. A. S. Mayants. Trudy Fiz. Inst. Akad. Nauk 5, 63 (1950).

NEW VARIANT OF THE METALLIC MODEL OF A MOLECULE

L. A. Borovinskii

Received 18 May 1959

A model of molecules with short chains of conjugate bonds is proposed. The molecular skeleton, which consists of the nuclei and the σ-electrons, is represented by a rigid charge evenly distributed along a straight line which is the same length as the conjugate bond chain. The motion of π-electrons in the field of this model of the skeleton is examined. An approximate separation of the longitudinal and transverse motion of the π-electrons is presented. In a zero approximation, the longitudinal part of the potential function can be replaced by the potential function of an harmonic oscillator and, correspondingly, the energy levels are determined to be the energy levels of the harmonic oscillator. For a more precise representation of the potential function the problem is solved using the semiclassical method of quantum mechanics. Calculated wavelengths of absorption bands are found to be in good agreement with experimental data.

A metallic model of molecules with conjugate bonds predicts a basic characteristic of the motion of π-electrons—their high mobility in the direction of the conjugate bond chains. However, the representation of the potential well inside of which the π-electrons move (which is basic in the model) corresponds poorly to the conditions of the motion of π-electrons in molecules with conjugate bonds. In real molecules, the π-electrons move in the field of the molecular skeleton which consists of the nuclei and the σ-electrons. The replacement of this field by a potential well with definite dimensions and shape, even in the case of a three-dimensional metallic model, represents an extremely crude approximation to actuality.

In this study a modified metallic model is proposed which, in our opinion, corresponds closer to the real conditions of π-electron motion in molecules with short chains of conjugate bonds.

We shall examine as a model of the molecular skeleton a rigid charge equal to the total charge of the nuclei and the σ-electrons of the molecule and evenly distributed along a straight line. The length of this line we shall make equal to the distance between the extreme atoms of the conjugate bond chain increased by a value of the order of one C—C bond length. The distance between the extreme atoms of the chain is equal to

$$a\,(N-1)\cos\frac{\pi}{6},$$

where a is the length of the C—C bond, N is the number of atoms in the chain, and the factor $\cos(\pi/6)$ arises from the zig-zag in the short chains of the conjugate bonds. In our model we shall make the length of the skeleton equal to

$$aN\cos\frac{\pi}{6}.$$

We shall examine the field of this model of the skeleton of a molecule. We shall use the cylindrical system of coordinates, the origin of which we take as the center of the skeleton model. The z model is directed along the axis of the skeleton. The linear density of the charge we call γ. An elementary calculation leads to the following expression for the field potential of the skeleton model of the molecule:

$$V=\gamma\ln\frac{\left[\sqrt{(L-z)^2+\rho^2}+(L-z)\right]\left[\sqrt{(L+z)^2+\rho^2}+(L+z)\right]}{\rho^2}, \quad (1)$$

where $L = [aN\cos(\pi/6)]/2$, the half-length of the skeleton model of the molecule.

We put the potential V into the form of a sum $V = V_1 + V_2$, where

$$V_1=\gamma\ln\frac{\left[\sqrt{(L-z)^2+\rho^2}+(L-z)\right]\left[\sqrt{(L+z)^2+\rho^2}+(L+z)\right]}{R^2}; \quad (2)$$

$$V_2=\gamma\ln\frac{R^2}{\rho^2}. \quad (3)$$

The value of R is arbitrary.

Since the motion of π-electrons occurs in a narrow cylinder along the short axis of the molecule we can consider that in the region of interest to us $\rho \ll L$. In view of this, we notice that the potential V_1 when $\rho^2 \ll (L \pm z)^2$ depends weakly on ρ. The dependence of V_1 on ρ is important only for the extremities, where z is close to $\pm L$. Therefore, we shall neglect the dependence of V_1 on ρ and replace, in Eq. (2), the coordinate ρ by the constant parameter r which characterizes the width of the region of π-electron motion. The division of the potential V into V_1 and V_2 and the neglect of the dependence of V_1 on ρ makes it possible, in the solution of the quantum mechanical problem, to carry out a separation of the variables z and ρ and also to carry out the transition from a three-dimensional model to a one-dimensional model. The one-dimensional Schrödinger equation for longitudinal motion of π-electrons has the form

$$-\frac{\hbar^2}{2m}\frac{d^2\psi}{dz^2}-eV_1\psi=E\psi. \quad (4)$$

The potential energy $U = -eV_1$ has a minimum in the center of the molecular model when z = 0. For a rough estimate of the energy levels and the dependence of wavelength on the number of atoms in the conjugate chain we shall solve the problem first for a still more simplified form of the potential function. For this, we assume that $\rho = 0$ and $R = 2L$ in Eq. (2).

The potential energy has the form

$$U(z) = -\gamma \ln\left(1 - \frac{z^2}{L^2}\right). \quad (5)$$

Expanding this expression as a power series in z and retaining only the quadratic term, we obtain

$$U(z) = \frac{\gamma}{L^2} z^2 = \frac{\varkappa z^2}{2}, \quad (6)$$

where

$$\varkappa = \frac{2\gamma}{L^2}.$$

Thus, in this approximation the potential energy has the same form as the potential energy of an harmonic oscillator. According to the equation for the energy levels of an harmonic oscillator we have,

$$E_n = \hbar\sqrt{\frac{\varkappa}{m}}\left(n + \frac{1}{2}\right) = \hbar\sqrt{\frac{2\gamma}{Lm}}\left(n + \frac{1}{2}\right); \quad (n = 0, 1, 2\ldots) \quad (7)$$

The linear density of charge along the skeleton is equal to

$$\gamma = \frac{eN}{2L} = \frac{e}{a\cos\frac{\pi}{6}},$$

It follows, however, that the shielding of the charge along the skeleton by the π-electrons must be computed. We introduce, therefore, into the expression for γ the factor p^2 which is a proper fraction of the order of unity. The expression for γ takes the form

$$\gamma = \frac{e}{a\cos\frac{\pi}{6}} p^2. \quad (8)$$

The transition frequencies in this approximation equal

$$\nu = \frac{1}{2\pi}\sqrt{\frac{2\gamma}{Lm}} = \frac{\sqrt{2}ep}{\pi a\cos\frac{\pi}{6}\sqrt{am\cos\frac{\pi}{6}}N} \quad (9)$$

Correspondingly, the wavelengths equal

$$\lambda = \frac{c}{\nu} = \frac{\pi a c\cos\frac{\pi}{6}\sqrt{2am\cos\frac{\pi}{6}}}{2ep} N. \quad (10)$$

Substituting the known values of the constants c, a, m, and e into Eq. (10) and carrying out the calculation, we obtain

$$\lambda = \frac{550}{p} N\,(\text{Å}). \quad (11)$$

As is seen from Table 2, the wavelengths of the absorption bands calculated from Eq. (11) for values of p close to unity agree well with the experimental data. Of course, in view of the crudeness of the model, the good agreement with experiment should be considered, in one way or another, accidental and connected with the empirical choice of the parameter p. The obtained results are interesting because in this approximation the quantum effects do not have an influence on the calculated frequencies of the absorption bands; the given calculations can be completely carried out on the basis of classical physics.

We shall now examine the motion of π-electrons in a field the potential of which is expressed by Eq. (2) with a substitution of ρ by the constant r. This constant can be considered equal in order of magnitude to a/2 = 0.7 A, i.e., the covalence radius of the carbon atom in molecules with conjugate bonds.

We perform the calculations for values of r equal to 0.7 and 0.91 A. All further calculations are carried out only for the first of these values of r. The value of R in this case is also, for convenience, set equal to r. Replacing the quantities ρ and R in (2) by a/2 and substituting the value of L, we have the expression

$$V_1(z) = \gamma \ln\left[\sqrt{\left(N\cos\frac{\pi}{6} - \frac{2z}{a}\right)^2 + 1} + \left(N\cos\frac{\pi}{6} - \frac{2z}{a}\right)\right] \times\left[\sqrt{\left(N\cos\frac{\pi}{6} + \frac{2z}{a}\right)^2 + 1} + \left(N\cos\frac{\pi}{6} + \frac{2z}{a}\right)\right]. \quad (12)$$

Solution of the Schrödinger Eq. (4) with a potential V_1 from (12) is beset by great numerical difficulties. Therefore, for the determination of energy levels and frequencies of transitions we use the semiclassical method of quantum mechanics. This method, as is well-known, applies to states which are characterized by large values of quantum numbers, but, in some cases, it gives legitimate results for the lowest states of electrons. In our problem the numbers for the levels between which transitions occur corresponding to the longest wavelength absorption bands are determined by the number of atoms in the chains of the conjugate bonds. As the approximation presented by Eq. (46.7) of Landau and Lifshits[1] shows, the semiclassical method is applicable when N ≥ 9.

Using Eq. (48.1) of Landau and Lifshits[1] we shall describe the quantum states in our case. The action function of an electron in our problem has the form

$$S = 4\int_0^{z_0} \sqrt{2m\,[E - U(z)]}\, dz, \quad (13)$$

where z_0 is the classical turning point of the electron at which $E = U(z_0)$.

For the conversion to dimensionless values, we set the energy quantity $e\gamma\ln 10$ equal to unity to make a change of variable: $z = (a/2)x$. Then the function U takes the form

$$U(x) = -\log\left[\sqrt{\left(N\cos\frac{\pi}{6} - x\right)^2 + 1} + \left(N\cos\frac{\pi}{6} - x\right)\right] \times\left[\sqrt{\left(N\cos\frac{\pi}{6} + x\right)^2 + 1} + \left(N\cos\frac{\pi}{6} + x\right)\right]. \quad (14)$$

The action we write in the form

$$S = 2a\sqrt{2me\gamma\ln 10}\cdot I, \quad (15)$$

where

$$I = \int_0^b \sqrt{E - U(x)}\, dx; \quad \left(b = \frac{2z_0}{a};\ E = U(b)\right). \quad (16)$$

The quantity I is the action in units of $2a(2me\gamma\ln 10)^{1/2}$. The quantum levels:

$$S_n = \hbar\left(n + \frac{1}{2}\right) \quad (17)$$

are written in our notation in the form

$$I_n = \frac{h}{2a\sqrt{2me\gamma\ln 10}}\left(n + \frac{1}{2}\right). \quad (18)$$

Replacing γ in (18) by the expression given in (8) and carrying out the computation we obtain

$$I_n = \frac{0.837}{p}\left(n + \frac{1}{2}\right). \quad (n = 0, 1, 2\ldots). \quad (19)$$

From (16), performing a numerical integration, we find the value of the quantity I for a number of values of b and energies E which correspond to them. Part of the results of these computations are shown in Table 1.

On the basis of the data in this table we constructed a graph of the dependence of action I on energy E. The

Table 1. Dependence of Action I on Energy E (in conventional units)

k	N-5		N-7		N-9		N-11		N-13		N-15	
	−E	I	−E	I	−E	I	−E	I	−E	I	−E	I
0	1.886	0	2.173	0	2.389	0	2.561	0	2.707	0	2.830	0
2	1.742	0.478	2.125	0.340	—	—	—	—	—	—	—	—
3	1.644	1.178	—	—	2.321	0.813	—	—	—	—	—	—
4	1.364	2.360	1.944	1.537	—	—	2.480	0.887	—	—	—	—
5	1.000	3.800	1.859	2.045	2.175	1.845	—	—	—	—	—	—
6	—	—	1.410	4.378	2.027	2.953	2.349	2.216	2.564	1.795	2.728	1.513
7	—	—	1.054	6.088	1.787	4.543	2.239	3.248	—	—	—	—
8	—	—	—	—	1.411	6.712	2.070	4.665	2.410	3.531	2.627	2.887
9	—	—	—	—	—	—	1.788	6.729	2.283	4.834		
10	—	—	—	—	—	—	1.393	9.271	2.086	6.632	2.451	5.055
11	—	—	—	—	—	—	—	—	1.760	9.219	2.306	6.661
12	—	—	—	—	—	—	—	—	1.370	11.980	2.079	8.575
13	—	—	—	—	—	—	—	—	—	—	1.712	11.962
14	—	—	—	—	—	—	—	—	—	—	1.346	14.785

energy levels of electrons were found from this graph for the permissible values of I determined from (19). As is known, in the semiclassical method the transition frequencies are determined from the equation

$$\nu = \frac{\Delta E}{\Delta S}, \tag{20}$$

where ΔS is the difference between two permissible values of action (energy E and action S are expressed in cgs units).

In our units the transition frequencies are expressed by the equation

$$\nu = \frac{ep\sqrt{\ln 10}}{2a\sqrt{2am\cos\frac{\pi}{6}}} \cdot \frac{\Delta E}{\Delta I}. \tag{21}$$

Correspondingly, the wavelengths of the absorption bands are determined from

$$\lambda = \frac{2ca}{ep\sqrt{\ln 10}} \sqrt{2ma\cos\frac{\pi}{6}} \cdot \frac{\Delta I}{\Delta E}. \tag{22}$$

We notice that Eq. (22) is different from Eq. (10) by the substitution of the factor $(\pi/2)N\cos(\pi/6)$ by the factor $(2/\sqrt{\ln 10})\Delta I/\Delta E$.

Putting the numerical values of the constants into (22) we get

$$\lambda = \frac{542}{p} \frac{\Delta I}{\Delta E} \text{ (A)}. \tag{23}$$

The wavelengths computed from (23) show an approximately linear dependence on the number of atoms in the chain of conjugate bonds, which agrees with experimental data. The calculations were carried out for a value of p equal to 0.46. We note that the choice of this empirical parameter was limited beforehand by the fact that p^2 must be a proper fraction of the order of unity. The computed wavelength was found in good agreement with the experimental data (see Table 2).

Table 2. Computed and Experimental Values of the Wavelength of the Absorption Bands of Molecules (I) and (II) (in A)

Number of atoms in the conjugate chain	Computed				Experimental	
	The usual metal model, Eq. (26)	Harmonic approximation for p = 0.87, (Eq. 11)	Semiclassical method Eq. (23)		I	II
			r = 0.7 A p = 0.46	r = 0.91 A p = 0.34		
5	2420	3220	4800	4760	4230	—
7	3390	4500	5760	5580	5575	—
9	4360	5790	6500	6400	6500	5900
11	5320	7070	7420	7300	7900	7100
13	6290	8360	8310	8110	8700	8300
15	7260	9650	9160	9180	9950	9300

Note. Nitrogen atoms are included in the number of atoms of the conjugate chain. The number of active π-electrons is taken equal to N − 1, i.e., it is assumed that two nitrogens give one mobile π-electron.

We shall compare the computed results for our model with the computed results for the usual metallic model. The wavelength of the first band of absorption of a linear molecule, which contains an odd number N of atoms in the chain of conjugate bonds and which is represented by a potential well of length l, is determined in the usual metallic model by the equation*

*The number of π-electrons can equal N or N − 1; we obtained identical results in both cases.

$$\lambda = \frac{8m l^2 \nu}{hN}. \tag{24}$$

If we take l = aN and put the numerical values into (24) then we shall get

$$\lambda = 646N \text{ (A)}. \tag{25}$$

This dependence of wavelength on N conforms well with experiment, and almost precisely agrees with Eq. (11) for values of p close to unity. However, we consider it incorrect to take the length of the potential well equal to aN. Due to the zig-zag shape of a chain of C—C bonds, the actual length of the molecule is $(\sqrt{3}/2)aN$. Since the width of the potential well is approximately the length of the C—C bond, the zig-zag shape of the molecule is completely accommodated within the potential well. Thus the motion of π-electrons occurs within a sufficiently broad band and not inside an infinitely narrow zig-zag well. If we assume

$$l = \frac{\sqrt{3}}{2} aN,$$

then in place of (25) we have

$$\lambda = 484N \text{ (A)}. \tag{26}$$

The comparison with experiment shows that the latter result gives too slow an increase of wavelength with an increase of the number of atoms in the conjugate chain.

Incidentally, we notice that the free motion of electrons inside the infinitely narrow potential well of zig-zag shape in general appears to us impossible. In our previous work,[2] conditions of joining the asymptotic expressions of wave functions with three branches terminating in one point were presented. These conditions can be applied to the angle points of the zig-zag potential well by assuming the wave function in one of the three branches is equal to zero.

We write the indicated conditions in the form:

$$\left.\begin{aligned} D\frac{d\psi}{dx_1}\Big|_{x_1=D} &= q_1\psi\Big|_{x_1=D} + q_2\psi\Big|_{x_2=D}; \\ D\frac{d\psi}{dx_2}\Big|_{x_2=D} &= q_2\psi\Big|_{x_2=D} + q_1\psi\Big|_{x_1=D}, \end{aligned}\right\} \tag{27}$$

where D is the width of the potential well; x_1 and x_2 are coordinates reckoned along each axis from the angle point; q_1 and q_2 are numerical coefficients. When D → 0, the left part of Eq. (27) converges to zero as $\sqrt{D}$. (The normalization factor of the wave function increases as $1/\sqrt{D}$). Since

$$q_1^2 \neq q_2^2,$$

then

$$\lim_{D\to 0}\psi\Big|_{x_1=D} = \lim_{D\to 0}\psi\Big|_{x_2=D} = 0.$$

Consequently at the angle points of the infinitely narrow potential well of zig-zag form, nodes are developed in the wave function which absolutely do not correspond to the fact of free mobility of the π-electrons along the chain of conjugate bonds.

As distinct from the usual metallic model, in our model there are no fixed limits to the potential well. The size of the region of motion of the electrons depends on their energy. The greater the energy of the electrons the further from the center of the molecule is the classical turning point, and the larger, consequently, is the effective size of the potential well. This circumstance leads to a drawing together of the computed energy levels in comparison with the usual metallic model and to a corresponding increase of the computed wavelength of the absorption bands.

The computed wavelengths and experimental data copied from Kuhn[3] are shown in Table 2.

The experimental data are given for molecules of the following types:

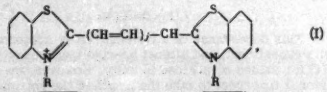

(I)

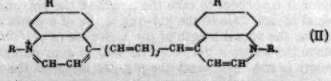

(II)

In molecules of these types the C—C bonds are more planar than in dimethyl- and diphenylpolyenes which is a condition for the great mobility of π-electrons along a conjugate bond chain. We suggest that the results of the calculation by the semiclassical method for N = 5,7 are not reliable, since the sufficient conditions of applicability of the semiclassical method are not fulfilled for these values of N. However, considering that the potential function (14) is close to parabolic, it may be assumed that for these values of N the semiclassical method gives satisfactory results, since in the case of a parabolic form of the potential function the energy levels obtained by the semiclassical method agree with the energy levels obtained by a solution of Schrödinger's equation for all values of quantum numbers.

In the harmonic approximation we computed the strength of the oscillator with the longest wavelength. In this approximation only one transition is permissible. Since this transition occurs between the levels (N − 1)/2 and (N + 1)/2, the oscillator strength (on account of the presence of two electrons in the upper level) is equal to

$$f = 2 \cdot \frac{4\pi^2 m \nu \left| z \right|^2_{\frac{N-1}{2},\frac{N+1}{2}} \cdot \nu}{3h}. \tag{28}$$

Substituting the value of the matrix element of the coordinate

$$\left| z \right|_{\frac{N-1}{2},\frac{N+1}{2}} = \sqrt{\frac{h}{2\pi m \nu}} \sqrt{\frac{N-1}{4}}, \tag{29}$$

we have

$$f = \frac{1}{3}(N-1). \tag{30}$$

Equation (30) gives a trivial result: for one-dimensional motion the sum of the oscillator strength must be equal to one-third the number of electrons. Although experimental data on oscillator strength are unknown to us, it is possible to assume that Eq. (30) gives too high a value of the strengths of oscillators of the longest wavelength transitions.

REFERENCE

1. L. D. Landau and E. M. Lifshits. "Kvantovaya Mekhanika." (Quantum Mechanics), Moscow, 1948.
2. L. A. Borovinsky. Izvest. Akad. Nauk SSSR, Ser. Fiz. 22, 1019 (1958).
3. H. Kuhn. Helv. Chim. Acta 31, 1441 (1948).

CALCULATION OF FREQUENCY AND FORM DERIVATIVES OF NORMAL VIBRATIONS OF MOLECULES POSSESSING SYMMETRY

L. S. Mayants

Received 21 May 1959

Methods are given for the calculation of derivatives of the frequencies and forms of the normal vibrations of molecules from symmetry-reduced equations.

When symmetry is present the frequencies and forms of normal vibrations of molecules are calculated separately for each symmetry species from the equation corresponding to this symmetry species. However, the method of calculating derivatives of the frequencies and forms of normal vibrations, which was reported previously,[1-3] started out from an equation in which the symmetry of the molecule was not taken into account.

Methods are developed below for calculating frequency and form derivatives of normal vibrations starting from equations which correspond to the various symmetry species. It will be shown that derivatives can be calculated also for degenerate vibrations, even when the variation of the parameter destroys the symmetry of the molecule.

The equations which determine the normal vibrations of a molecule have the well-known form,

$$(W - \lambda K) r = 0, \tag{1}$$

where W and K are certain quadratic matrices, the order n of which is equal to the number of vibrational degrees of freedom considered in the calculation, r is a certain column matrix with n elements, and $\lambda = \omega^2$ is the square of a vibrational frequency of the molecule.

If symmetry is present in the molecule, the matrices W and K also possess definite symmetry. This is shown by the fact that a similarity transformation by a certain matrix R, the elements of which depend only on the symmetry of the molecule, reduces the matrices W and K to stepped (quasi-diagonal, block) matrices of the same structure:

$$W' = R^{-1}WR = \begin{Vmatrix} W'_{11} & 0 & 0 & \cdots & 0 \\ 0 & W'_{22} & 0 & \cdots & 0 \\ 0 & 0 & W'_{33} & \cdots & 0 \\ \cdots & \cdots & \cdots & \cdots & \cdots \\ 0 & 0 & 0 & \cdots & W'_{mm} \end{Vmatrix} \tag{2}$$

$$K' = R^{-1}KR = \begin{Vmatrix} K'_{11} & 0 & 0 & \cdots & 0 \\ 0 & K'_{22} & 0 & \cdots & 0 \\ 0 & 0 & K'_{33} & \cdots & 0 \\ \cdots & \cdots & \cdots & \cdots & \cdots \\ 0 & 0 & 0 & & K'_{mm} \end{Vmatrix} \tag{2a}$$

Each block of the matrices W′ and K′ corresponds to the molecular vibrations belonging to a given symmetry species; corresponding to 1-fold degenerate vibrations there are 1 identical blocks in the matrix W′ and, consequently, also in K′.

If we designate the blocks of elements of the stepped matrices W′ and K′ by W'_{ij} and K'_{ij}, respectively, we can write

$$\left.\begin{aligned} W'_{ij} &= (R^{-1})_i W R_j = \delta_{ij} W'_{ii} \\ K'_{ij} &= (R^{-1})_i K R_j = \delta_{ij} K'_{ii} \end{aligned}\right\} \quad (i, j = 1, 2, \ldots, m), \tag{3}$$

where R_j is a rectangular submatrix of the matrix R, consisting of the columns of the latter which correspond to the jth block of W′ and K′, $(R^{-1})_i$ is a rectangular submatrix of the matrix R^{-1}, consisting of the rows of the latter which correspond to ith block of W′ and K′, and δ_{ij} is the Kronecker symbol.

Let $\lambda_i = \omega_i^2$ be the square of the frequency of a given vibration of the jth symmetry species, and $r^{(j)}$ the column matrix for this vibration which appears as the solution of Eq. (1) for $\lambda = \lambda_i$. Then the following identity holds:

$$(W - \lambda_i K) r^{(i)} = 0. \tag{4}$$

Introducing the column matrix,

$$r^{(i)\prime} = R^{-1} r^{(i)} \tag{5}$$

multiplying both terms of the identity (4) on the left with the matrix R^{-1}, and taking Eqs. (2) and (2a) into account we obtain

$$(W' - \lambda_i K') r^{(i)\prime} = 0. \tag{6}$$

Since the matrix $W' - \lambda K'$ is stepped, in the case of nondegenerate vibrations only those elements of the column matrix $r^{(i)\prime}$ can be different from zero which refer to the jth block of $W' - \lambda K'$, corresponding to the given vibrational species; in the case of degenerate vibrations, those elements are different from zero which refer to all the other blocks of the matrix, corresponding to the given degenerate vibrational species.

For nondegenerate vibrations it therefore follows from the identity (6) that

$$(W'_{jj} - \lambda_i K'_{jj}) r^{(i)}_{(j)} = 0, \tag{7}$$

where $r^{(i)}_{(j)\prime}$ is the corresponding submatrix of $r^{(i)\prime}$, clearly identical with the solution of the equation

$$(W'_{jj} - \lambda K'_{jj}) r'_{(j)} = 0 \tag{8}$$

with $\lambda = \lambda_i (r'_{(j)})$ is a column matrix with elements equal in number to the degree of matrices W'_{jj} and K'_{jj}).

From equality (5) it follows that

$$r^{(i)}_{(j)} = (R^{-1})_j r^{(i)}, \tag{9}$$

We will now consider the identity

$$\tilde{p}^{(i)} (W - \lambda_i K) = 0, \tag{10}$$

where $\tilde{p}^{(i)}$ is a row matrix which satisfies the equation

$$\tilde{p}(W - \lambda K) = 0 \tag{11}$$

for $\lambda = \lambda_i$.

Introducing the row matrix,

$$\tilde{p}^{(i)\prime} = \tilde{p}^{(i)} R \tag{12}$$

and multiplying both terms of identity (10) on the right by R, we obtain

$$\tilde{p}^{(i)\prime} (W' - \lambda_i K') = 0. \tag{13}$$

For nondegenerate vibrations only those elements of the row matrix $\tilde{p}^{(i)\prime}$ can be different from zero which refer to the jth block of $W' - \lambda K'$; for degenerate vibrations all those elements of $\tilde{p}^{(i)\prime}$ are different from zero which refer to the other blocks of the matrix corresponding to this same degenerate species.

For nondegenerate vibrations it therefore follows from the identity (13) that

$$\tilde{p}^{(i)\prime}_{(j)} (W'_{jj} - \lambda_i K'_{jj}) = 0, \tag{14}$$

where $\tilde{p}^{(i)\prime}_{(j)}$ is the corresponding submatrix of $\tilde{p}^{(i)\prime}$, clearly identical with the solution of the equation

$$\tilde{p}'_{(j)} (W'_{jj} - \lambda K'_{jj}) = 0 \tag{15}$$

for $\lambda = \lambda_i$.

From equality (12) it follows that for this case

$$\tilde{p}^{(i)\prime}_{(j)} = \tilde{p}^{(i)} R_j. \tag{16}$$

The following equation, obtained by differentiating identity (4),

$$(W - \lambda_i K) \frac{dr^{(i)}}{dt} - K r^{(i)} \frac{d\lambda_i}{dt} = -\left(\frac{dW}{dt} - \lambda_i \frac{dK}{dt}\right) r^{(i)}, \tag{17}$$

forms the initial equation for determining the frequency and form derivatives of a given vibration with respect to a parameter t on which the matrices W and K depend.

For the determination of $d\lambda_i/dt$ in the case of nondegenerate vibrations, we multiply both sides of Eq. (17) with the column matrix $\tilde{p}^{(i)}$ which occurs in identity (10). We then obtain

$$\tilde{p}^{(i)} K r^{(i)} \frac{d\lambda_i}{dt} = \tilde{p}^{(i)} \left(\frac{dW}{dt} - \lambda_i \frac{dK}{dt}\right) r^{(i)}. \tag{18}$$

But from formula (5) it follows that

$$r^{(i)} = R r^{(i)\prime} = R_j r^{(i)}_{(j)\prime}, \tag{19}$$

and from formula (12),

$$\tilde{p}^{(i)} = \tilde{p}^{(i)\prime} R^{-1} = \tilde{p}^{(i)}_{(j)} (R^{-1})_j. \tag{20}$$

We have, therefore,

$$\tilde{p}^{(i)} K r^{(i)} = \tilde{p}^{(i)\prime}_{(j)} K'_{jj} r^{(i)}_{(j)\prime}, \tag{21}$$

$$\tilde{p}^{(i)} \left(\frac{dW}{dt} - \lambda_i \frac{dK}{dt}\right) r^{(i)} = \tilde{p}^{(i)\prime}_{(j)} \left(\frac{dW'_{jj}}{dt} - \lambda_i \frac{dK'_{jj}}{dt}\right) r^{(i)}_{(j)\prime}, \tag{22}$$

if we take into account the relations,

$$\frac{dW'_{ij}}{dt} = (R^{-1})_i \frac{dW}{dt} R_j; \quad \frac{dK'_{ij}}{dt} = (R^{-1})_i \frac{dK}{dt} R_j \; (i, j = 1, 2, \ldots, m). \tag{23}$$

Solving Eq. (18) for $d\lambda_i/dt$ and taking formulas (21) and (22) into account, we find

$$\frac{d\lambda_i}{dt} = \frac{\tilde{p}^{(i)\prime}_{(j)} \left(\frac{dW'_{jj}}{dt} - \lambda_i \frac{dK'_{jj}}{dt}\right) r^{(i)}_{(j)\prime}}{\tilde{p}^{(i)\prime}_{(j)} K'_{jj} r^{(i)}_{(j)\prime}}. \tag{24}$$

The evaluation of the column matrix $\overline{r}^{(i)}_{(j)}{}'$ can be carried out without difficulty with the same scheme of computation as was used for the evaluation of $r^{(i)}_{(j)}$ (cf. reference 3); this scheme occurs in the last step of the iteration process for evaluating λ_j, when the "method of increasing precision of the roots...'[1], [2] is used. If the matrices W'_{jj} and K'_{jj} are symmetrical, then $\overline{r}^{(i)}_{(j)}{}' = r^{(i)}_{(j)}{}'$, and both formula (24) and the calculation involved in it are correspondingly simplified.

If $dr^{(i)}/dt$ is also to be evaluated (to determine the derivative of the form of the vibration with respect to t), then, multiplying both sides of Eq. (17) with R^{-1} and using the column matrix $r^{(i)\prime}$ and the relation

$$\frac{dr^{(i)\prime}}{dt} = R^{-1}\frac{dr^{(i)}}{dt}, \tag{25}$$

we obtain

$$(W' - \lambda_i K')\frac{dr^{(i)\prime}}{dt} - K' r^{(i)\prime}\frac{d\lambda_i}{dt} = -\left(\frac{dW'}{dt} - \lambda_i\frac{dK'}{dt}\right) r^{(i)\prime}, \tag{26}$$

where

$$\frac{dW'}{dt} = R^{-1}\frac{dW}{dt}R; \quad \frac{dK'}{dt} = R^{-1}\frac{dK}{dt}R. \tag{26a}$$

Taking into account the stepped form of the matrix $W' - \lambda K'$ and the form of the column matrix $r^{(i)\prime}$ we can represent Eq. (26) for the case of nondegenerate vibrations by the following set of equations:

$$(W'_{jj} - \lambda_i K'_{jj})\frac{dr^{(i)\prime}_{(j)}}{dt} - K'_{jj} r^{(i)\prime}_{(j)}\frac{d\lambda_i}{dt} = -\left(\frac{dW'_{jj}}{dt} - \lambda_i\frac{dK'_{jj}}{dt}\right) r^{(i)\prime}_{(j)}, \tag{27}$$

$$(W'_{kk} - \lambda_i K'_{kk})\frac{dr^{(i)\prime}_{(k)}}{dt} = -\left(\frac{dW'_{kj}}{dt} - \lambda_i\frac{dK'_{kj}}{dt}\right) r^{(i)\prime}_{(j)} \quad (k \neq j), \tag{28}$$

where $dr^{(i)}_{(j)}/dt$ and $dr^{(i)\prime}_{(j)}/dt$ are corresponding submatrices of the matrix $dr^{(i)\prime}/dt$.

To solve Eq. (27) we put $dr^{(i)}_{1}{}'/dt = 0$ and represent the equation by the set of two equations

$$w^{(i)}\frac{dr^{(i)0}_{(j)}}{dt} - K_1 r^{(i)\prime}_{(j)}\cdot\frac{d\lambda_i}{dt} = -f^{(i)}_{(j)1} \tag{29}$$

$$W^{(i)}\frac{dr^{(i)0}_{(j)}}{dt} - K_2 r^{(i)\prime}_{(j)}\cdot\frac{d\lambda_i}{dt} = -f^{(i)0}_{(j)}, \tag{30}$$

where K_1 is the first row of the matrix K'_{jj}, K_2 is the rectangular matrix obtained by deleting the first row of the matrix K'_{jj}, $f^{(i)0}_{1}$ is the column matrix obtained by discarding the first element $f^{(i)}_{k1}$ of the column matrix,

$$f^{(i)}_{(j)} \equiv \left(\frac{dW'_{jj}}{dt} - \lambda_i\frac{dK'_{jj}}{dt}\right) r^{(i)\prime}_{(j)}; \tag{30a}$$

$dr^{(i)0}_{(j)}/dt$ is the column matrix obtained by discarding the first element $dr^{(i)}_{1}{}'/dt$ of the column matrix $dr^{(i)}_{(j)}{}'/dt$, $v^{(i)\prime}$ is the first row of the matrix $W'_{jj} - \lambda_i K'_{jj}$ without its first element, and $W^{(i)}$ is the quadratic matrix obtained by discarding the first column and the first row of the matrix $W'_{jj} - \lambda_i K'_{jj}$.

Solving the set of equations (29) and (30) we obtain

$$\frac{d\lambda_i}{dt} = \frac{f^{(i)}_{(j)1} - v^{(i)\prime}W^{(i)-1}f^{(i)0}_{(j)}}{K_1 r^{(i)\prime}_{(j)} - v^{(i)\prime}W^{(i)-1}K_2 r^{(i)\prime}_{(j)}}, \tag{31}$$

$$\frac{dr^{(i)0}_{(j)}}{dt} = -W^{(i)-1}f^{(i)0}_{(j)} + W^{(i)-1}K_2 r^{(i)\prime}_{(j)}\frac{d\lambda_i}{dt}. \tag{32}$$

To evaluate $d\lambda_i/dt$ and $dr^{(i)}_{(j)}{}'/dt$ with these formulas it is necessary to find first of all the column matrices $W^{(i)-1}K_2 r^{(i)}_{(j)}{}'$ and $W^{(i)-1}f^{(i)0}_{(j)}$. This is not difficult to do with the computation scheme used in the last step of the iteration process which leads to the evaluation of λ_i and $r^{(i)}_{(j)}{}'$, if the "method of increasing precision of the roots..."[1], [2] is used.

If in addition we calculate $dr^{(i)}_{(j)}{}'/dt$ for $k \neq j$ from Eq. (28), which is always possible since in the case of nondegenerate vibrations $|W'_{kk} - \lambda_i K'_{kk}| \neq 0$, we can construct $dr^{(i)\prime}/dt$ and then we can obtain $dr^{(i)}/dt$ from the formula

$$\frac{dr^{(i)}}{dt} = R\frac{dr^{(i)\prime}}{dt}. \tag{33}$$

The problem is simplified if the variation of the parameter t does not destroy the symmetry of the molecule, since in this case the symmetry of the matrices dW/dt and dK/dt is the same as the symmetry of the matrices W and K. At the same time dW'/dt and dK'/dt also appear as stepped matrices with the same structure as W' and K', and consequently $dW'_{kj}/dt = 0$ and $dK'_{kj}/dt = 0$ $(k \neq j)$.

In this case it is evident that

$$\frac{dr^{(i)\prime}_{(k)}}{dt} = 0 \quad (k \neq j) \tag{34}$$

and formula (33) goes over into

$$\frac{dr^{(i)}_{(j)}}{dt} = R_j\frac{dr^{(i)\prime}_{(j)}}{dt}. \tag{35}$$

We will now consider the case of degenerate vibrations.

As was shown above, to the l-fold degenerate vibrations there correspond l identical blocks of the matrix W' and the same number of corresponding blocks of the matrix K'. Without limiting the generality we will consider them to be the first blocks and will designate them $W'_{j1}, W'_{j2}, \ldots W'_{jl}$ and $K'_{j1}, K'_{j2}, \ldots K'_{jl}$, respectively. If λ_i refers to an l-fold degenerate vibration, the corresponding solution of Eq. (1) has the form

$$r^{(i)} = \sum_{\alpha=1}^{l} c_\alpha r^{(\alpha)}, \tag{36}$$

where the c_α $(\alpha = 1, 2, \ldots, l)$ are arbitrary numbers.

Consequently the column matrix $r^{(i)\prime}$, which enters into Eq. (26), on the basis of formula (5) has the form

$$r^{(i)\prime} = \sum_{\alpha=1}^{l} c_\alpha R^{-1} r^{(\alpha)} = \sum_{\alpha=1}^{l} c_\alpha r^{(\alpha)\prime}, \tag{37}$$

where

$$r^{(\alpha)\prime} = R^{-1} r^{(\alpha)} \quad (\alpha = 1, 2, \ldots, l). \tag{38}$$

The column matrix $r^{(\alpha)}$ can always be chosen so that in each of the submatrices $r^{(\alpha)\prime}$, which are determined by formulas (38), elements different from zero occur only in the submatrix $r^{(\alpha)\prime}_{(\alpha)}$. For this it suffices to put

$$r^{(\alpha)} = R_\alpha r^{(\alpha)\prime} \quad (\alpha = 1, 2, \ldots, l), \tag{39}$$

where $r^{(\alpha)\prime}$ is the solution of Eq. (8) with $\lambda = \lambda_i$ (for $j = 1, 2, \ldots l$).

If we use in Eq. (26) the column matrix $r^{(i)\prime}$, determined by relations (37) and (39), we obtain from this equation the following set of equations

$$(W'_{jj} - \lambda_i K'_{jj})\frac{dr^{(i)\prime}_{(j)}}{dt} - c_j K'_{jj} r^{(i)\prime}\cdot\frac{d\lambda_i}{dt} = -\sum_{\alpha=1}^{l} c_\alpha\left(\frac{dW'_{j\alpha}}{dt} - \lambda_i\frac{dK'_{j\alpha}}{dt}\right) r^{(\alpha)\prime}, \tag{40}$$

$$(j = 1, 2, \ldots, l)$$

$$(W'_{jj} - \lambda_i K'_{jj}) \frac{d\lambda_i^{(j)}}{dt} = -\sum_{\alpha=1}^{l} c_\alpha \left(\frac{dW'_{j\alpha}}{dt} - \lambda_i \frac{dK'_{j\alpha}}{dt} \right) r_i^{(j)} \quad (j > l). \quad (41)$$

If the variation of the parameter t does not destroy the symmetry of the molecule, Eqs. (40) and (41) are simplified and take the respective forms,

$$(W'_{jj} - \lambda_i K'_{jj}) \frac{d\lambda_i^{(j)}}{dt} - c_j K'_{jj} \lambda_i^{(j)} \frac{d\lambda_i}{dt} = -c_j \left(\frac{dW'_{jj}}{dt} - \lambda_i \frac{dK'_{jj}}{dt} \right) r_i^{(j)}, \quad (42)$$

$$(j = 1, 2, \ldots, l)$$

$$(W'_{jj} - \lambda_i K'_{jj}) \frac{d\lambda_i^{(j)}}{dt} = 0 \quad (j > l). \quad (43)$$

In this case not only are all the matrices $W'_{jj} - \lambda_i K'_{jj}$ ($j = 1, 2, \ldots l$) equal to one other, but also all the matrices $(dW'_{jj}/dt) - \lambda_i (dK'_{jj}/dt)$ ($j = 1, 2, \ldots l$) are equal to one other. Therefore, Eqs. (42), corresponding to different values of the index j ($j = 1, 2, \ldots l$), differ from one another only in the designation of the unknowns, $dr_\beta^{(j)\prime}/dr$, and in the designation of the arbitrary constant, c_j. It follows that the solutions of all these equations coincide apart from the normalization of the $dr_\beta^{(j)\prime}/dt$ and can be obtained from any one of them. Moreover, for $j > l$, relation (34) holds.

Since we are not considering here (or in the following) accidental degeneracy, it is possible to find $d\lambda_i/dt$ and $dr_\beta^{(j)\prime}/dt$ from one of the Eqs. (42) by the methods given above, namely: if only $d\lambda_i/dt$ is to be found, one can use formula (24); if both $d\lambda_i/dt$ and $dr^{(j)}/dt$ are to be evaluated, one can use formulas (31) and (32), and then formula (33).

If the variation of the parameter t destroys the symmetry of the molecule, in order to find $d\lambda_i/dt$ and $dr^{(j)\prime}/dt$ it is necessary to solve Eqs. (40) and (41) directly. In this case equations in (40), corresponding to different indices j ($j = 1, 2, \ldots l$), differ from one another also in their free terms.

Each of the Eqs. (40) has a solution for arbitrary values of the constants c_α ($\alpha = 1, 2, \ldots l$) (if $c_j \neq 0$), and these solutions, and thus also the $d\lambda_i/dt$, depend on the choice of the c_α ($\alpha = 1, 2, \ldots l$). In order that the values of $d\lambda_i/dt$ determined from Eqs. (40) be the same for different values of j ($j = 1, 2, \ldots l$), that is, in order that Eqs. (40) be compatible, it is necessary that there exist specific relations between the c_α ($\alpha = 1, 2, \ldots l$).

Actually, the calculation of $d\lambda_i/dt$ from each of the Eqs. (40) gives

$$\frac{d\lambda_i}{dt} = \frac{\sum_{\alpha=1}^{l} c_\alpha p_i^{(j)\rho} \left(\frac{dW'_{j\alpha}}{dt} - \lambda_i \frac{dK'_{j\alpha}}{dt} \right) r_i^{(j)\rho}}{c_j p_i^{(j)\rho} K'_{jj} r_i^{(j)\rho}}, \quad (44)$$

where $\overline{p}^{(j)\prime\prime}$ is the column matrix satisfying Eq. (15) with $\lambda = \lambda_i$.

Formula (44) gives identical results for different values of j ($j = 1, 2, \ldots l$) only if the relations

$$\frac{\sum_{\alpha=1}^{l} c_\alpha p_i^{(j)\rho} \left(\frac{dW'_{1\alpha}}{dt} - \lambda_i \frac{dK'_{1\alpha}}{dt} \right) r_i^{(j)\rho}}{c_1} = \ldots = \ldots = \frac{\sum_{\alpha=1}^{l} c_\alpha p_i^{(j)\rho} \left(\frac{dW'_{l\alpha}}{dt} - \lambda_i \frac{dK'_{l\alpha}}{dt} \right) r_i^{(j)\rho}}{c_l}. \quad (45)$$

are satisfied.

The conditions (45) define the values of c_α ($\alpha = 1, 2, \ldots l$), for which Eqs. (40) are compatible. Since these conditions are homogeneous with respect to all the c_α, one of the c_α can be chosen arbitrarily. Thus, conditions (45) will give $l - 1$ equations of the second degree in the $l - 1$ unknowns. By solving these equations it is possible to find the required values of c_α, and then, by formula (44), the values of $d\lambda_i/dt$ which correspond to them. If the $dr^{(j)}/dt$ are to be found in addition, one must determine $dr^{(j)\prime}/dt$ from Eqs. (40) and (41) with the known values of c_α ($\alpha = 1, 2, \ldots l$) and the corresponding values of $d\lambda_i/dt$, and then obtain $dr^{(j)}/dt$ from formula (33).

In the practical application of the various methods considered above for the calculation of derivatives one should keep in mind the following.

If the symmetry of the molecule is not destroyed in the variation of the parameter t, dW'_{jj}/dt and dK'_{jj}/dt are obtained from the matrices dW/dt and dK/dt, respectively, in the same way as W'_{jj} and K'_{jj} are obtained from the matrices W and K (cf., for example, reference 4). If, however, the symmetry of the molecule changes when the parameter t is varied, it is necessary to use the general relations (23). In this one must keep in mind that if the matrix R is orthogonal, then $(R^{-1})_j = \overline{R}_j$. If on the other hand R is not orthogonal, then it is easy to obtain $(R^{-1})_j$ from $\overline{R}_j$ by using chemical coordinates; however, we will consider this in greater detail elsewhere.

For the evaluation of the derivative of the vibrational frequency with respect to the parameter t one must use the obvious relation

$$\frac{d\omega_i}{dt} = \frac{1}{2\omega_i} \cdot \frac{d\lambda_i}{dt}. \quad (46)$$

The definitive formula for calculations with a specific parameter t can be reduced to some form more practical for computation (cf. reference 3).

For the calculation of the derivative of the vibrational form with respect to the parameter t it is necessary to relate $dr^{(j)}/dt$ to the required derivative. Specifically, if $W = T^{-1}U$ and $K = E$, where T^{-1} is the matrix of the kinematic coefficients, U the matrix of the forces coefficients, and E the unit matrix, the calculation of $dr^{(j)}/dt$ gives the required derivative directly. We note that in this case the formulas derived above are correspondingly simplified. Moreover, if U'_{jj} and $(T^{-1})'_{jj}$ are symmetrical matrices, it is not difficult to show that the matrices $\overline{p}_\beta^{(j)\prime}$ and $\overline{p}^{(j)\prime\prime}$ are connected (except for some factor) with the matrices $r_\beta^{(j)\prime}$ and $r^{(j)\prime\prime}$ by the relations

$$p_\beta^{(j)\rho} = \lambda_j^{(j)} U'_{j\beta}, \quad (47)$$

$$p^{(j)\rho} = r^{(j)\rho} U'_{jj}. \quad (48)$$

These relations can also serve as an auxiliary control on the accuracy of a calculation of $\overline{p}_\beta^{(j)\prime}$ and $\overline{p}^{(j)\prime\prime}$ directly from the computation scheme (the computational work involved using the computation scheme and using relations (47) and (48) is identical). Similar relations can be set up also for the case in which U'_{jj} and $(T^{-1})'_{jj}$ are not symmetrical matrices. However, we will not dwell on this question here.

REFERENCES

1. L. S. Mayants. Doklady Akad. Nauk SSSR 50, 121 (1945).

2. L. S. Mayants. Doctoral dissertation, Fiz. Inst. Akad. Nauk, Moscow, 1947; Trudy Fiz. Inst. Akad. Nauk 5, 63 (1950).
3. L. S. Mayants. Opt. i Spektr. 5, 378 (1958).
4. L. S. Mayants. Zhur. Eksptl. i Teoret. Fiz. 25, 393 (1953).

PHOTOELECTRIC INVESTIGATION OF RAMAN SPECTRA OF GASES AT LOW PRESSURES

P. A. Bazhulin and Iu. A. Lazarev

Received 22 June 1959

The line shapes and widths of rotational and rotational-vibrational spectra of the simple gases H_2, O_2, N_2, CO_2, and CH_4 were investigated over the pressure interval of 1-10 atm, using a photoelectric method. The effective optical cross sections of the gases H_2, O_2, N_2, and CO_2 were calculated from the magnitude of line broadening of rotational Raman spectra.

Lately, papers have been systematically appearing in the literature on the detailed investigation of Raman spectra of vapors and gases at low pressures, near atmospheric, using instruments of high dispersion and resolution.[1, 2]

Such investigations have become possible only recently, due to the development of cooled high-intensity mercury arcs with[1, 2] highly efficient, multiple-reflection mirror cells.[2] (See also reference 33.)

Most investigators have restricted themselves to frequency analysis. Such results give extensive information concerning the molecule, particularly about its dynamics and structure, and permit highly precise calculation of interatomic distances. Unfortunately, very few investigators have attempted the measurement of integrated intensities and polarizations of vibrational lines.[4, 5]

Up till now, investigations of line shapes and widths in Raman spectra of gases at low pressures have been almost completely absent from the literature, This is obviously due to the existence of serious experimental difficulties. However, the study of this very parameter as as a function of the structure of the molecule, type of vibration, temperature, pressure, and state of aggregation would make it possible to solve one of the most important problems in molecular spectroscopy; namely, the nature of line-width in Raman spectra. The question of the nature of line-width has been raised by many authors.[4, 6-8, 34] Very thorough experimental investigations of Raman spectra of the gases N_2 and O_2 at high pressures have been performed recently by Mikhailov,[9, 10] who showed in particular that the line-width in the vibrational spectrum changes very little between 10 and 100 atm, and that the observed shape of these lines can be explained by a splitting of the Q branch due to vibration-rotation interaction. However, up till now, the question of the nature of line-width in Raman spectra has remained unsolved.

It is therefore of considerable interest to perform further detailed investigations, beginning with the simplest nonpolar molecules whose structure is well-known and whose molecular constants have been accurately measured at pressures close to atmospheric, so that molecular interaction can either be neglected or corrected for.

METHOD OF MEASUREMENT

Until recently, Raman spectra of gases were investigated photographically. The inadequate resolution of photographic plates forced the use of instruments with high linear dispersion and, as a rule, of low speed, thus leading to long exposure times (several tens of hours) and necessitating a large number of precautions.[2]

It is only relatively recently that papers have appeared in the literature[5, 11] with detailed descriptions of photoelectric methods of measuring the integrated intensity of lines in the vibrational Raman spectra of gases at low pressures.

We have constructed an instrument which allowed us to record spectra photoelectrically, and to measure the intensities, widths, and shapes of the rotational and vibrational lines in the Raman spectra of vapors and gases between 1 and 10 atm at 30-250°C. SKF-32 and SKF-26 fluorinated plastics were used for the gaskets because of their high chemical and thermal stability. The apparatus consisted of the following principal components: (a) DFS-4 spectrometer with a plane reflection grating of 1200 lines/mm, linear dispersion 6.4 A/mm and relative aperture 1:10; (b) a multiple-reflection gas cell, 600 mm long and 40 mm in diameter, with a mirror and two focusing condensers; (c) two, cooled-discharge, low-pressure mercury lamps 600 mm long; (d) protective housing sprayed on the inside with MgO. The mirrors of the cell were made of a dielectric with a coefficient of reflection not less than 95% in the region 4000-5000 A. In some experiments we used aluminized mirrors whose coefficient of reflection in this region was 90%. The working current through the lamps never exceeded 25 amp. An FEU-17 photomultiplier specially selected for the highest signal-noise ratio[12] was used as the detector. The working voltage across the photomultiplier was 600 volts, its dark current was $2\text{-}3 \times 10^{-13}$ amp; and the useful signal current was 10^{-12}-10^{-11} amp. The voltage was supplied to the FEU-17 by batteries.

The objects of our investigation were the simple gases H_2, O_2, N_2, CO_2, and CH_4 in the pure state, and as mixtures with inert gases (Ar, He). The gases were taken from commercial-grade cylinders and purified by passage through silica gel. In the case of CH_4, the purification was more careful. The cartridge containing the silica gel was immersed in liquid nitrogen, and the liquefied methane was then slowly transferred into the cell until the required pressure was obtained.

The spectral slit-widths used in recording the rotational spectra of the gases were of the order of 0.5-0.6 cm^{-1}; in the registration of vibrational spectra (Q-branch) the slit-widths were 0.3-1.5 cm^{-1}, and in the recording of rotational-vibrational spectra (Q, P, R, S-branches) they were 2-3 cm^{-1}. In all cases, the exit slit-width was equal to the entrance slit-width. The half-width of the slit function measured at slit-widths of 0.1 cm^{-1} was 0.5-0.7 cm^{-1} (depending on the wavelength). The slit height used was 15 mm. The scanning rate was 3.5 cm^{-1}/min. The spectrogram of O_2 is shown in Fig. 1. The treatment of the observed band shapes and the calculation of true widths of the isolated simple lines were performed using methods described in references 8, 13, and 14, utilizing Voigt's function. In the case of overlapping lines special methods,

partly described in references 14 and 15, were used.

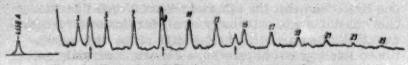

Fig. 1. Rotational Raman spectrum of gaseous oxygen at a pressure of 3 atm (slit—0.7 cm^{-1}). The dots correspond to the theoretically calculated distribution of intensity as function of frequency for the case of free rotation; the arrows indicate grating ghosts.

EXPERIMENTAL RESULTS AND DISCUSSION

Rotational spectra. The study of pure rotational spectra shows that the true shape of a single rotational component approximates the dispersion shape, and that the true width of a rotational component is a linear function of pressure. Starting with the collision theory of broadening[16-18] the intensity distribution across the line profile is given by the expression

$$I(\omega) = \frac{\gamma/2}{(\omega - \omega_0)^2 + (\gamma/2)^2},$$

and the line-width, for a homogeneous gas, is given by

$$\gamma = \frac{z}{\pi} = 0.5\frac{pd^2}{\sqrt{\mu T}},$$

where z is the number of collisions per second, p is the gas pressure (in atm), d is the effective optical collisional cross section (A), μ is the molecular weight, and T is the absolute temperature (with γ expressed in cm^{-1}). For a mixture of gases,

$$\gamma_1 = 0.5\frac{p_1 d_{11}^2}{\sqrt{\mu_1 T}} + 0.5\sqrt{\left(\frac{1}{\mu_1} + \frac{1}{\mu_2}\right)\frac{1}{2T}}\, p_2 d_{12}^2,$$

where p_1, d_{11} and μ_1 are the above-mentioned variables for the main gaseous component, and p_2, d_{12}, and μ_2 are the corresponding quantities for the added component.

The slope of the straight-line plot of true width as a function of pressure permits the calculation of the effective optical cross section (see Fig. 2 and Table 1). Within the limits of experimental error, there does not seem to be any dependence of the optical cross section (or the line-width) on the rotational quantum number j.

Table 1. Optical Cross Sections (in A) of Various Gases, Obtained from Broadening of Lines in the Rotational Spectrum at T = 300°K

Literature source	O_2	O_2+Ar	O_2+He	N_2	N_2+Ar	CO_2	CO_2+Ar	H_2
Our data	4.2	3.9	2.2	4.1	3.8	9	6	<1
Data from reference 10	4.5	—	—	5.4	—	—	—	—
Data from reference 19	4.35	3.57	—	—	—	—	—	—

The rotational line-widths for N_2 at p = 5 atm coincide with the ones obtained by Iozenas (Moscow State University) using a photographic method.

The effective optical cross section of oxygen (see Table 1) which we obtained from the rotational Raman spectrum between 1 and 10 atm is in good agreement with the value obtained by Mikhailov from the rotational Raman spectrum between 10 and 100 atm,[19] and with the cross section obtained by Andersen from the rotational microwave spectrum of O_2 (magnetic absorption) between 0.1 and 12 mm Hg.[19]

Table 2 gives the values of the gas-kinetic collisional cross sections. As can be seen from the results given, the largest deviation of the optical cross section from the gas-kinetic cross section occurs in the case of H_2, where the probability of energy transfer from the translational degree of freedom to the rotational one is very small,[20] and in the case of CO_2, where intermolecular attraction forces are stronger than in the other gases investigated.

Table 2. The Gas-Kinetic Collisional Cross Sections (in A) of Various Gases at T = 300°K[22]

H_2	O_2	N_2	CO_2	Ar	He	CH_4
2.7	3.6	3.7	4.5	3.6	2.1	4.1

Rotational wings of rotational-vibrational bands. Since the intensity of the rotational component of the rotational-vibrational bands is about two orders of magnitude smaller than that of the lines in the pure rotational spectrum, its registration is much more difficult, and the line-width measurement even more so. Nevertheless, we were able to obtain the rotational-vibrational spectra of oxygen and methane at 10 atm, and evaluate the half-width of the rotational-vibrational component (see Fig. 3). The line half-widths given in Table 3 are the averages of 4 or 5 spectrograms and correspond to transitions from the most populated levels.

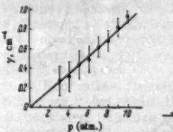

Fig. 2

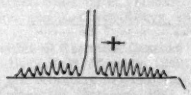

Fig. 3

Fig. 2. Plot of the half-width of lines in the rotational spectrum of oxygen, as a function of pressure.
Fig. 3. The rotational-vibrational spectrum of oxygen at 10 atm pressure (slit, 3 cm^{-1}).

In the case of O_2, comparison with the pure rotational spectrum taken at 10 atm shows that the width of the rotational components of the rotational-vibrational lines is three times greater than the width of lines of the pure rotational spectrum. This is apparently due to the greater optical cross section in the excited vibrational state.

Table 3. The Half-Widths of the Rotational Components (in cm^{-1}) of the Rotational-Vibrational Lines of Various Gases at 10 atm

O_2	$\nu_3 CH_4$	$\nu_4 CH_4$
3±1	≤1.5	≤2

Q-branches of rotational-vibrational bands. Treatment of the vibrational spectra led to the following results: (a) all broad lines are asymmetric, either toward the ultraviolet or the infrared; (b) the shape and width of the strongly polarized lines (H_2, O_2, N_2, CO_2 (ν_1 and $2\nu_2$)) (1-10 atm) are independent of pressure within the limits of experimental error (±0.2 cm^{-1}) over the range of pressures investigated.

It is known from the theory of molecular spectra[7,21,22] that Q-branches are complex bands consisting of separate components, which are usually (except in the case of H_2) unresolvable experimentally. For simple molecules whose parameters (such as the rotational constant, vibrational-rotational interaction constants, statistical weights of rotational levels, etc.) are known, it is possible to calculate the splitting of the Q-branch and the distribution of intensity within the individual components. Assuming a dispersion shape for each separate component, knowing the width and shape of the slit function* with which the vibrational spectra were recorded, and taking into consideration the overlap of separate components, it is possible to construct the shape of the Q-band envelope. Furthermore, by varying the width of an individual component and comparing the calculated shape with the observed one, it is possible to evaluate the true width of a component. In the case of H_2, the Q-branch components are fully resolved, thus permitting direct measurement of their widths. Figure 4 shows a comparison of the calculated and observed shapes. Table 4 gives estimates of the true half-widths of components obtained at 10 atm.

*In our case, it was either a Gaussian function or Volgt's function (depending on the slit-width).

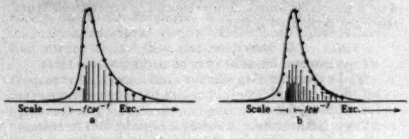

Fig. 4. Rotational-vibrational band shapes of oxygen (a), nitrogen (b), and methane (c). Line frequency (ν), half-width of the slit-function (α_{app}), and the true line half-width (δ_{true}) in cm^{-1}. (a), O_2; $\nu = 1580$, $\alpha_{app} = 1.6$, $\delta_{true} = 0.3$; (b), N_2; $\nu = 2330$, $\alpha_{app} = 1.4$, $\delta_{true} = 0.3$; (c), $\nu_2 CH_4$, $\nu = 1535$, $\alpha_{app} = 2.8$, $\delta_{true} = 1.5$. (Continuous line—observed shape at 10 atm pressure; points indicate the calculated envelope.)

It must be noted in particular that for the vibrational frequencies ν_1 and $2\nu_2$ of the CO_2 molecule, it was not possible to determine the half-width of either a single component nor of the whole Q-branch over the entire range of pressures investigated (1-10 atm) because of insufficient experimental accuracy. This was probably due to the fact that the vibrational-rotational interaction constants are extremely small for these two frequencies.[23] Estimates of the half-widths of the above-mentioned lines, given in reference 24, are apparently quite a bit too high.

Table 4. Degrees of Depolarization and Half-Widths of Lines of Various Gases

	H_2	O_2	N_2	CO_2		CH_4		
	Frequency (cm^{-1})							
	ν = 4160	ν = 1580	ν = 2330	ν_1 1389	$2\nu_2$ 1285	ν_3 2915	ν_2 1535	ν_3 3017
Degree of depolarization	0.05	0.11	0.1	0.05	0.08	0.00	Depol.	Depol.
Spectral slit-width (cm^{-1})	0.8	1	1	0.6	0.6	0.3	2	1
Half-width of the observed Q-branch (cm^{-1})	—	3	2.7	—	—	1.3	6.3	—
Calculated half-width of a single component of the Q-branch (cm^{-1}) (p-10 atm.)	<0.2	<0.3	<0.3	<0.2	<0.2	—	1.5 ± 0.7	—

In the case of the ν_2 vibration mode of CH_4, the moment of inertia in the excited state is less than that in the ground state,[25] and hence the Q-branch is degraded toward higher frequencies (as opposed to the cases of O_2 and N_2). The Q-branch of the ν_2 mode of CH_4 (corresponding to thrice-degenerate vibrations of the molecule), exhibits additional splitting due to removal of degeneracy as a result of Coriolis coupling of vibrations,[25,26] thus leading to the presence of a double maximum (see Fig. 5).

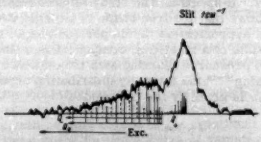

Fig. 5. Shape of the rotational-vibrational line of methane ($\nu_3 = 3018$ cm^{-1}) at 10 atm.

As a result of treatment and analysis of experimental results, it can be concluded that for linear and spherical top molecules, the following regularities are observed: (a) the asymmetry and width of the Q-band is completely explained by the splitting of the Q-branch due to vibrational-rotational interaction and Coriolis interaction of vibrations, thus supporting the conclusions of previous investigations;[7,9] (b) the true half-width of a single component of the Q-branch of strongly polarized lines is small in the pressure interval investigated, (less than 0.3 cm^{-1}) and the possibility of determining it is outside our experimental limits; (c) the single components of the Q-branch of the depolarized line ν_2 of CH_4, measured at 10 atm pressure, are broadened (1.5 cm^{-1}), as well as the rotational components of the vibrational-rotational wing.*

*Similar results were apparently obtained from infrared spectra in reference 27.

The general picture of the phenomenon is the following: if, at the instant of scattering, there occurs a transition into the excited vibrational state accompanied by a change in the magnitude of the rotational moment (rotational wings of the rotational-vibrational band) or only in its direction (Q-branch of anisotropic scattering), then the width of lines corresponding to the given transitions will exhibit an effect of the nature of the rotational motion of the molecule. On the other hand, if the transition into the excited vibrational state is not accompanied by change in neither the magnitude nor the direction of the rotational moment (Q-branch of the isotropic scattering), then the width of lines corresponding to such transitions will be independent of the nature of the rotational motion of the molecules. Thus, the great difference in the broadening of isotropic and anisotropic scattering must be due to the influence of collisions which inhibit the free rotation of molecules.

Let us examine the factors causing the broadening of lines in isotropic scattering. Experiments on dispersion and absorption of ultrasonic waves, as well as experiments on resonance fluorescence, show that in the case of simple molecules, the probability of energy transfer from the exterior (translational and rotational) de-

grees of freedom to the inner (vibrational) degrees of freedom is extremely small.[30] Thus, the lifetime of a vibrational level is rather long, as has been substantiated by direct measurements.[28]

Thus, inelastic collisions can not be an appreciable factor in the line broadening of vibrational spectra, at least in the molecules we studied.

In the general case, it is necessary to take into consideration the perturbing influence of elastic collisions. In particular, as was noted in references 29 and 30, even when the optical cross section is much smaller than the collisional gas-kinetic cross section, the broadening caused by the Doppler effect depends on the number of collisions. However, experiments with simple molecules not possessing a permanent dipole moment, such as O_2 and N_2[9,10] or CO_2[31] show that high pressure and even transition to the liquid phase (at constant temperature) do not appreciably affect the width of lines corresponding to isotropic scattering. This would seem to indicate that the perturbing influence of the intermolecular field on such vibrations is usually very small.

Hence, in the case of simple molecules not possessing a permanent dipole moment, the main factor which determines the large width of vibrational lines of Raman scattering in gases is the presence of rotational degrees of freedom (the presence of rotational-vibrational wings, splitting of Q-branches as a result of vibrational-rotational interaction and of Coriolis coupling of vibrations, broadening of lines due to hindrance of free rotation during collisions between molecules).

At present, unfortunately, there is no satisfactory quantum theory explaining the great difference in the broadening of lines in isotropic and anisotropic scattering. An attempt at quantum mechanical interpretation was made in reference 31. The authors there considered the broadening of lines in the anisotropic scattering as due to the removal of degeneracy of rotational levels (with regard to "m") in the intermolecular fields, but in explaining the small width of lines in the isotropic scattering, they assume, without sufficient basis, that the broadening of a single component of a rotational level is small.

It must be noted in this discussion that both the observed difference in line broadening in the isotropic and anisotropic scattering, and independence of line-width in the vibrational spectrum of the width of the rotational level, are apparently due to the fact that complete conservation of rotational energy in a vibrational transition* occurs only in the case of isotropic scattering.

*Disregarding any shift in the rotational level in the excited vibrational state due to vibrational-rotational interaction.

In conclusion, we would like to express our deep gratitude to I. I. Sobelman for his interest in our work and for valuable discussions.

REFERENCES

1. B. P. Stoicheff. Canad. J. Phys., 32, 630 (1954).
2. H. L. Welsh, E. J. Stansbury, J. Romanko, and T. Feldman. J. Opt. Soc. Am., 45, 338 (1955).
3. H. L. Welsh, C. Cumming, and E. J. Stansbury. J. Opt. Soc. Am., 41, 712 (1951).
4. H. L. Welsh, M. F. Crawford, T. R. Thomas, and G. R. Love. Canad. J. Phys., 30, 577 (1952).
5. T. Yoshino and H. J. Bernstein. J. Mol. Spec. 2, 213 (1958).
6. Kh. E. Sterin. Izvest. Akad. Nauk SSSR, Ser. Fiz. 14, 411 (1950).
7. I. I. Sobelman. Izvest. Akad. Nauk SSSR, Ser. Fiz. 17, 554 (1953).
8. M. M. Sushchinskii. Dokt. diss., Fiz. Inst. Akad. Nauk SSSR, 1957.
9. G. V. Mikhailov. Zhur. Eksptl. i Teoret. Fiz. 36, 1368 (1959).
10. G. V. Mikhailov. Zhur. Eksptl. i Teoret. Fiz., in press.
11. Ya. S. Bobovich and V. M. Pivovarov. Uspekhi Fiz. Nauk 60, 689 (1956);
V. M. Pivovarov and Ya. S. Bobovich. Opt. i Spektr. 6, 249 (1959).
12. N. O. Chechik, S. M. Fainshtein, and T. M. Lifshitz. "Electronic Photomultipliers". Gosudarst. Izd. Tekh.-Teoret. Lit., Moscow, 1957.
13. G. S. Landsberg, P. A. Bazhulin, and M. M. Sushchinskii. "The Fundamental Parameters of Raman Spectra of Hydrocarbons." Izd. Akad. Nauk SSSR, Moscow, 1956.
14. S. G. Rautian. Uspekhi Fiz. Nauk 66, 475 (1958).
15. B. K. Ablekov. Opt. i Spektr. 6, 562 (1959).
16. M. Born. "Optik" Gosudarst. Nauch. Tekh.-Fiz. Ukrainy, Kharkov-Kiev, 1937.
17. V. Vaiskopf. Uspekhi Fiz. Nauk 13, 552 (1933).
18. I. I. Sobelman. Uspekhi Fiz. Nauk 54, 551 (1952).
19. S. Anderson, W. V. Smith, and W. Gordy. Phys. Rev. 87, 561 (1952).
20. V. N. Kondratiev. "Kinetics of Chemical Gaseous Reactions." Izd. Akad. Nauk SSSR, Moscow, 1958.
21. G. Herzberg. "Spectra and Structure of Diatomic Molecules." Izd. Inostrannoi Lit., Moscow, 1949.
22. G. Herzberg. "Vibrational and Rotational Spectra of Polyatomic Molecules." Izd. Inostrannoi Lit., Moscow, 1949.
23. B. P. Stoicheff. Canad. J. Phys., 36, 218 (1958).
24. H. L. Welsh, P. E. Poshler, and B. P. Stoicheff. Canad. J. Phys., 30, 99 (1952).
25. T. Feldman, J. Romanko, and H. L. Welsh. Canad. J. Phys., 33, 138 (1955).
26. B. P. Stoicheff, C. Cumming, G. E. John, and H. L. Welsh. J. Chem. Phys., 20, 498 (1952).
27. G. N. Zhizhin. Thesis, Moskov. Fiz.-Tekh. Inst., 1959.
28. P. V. Slobodskaya. Izvest. Akad. Nauk SSSR, Ser. Fiz. 12, 656 (1948).
29. I. I. Sobelman. Kand. diss., Inst. Fiz. Akad. Nauk SSSR, 1955.
30. V. L. Ginsburg. Doklady Akad. Nauk SSSR 30, 397 (1941).
31. M. F. Crawford, H. L. Welsh, and J. H. Harrold. Canad. J. Phys., 30, 81,(1952).
32. Landolt-Börnstein. b. 1, T. I, S. 369, 1950.
33. V. I. Tiulin and V. M. Tatevskii. Opt. i Spektr. 2 820 (1957).
34. N. I. Rezaev. Vestnik Moskov Univ. 2, 145 (1957).

TOTAL LUMINESCENCE BRIGHTNESS OF ZnS-Cu AND ZnS-Cu,Mn ELECTROLUMINOPHORS IN A PULSATING FIELD

G. S. Kozina and L. P. Poskacheeva

Received 25 May 1959

Measurements of the luminescence brightness of yellow and green electroluminophors in a pulsating field are presented. The electroluminescence brightness of yellow luminophors in this mode of operation exceeds the luminescence brightness of the same layers in a bipolar field by several fold. The brightness of green luminophors in a pulsating field is somewhat lower than their brightness in a bipolar field. The variation of brightness is connected with the occurrence of an appreciable conduction current through the layer. The increase of brightness is explained by the joint effects of electroluminescence in dc and alternating fields.

According to data in the literature,[1,2] the electroluminescence brightness of layers made of "green" ZnS electroluminophors decreases when the layers are subjected to a pulsating unipolar voltage (in contrast to the brightness in an alternating bipolar field). At present, the authors do not know of any similar data for layers of "yellow" ZnS-Cu,Mn luminophors. The following results show variation of the total luminescence brightness of green and yellow electroluminophors for sinusoidal and square pulses.

METHOD OF MEASUREMENT

An electroluminescent layer 100 μ thick was prepared by applying a (pulverized) mixture of the luminophor and a dielectric material to a glass plate with a transparent conducting film (one of the electrodes). An aluminum layer, vapor-deposited in vacuum, was used for the second electrode. An alternating voltage of square or sinusoidal form was applied to the electrodes, or this alternating voltage was superimposed on a constant (dc) voltage equal to the amplitude of the alternating voltage, thus creating a pulsating voltage. The essential electrical diagram of the arrangement is shown in Fig. 1.

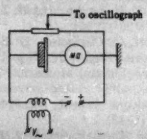

Fig. 1. Electrical diagram for measurement of electroluminescence in alternating and pulsating fields.

The voltage was controlled with the aid of an oscilloscope, and the brightness measured with a selenium cell whose sensitivity was corrected by a light filter in accordance with the visibility curve.

ELECTROLUMINESCENCE BRIGHTNESS OF YELLOW ZnS-Cu,Mn LUMINOPHORS WITH BIPOLAR AND UNIPOLAR VOLTAGE SUPPLY

The dependence of the electroluminescence brightness of yellow electroluminophor layers on the amplitude of an alternating square voltage for two frequencies is shown in Fig. 2. In the same figure, we show the variation of the conductivity current I when a pulsating voltage is applied to the layer.

Figure 2 shows that the brightness values for the two modes of operation coincide at small amplitudes (100-200 volts). At high voltages, the brightness in the pulsating mode exceeds the brightness in the alternating field. This difference in brightness occurs at the same voltage values for which the conductivity current increases sharply. At about 300 volts, the brightness of the layer in the unipolar mode exceeds the brightness of this layer in the alternating field by 2.7 times at 500 cps and by 6 times at 100 cps.

An analogous picture is observed when the voltage is sinusoidal (Fig. 3). At about 250 volts and a conductivity current of 490 μamp the brightness in the unipolar field exceeds the luminescence brightness in the alternating field by 2.3 times at a frequency of 1000 cps and 5 times at a frequency of 100 cps.

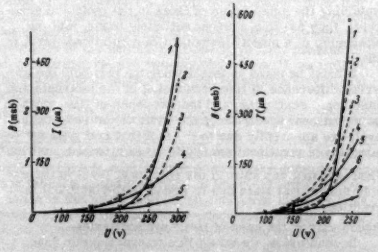

Fig. 2

Fig. 3

Fig. 2. Dependence of conductivity current I (curve 1) and luminescence brightness B of a yellow electroluminophor in bipolar (curves 4, 5) and pulsating (curves 2, 3) fields on the voltage of a square waveform at various frequencies. Frequencies (in cps): curves 1, 3, 5—100; curves 2, 4—500.

Fig. 3. Dependence of conductivity current I (curve 1) and luminescence brightness B of a yellow electroluminophor in bipolar (curves 5, 6, 7) and pulsating (curves 2, 3, 4) fields on sinusoidal voltage at various frequencies. Frequencies in (cps): curves 1, 4, 7—100; curves 3, 6—500; curves 2, 5—1000.

ELECTROLUMINESCENCE BRIGHTNESS OF GREEN ZnS-Cu LUMINOPHORS WITH BIPOLAR AND UNIPOLAR VOLTAGE SUPPLY

In Fig. 4 we present the dependence of the electroluminescence brightness of green luminophors on the amplitude of a sinusoidal bipolar and a pulsating unipolar voltage. Curves for three frequency values were obtained: 100, 500, and 100 cps. In the same Figure, curve 1 shows the conductivity current in the presence of a pulsating voltage.

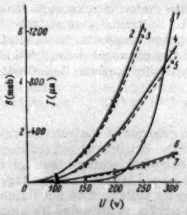

Fig. 4. Dependence of conductivity current I (curve 1) and luminescence brightness B of a green electroluminophor in bipolar (curves 2, 4, 6) and pulsating (curves 3, 5, 7) fields on sinusoidal voltage at various frequencies. Frequencies (in cps): curves 1, 6, 7—100; curves 4, 5—500; curves 2, 3—1000.

As may be seen from Fig. 4, the brightness values coincide at small voltages; with increasing voltage, the luminescence brightness in the pulsating mode of operation lags very slightly behind the brightness in the bipolar mode. As in the case of the yellow luminophor, the difference in brightness occurs along with a sharp rise of the conductivity current through the layer.

The dependence of brightness and current on the amplitude of square voltage pulses in bipolar and unipolar modes of operation is also depicted in Fig. 4.

DISCUSSION OF RESULTS

The following conclusions may be drawn from these experimental data:

1. For layers of the yellow ZnS-Cu,Mn luminophor, the electroluminescence brightness in a unipolar pulsating field does not differ from the brightness in an alternating bipolar field at small (100-200 volts) voltages, but considerably (5-6 times) exceeds it at higher voltages.

2. For layers of the green ZnS-Cu luminophor, the brightness is the same for both modes of operation at small voltages (100-200 volts) and there is an insignificant reduction of brightness in the pulsating mode (6-7%) at higher voltages.

3. In both cases, differences of brightness occur simultaneously with a sharp increase of the conductivity current through the layer.

4. In yellow luminophors, the rapid increase of brightness with increasing voltage in the pulsating mode of operation is accompanied by a rapid increase in the conductivity current through the layer.

5. The excess of brightness in the pulsating mode of operation over the brightness in the bipolar field decreases with increasing frequency (270% at 500 cps and 600% at 100 cps).

The above-mentioned luminescence characteristics indicate that the simultaneous action of an alternating and a dc voltage, which by their nature double the voltage in the layer and decrease its frequency by a factor of two, has practically no influence on the electroluminescence of green luminophors, but very substantially changes the brightness of yellow electroluminophors. The fact that layers made of green and yellow luminophors have roughly the same conductivity makes it impossible to assume that essentially different voltages are acting upon the separate granules of the green and yellow luminophors suspended in the dielectric medium.

The above-described difference in the total brightness of yellow electroluminophors in a pulsating field, and the certain connection of this phenomenon with the appearance of a conductivity current in the layer, are compatible with sharp distortion of the electroluminescence light pulses of the indicated luminophors under these same conditions.[3] This correspondence permits a possible qualitative explanation of the joint effect of electroluminescence in a dc field and in an alternating one. Inasmuch as layers made of the yellow ZnS-Cu,Mn electroluminophors are able to luminesce in a dc field with conductivity current flowing through them, the increase of brightness in the pulsating mode of operation evidently takes place as a result of the development of luminescence in the dc field under the action of both voltages at times when they add. The simultaneous rapid increases of brightness and conductivity current with increasing voltage in the pulsating mode of operation confirm this supposition.

The dependence of brightness on frequency in the pulsating mode, in particular the decrease of growth of brightness at high frequencies, may be explained by inertia in the development of luminescence in a dc field. The small decrease in the brightness of green luminophors in the pulsating mode also corresponds to observable changes in light pulses, and may be explained as a small weakening of luminescence in the alternating field, due to the presence of conductivity.

REFERENCES

1. P. Zalm. Philips Res. Repts. 11, 353, 417 (1956).
2. B. Kazan. Proc. I.R.E. 45, 1358 (1957).
3. G. S. Kozina, V. N. Favorin, and I. D. Anisimova. Opt. i Spektr. 8, 218 (1960).

ELECTRLUMINESCENCE LIGHT PULSES UNDER THE SIMULTANEOUS ACTION OF DC AND AC VOLTAGE

G. S. Kozina, V. N. Favorin, and I. D. Anisimova

Received 25 May 1959

In this paper we discuss alterations of the form of electroluminescence light pulses of a yellow ZnS-Cu,Mn luminophor caused by changing the ratio of dc to ac voltage applied to the layer (for square and sinusoidal ac waveforms). We also examine the connection between these changes and the conductivity of the layer. Nonadditivity of the combined action of dc and ac voltages is established. The absence of analogous changes of light pulse shapes in the case of a green electroluminophor under the same conditions is indicated. The phenomena described are explained in terms of the combination of the electroluminescence effects of the ZnS-Cu,Mn luminophor in dc and ac fields.

Under the simultaneous action of dc and ac voltages on electroluminescent layers, an essential difference can be observed between the behavior of electroluminophors which contain manganese as activator ("yellow" ZnS-Cu, Mn) and those which do not ("green" ZnS-Cu).[1,2]

In this paper we present the results of an investigation of the electroluminescence light pulse shapes of yellow and green electroluminophors under the simultaneous action of dc and ac voltages.

EXAMPLES AND METHOD OF MEASUREMENT

Electroluminescent layers were prepared by applying a mixture of the electroluminophor and the dielectric binding material (pulverized) to a glass plate coated with a transparent conducting electrode. After drying, a second aluminum electrode was vaporized onto the surface of the layer in vacuum. The thickness of the luminophor layer was 50-100 μ.

DC and ac voltages were applied to the electrodes of this electroluminescent condenser as depicted in Fig. 1.

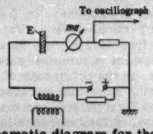

Fig. 1. Schematic diagram for the investigation of electroluminescence. E—electroluminophor layer.

The conductivity current through the layer was controlled with the apparatus shown on the diagram; observations of light pulse shapes were carried out with the help of an FEU-27 photomultiplier and two oscillographs connected in parallel: an ENO-1 (to measure dc components) and a double-beam 2KO-721 (for comparisons of voltage waves).

The square and sinusoidal alternating voltage waveforms were applied at a frequency of 100 cps.

Oscillograms of voltage V and electroluminescence brightness B under the simultaneous action of dc and ac fields are presented in Fig. 2 (for green, copper-activated luminophors) and in Fig. 3 (for yellow, containing manganese as an activator). From the Figures we can see that the green as well as the yellow electroluminophors, under excitation by a rectangular voltage wave, have qualitatively similar types of light pulses, with two peaks occurring at sign changes of the voltage wave. However, the decay time of the brightness is considerably longer for the yellow electroluminophors than for the green ones. In the case of the green layers, a dc voltage acting simultaneously with the ac voltage does not influence the form of the light pulse except to diminish its amplitude slightly (Fig. 2). Application of a dc voltage to the layer of yellow electroluminophor simultaneously with the ac voltage, and the resulting upward displacement of the ac "zero" line, cause a change in the shape of the light pulse. With increasing voltage one notices that simultaneously with the increase of peak amplitude there is a more rapid increase in the area between the peaks, so that the light pulse acquires a rectangular form for a sufficiently large dc voltage (Fig. 3, b).

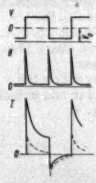

Fig. 2

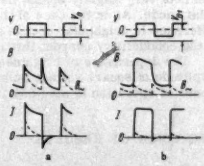

Fig. 3

Fig. 2. Oscillograms of voltage V, brightness B, and current I for a green electroluminophor in an alternating field (broken curve), and under the simultaneous action of direct and alternating fields (continuous curve). Density of the dc conductivity current: 40 $\mu a/cm^2$.

Fig. 3. Oscillograms of voltage V, brightness B, and current I for a yellow electroluminophor in an alternating field (broken curves) and under the simultaneous action of alternating and direct fields (continuous curves) ($B_\sim$ is the brightness level in the alternating field). Density of the dc conductivity current (in $\mu a/cm^2$): a—6, b—80.

The shape of the light pulses of a yellow electroluminophor under the simultaneous action of different voltages is determined by the ratio of the components: increasing the amplitude of the alternating voltage increases the sharp peaks of the light pulse (Fig. 4, a); increasing the dc component causes a more rapid in-

crease in the area between the peaks (Fig. 4, b). In all cases of simultaneous action of dc and ac voltages on a yellow luminophor, one observes a brightness greater than that of either component separately, and also greater than the sum of these brightnesses.

CHANGES IN THE SHAPE OF LIGHT PULSES AS A FUNCTION OF THE CONDUCTIVITY OF THE ELECTROLUMINOPHOR LAYER

All changes in the shape of the light pulse described in the previous section can take place only in the presence of a dc conductivity current through the layer. The value of the conductivity current necessary for alteration of the form of the light pulse depends on the amplitude of the alternating voltage: at small amplitudes, alteration of the light pulse shape may be observed at conductivity current densities as low as 10^{-8} to 10^{-7} amp/cm² (Fig. 5, a).

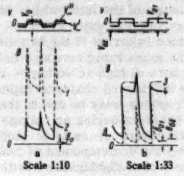

Fig. 4

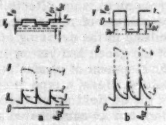

Fig. 5

Fig. 4. Oscillograms of voltage V and light pulses B for a yellow electroluminophor (a) with fixed dc voltage (V_0) and different alternating voltages ($V_\sim'$ and $V_\sim''$), and (b) with fixed alternating voltage (V) and different dc fields (V_{01} and V_{02}). (B_0 and $B_\sim$ are the brightnesses under the action of the dc and ac fields respectively.) DC conductivity current density (in μa/cm²): curve 1—1.1; curve 2—0.5; curve 3—6; curve 4—3.6.

Fig. 5. Oscillograms of voltage V and light pulse form B under the simultaneous action of a dc voltage and an ac field of low (a) and high (b) amplitude (corresponding V and B curves are represented by similar types of lines). DC conductivity current density (in μa/cm²): curve 1—0.16; curve 2—0.08; curve 3—0.04; curve 4—60; curve 5—10. Amplitude of the alternating voltage: a—30; b—200.

When high ac voltages are applied to the same layer (Fig. 5, b) the alteration starts at currents of 10 μa/cm² (150 volts) but rectangular light pulses are observed only for currents higher than 60 μa/cm². Thus, in order to change the shape of the light pulse, the conductivity current must be higher for higher ac voltages.

The shape and amplitude of the light pulse also depend on the conductivity current which flows through the layer under the action of the dc component of the voltage alone. In the absence of appreciable conductivity under the action of dc only, ($B_0 = 0$), the light pulse has sharp peaks and its height is greater than the value attained in a dc field whose magnitude is equal to the sum of the two voltages ($B_{V_{dc}}$ in Fig. 6, a). If, however, the dc voltage on the layer is sufficient to cause appreciable conductivity, then the peaks are not as sharp and in the limit the light pulse has a rectangular shape; the brightness is less than or equal to the luminescence brightness in a dc field equal in magnitude to the sum of the ac and dc fields (Fig. 6, b). Comparison of the curves in Figs. 6a and b shows that at the same maximum total voltage, completely different shapes and amplitudes of light pulse are possible.

Similar alternations of the light pulse may be observed when a sinusoidal alternating voltage and a dc voltage are impressed simultaneously on a layer of yellow electroluminophor (Fig. 7).

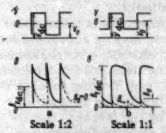

Fig. 6

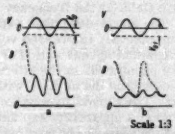

Fig. 7

Fig. 6. Oscillograms of voltage V and light pulse form B (solid lines) under the simultaneous action of dc and ac fields (a) in the absence of noticeable conductivity ($B_0 = 0$) and (b) in the presence of noticeable luminescence in the dc field ($B_0 \neq 0$) (broken lines: $B_\sim$ is the brightness in the alternating field).

Fig. 7. Oscillograms of voltage V and light pulse form B for a yellow electroluminophor in an ac field (solid lines) and under the simultaneous action of a dc and an ac field (broken curves). DC conductivity current density (in μa/cm²): a—10, b—60.

ELECTROLUMINESCENCE LIGHT PULSES AND CURRENT PULSES UNDER THE SIMULTANEOUS ACTION OF DC AND SQUARE ALTERNATING VOLTAGES

Current impulses in the electroluminescent layer circuit were studied with the aid of the ENO-1 oscillograph. Oscillograms of current I for a square wave ac voltage applied to a layer of yellow electroluminophor are shown in dotted curves in Figs. 3, a and b, together with oscillograms of voltage V and brightness B. An oscillogram of the current I for a green electroluminophor is shown in Fig. 2, also by a dotted curve. It follows from the Figures that oscillograms of current for green and yellow electroluminophors field are not essentially different in square-wave ac fields.

Oscillograms of the current I for simultaneous dc and alternating voltages on a layer of the yellow electroluminophor are shown in Fig. 3 as solid curves. The dc component of the voltage by itself does not give rise to noticeable conductivity current, but its joint action with the alternating voltage leads to a sharp increase in current during the half-cycle in which the voltages add together. In general, the current traces resemble the light pulses (Fig. 3, a). Further increase of the dc voltage leads to rapid growth and changes in shape of the current impulses during the half-cycle of increased voltage, as a result of which the oscillograms of current and brightness acquire the general character of the voltage curves (Fig. 3b). In Fig. 2 we present an oscillogram of the current in a layer of the green electroluminophor subjected simultaneously to dc and ac voltages. As in the case of the yellow electroluminophor, increased impulse current may be observed during periods of increased voltage, although the shape of the light pulse does not change, except for some scaling down.

CONCLUSIONS

Green electroluminophor layers containing manganese as one activator have been studied. These layers are distinguished by the presence of electroluminescence in a dc field whose brightness depends on the magnitude of the direct current passing through the layer, and is sharply altered as the applied dc voltage increases. The spectral characteristics of the dc luminescence do not differ from those of the electroluminescence in an alternating field (at the frequency studied).[1]

The above-described experimental data taken under simultaneously impressed voltages may be accounted for by the simultaneous action of two effects: electroluminescence phenomena in the alternating field and luminescence phenomena in the dc field with current flowing through the layer. The nonadditive action of the dc and alternating voltages is apparently explained by the fact that the alternating voltage not only excites electroluminescence itself, but when added to the dc voltage, leads to increased conductivity current (cf. the current variations on the oscillograms) and strengthens the dc luminescence during the time of additive voltage action.

The rectangular light pulses having sharp peaks which coincide with the edges of the voltage impulses (see, for example, Fig. 4) may be regarded as the result of superposing two types of waveforms: peaked waveforms excited by the alternating field, and rectangular light pulses arising from the combined action of the dc and rectangular ac voltages. Occurring simultaneously with alteration of the light pulse shape, the gradual transformation of the exponential current curve (characteristic of the charging of the capacitance constituted by the electroluminescent layer) into a square-wave repeating the voltage waveform indicates that under the action of additive voltages, the electroluminescent condenser is transformed into a nonlinear ohmic resistance. Observation under these conditions of similar pulse shapes for light, current, and voltage (see Figs. 3, b or 6, b where the combined brightness at a minimum may be less than the brightness of the dc component) and the quantitative agreement of the maximum combined brightness with the brightness due to dc field equal to the sum of the dc and ac components (Fig. 6, b) compels us to suppose that with the increase of conductivity there is a decrease of ac luminescence, with the fundamental role passing to the dc field and the current flow. The fact that the presence of a previously existing small conductivity is necessary for it to be manifested during a half-cycle (see Fig. 6) indicates the inertia of the dc luminescence effect.

A green electroluminophor layer does not show noticeable electroluminescence in a dc field. Therefore, in spite of its considerable conductivity and the presence of the same alteration of current as found in the yellow electroluminophors, this layer does not show any change in light pulse form under simultaneously impressed dc and ac voltages. Under conditions of considerable layer conductivity some decrease of brightness takes place, which may be regarded as a weakening of the luminescence effect in the alternating field as the result of a decrease of local potential gradients.

The different rates of change of the integral brightness of yellow and green electroluminophors in an alternating field may be explained in terms of the two electroluminescence effects.[3] The more rapid increase in the brightness of yellow luminophors at high ac voltages, resulting in the crossing of the brightness characteristics of the green and yellow luminophors, may be due to the development of conductivity currents during ac voltage pulses. Here, a type of electroluminescence is developed in the dc field which increases the dc component of radiation, and an accelerated growth of total brightness with increasing voltage is observed.

REFERENCES

1. V. N. Favorin, G. S. Kozina, and L. K. Tikhonova. Opt. i Spektr. 7, 703 (1959).
2. G. S. Kozina and L. N. Poskacheeva. Opt. i Spektr. 8, 214 (1960).
3. V. N. Favorin and L. P. Poskacheeva. Opt. i Spektr. 8, 706 (1959).

POLARIZATION OF LUMINESCENCE IN A SYSTEM OF PARTICLES WITH THREE ENERGY LEVELS AS A FUNCTION OF THE EXCITING LIGHT INTENSITY

B. I. Stepanov and V. P. Gribkovskii

Received 22 June 1959

The polarization, absorption coefficient, dichroism, and intensity of α-phosphorescence are calculated as functions of the intensity of the incident radiation. It is shown that these are all nonlinear functions and are connected with the accumulation of particles in a metastable state.

1. Vavilov's works contain a number of problems in nonlinear optics.[1] Nonlinear phenomena arise, as is well known, upon illuminating the object under investigation with very intense light beams. Appreciable deviations from linearity develop first of all as a violation of Bouguer's law.[2] They also develop in the emergence of dichroism and in the depolarization of luminescence. The depolarization of luminescence under saturating light conditions was predicted by Feofilov and detected experimentally by Sveshnikov.[3] It becomes appreciable in the luminescence of molecules which possess significant phosphorescence, and is connected with the existence of a metastable state. Sveshnikov also showed that the decrease in the degree of polarization of luminescence in proportion to the increase in the intensity of the illumination is accompanied by a simultaneous increase in the degree of violation of Boufuer's Law.

In the present paper a rigorous calculation is made of the dependence of the polarization of luminescence on the intensity of the incident light for a system of particles with three energy levels, i.e., for molecules having normal, unstable, and metastable levels. The calculations carried out by Feofilov[4] pertain in essence to a system of particles with two energy levels, and his results are

only approximate.* In calculating the degree of polarization, we used the usual probability method used by Sveshnikov[7] in a study of various phosphorescence properties of organic molecules.

*A more accurate calculation of the luminescence polarization of a system of particles with two energy levels is carried out in reference 6. In contrast to reference 6, the background of thermal radiation is neglected in the present paper.

At the same time, we considered other nonlinear effects closely connected with the emergence of depolarization of luminescence.

2. We shall assume that the excitation of luminescence is carried out by means of polarized light directed along the x-axis. The electric vector of the incident wave is oriented along the z-axis, and the direction of observation coincides with the y-axis. Figure 1 shows the symbols for the transition probabilities between the levels. The quantities p_{ij} represent the sum of the probabilities of all the optical and nonoptical transitions, the frequency

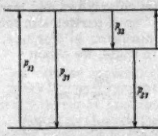

Fig. 1. Diagram for a system with three energy levels (arrows show the possible transitions).

of the incident radiation being equal to $E_3 - E_1$. In this case, the expressions for the transition probabilities between the normal and unstable levels are written in the form

$$p_{13} = 3B_{13} \cdot s\Delta\Omega' \cos^2\Theta, \tag{1}$$

$$p_{31} = A_{31} + 3B_{13} s\Delta\Omega' \cos^2\Theta + d_{31}. \tag{2}$$

Here $3B_{13}\cos^2\Theta$ is the Einstein differential absorption coefficient and s is the density of the incident radiation within the cell, calculated for unit solid angle; $\Delta\Omega'$ is the solid angle of the exciting radiation, A_{31} is the Einstein integral coefficient for spontaneous emission, d_{31} is the probability of the radiationless transition 3 – 1, and Θ is the angle between the electric vector and the dipole moment of the molecule. In making the calculation we corrected for induced emission, which substantially affects the degree of polarization. We shall also assume that up until excitation all molecules are randomly oriented and that there is no rotation of excited molecules (inelastic medium). The transition probabilities p_{23}, p_{32}, p_{21} do not depend on the angle Θ in the given case.

The distribution of the particles among the energy levels under constant illumination is found from the energy balance relationships

$$n_1 p_{13} - n_2 p_{21} - n_3 p_{31} = 0, \quad n_2 (p_{21} + p_{23}) - n_3 p_{32} = 0, \quad n_3 (p_{31} + p_{32}) - n_1 p_{13} - n_2 p_{23} = 0, \tag{3}$$

$$n_1 + n_2 + n_3 = \frac{n}{4\pi}. \tag{4}$$

where n_1, n_2, n_3 are the numbers of particles calculated in a unit solid angle corresponding to the direction Θ, ϕ, and n is the total number of particles. In the calculation, no account is taken of the thermal radiation background (u = 0). Solving Eqs. (3) and (4), we obtain

$$n_3 = \frac{3}{4\pi} n \frac{(p_{21} + p_{23}) B_{13} s\Delta\Omega' \cos^2\Theta}{K + L\cos^2\Theta}, \tag{5}$$

$$n_2 = \frac{3}{4\pi} n \frac{p_{32} B_{13} s\Delta\Omega' \cos^2\Theta}{K + L\cos^2\Theta}, \tag{6}$$

$$n_1 = \frac{1}{4\pi} n \frac{(p_{21} + p_{23})(A_{31} + d_{31} + 3B_{31} s\Delta\Omega' \cos^2\Theta) + p_{23} p_{31}}{K + L\cos^2\Theta}, \tag{7}$$

where

$$K = (A_{31} + d_{31})(p_{21} + p_{23}) + p_{21} p_{23}, \tag{8}$$

$$L = 3B_{13} s\Delta\Omega' (2p_{21} + 2p_{23} + p_{32}). \tag{9}$$

Formulas (5)-(9) differ from the corresponding formulas of Sveshnikov[7] by the inclusion of induced emission. Besides this, in the present case we compute the dependence of the transition probability on the angle Θ, making it possible to determine the orientation of the excited molecules. The luminescent power at frequency ν_{21} observed in the y-direction, with the electric vectors oriented along the z- and x-axes, calculated for unit solid angle of observation, is equal to

$$W_{21}^z = \int_\Omega n_3(\Omega) A_{21}^z(\Omega) h\nu_{21} d\Omega, \tag{10}$$

$$W_{21}^x = \int_\Omega n_3(\Omega) A_{21}^x(\Omega) h\nu_{21} d\Omega. \tag{11}$$

$A_{21}^z(\Omega)$ and $A_{21}^x(\Omega)$ are the differential Einstein coefficients for spontaneous emission, connected with the integral coefficient by the relations

$$A_{21}^z(\Omega) = \frac{3}{8\pi} A_{21} \cos^2\Theta, \tag{12}$$

$$A_{21}^x(\Omega) = \frac{3}{8\pi} A_{21} \sin^2\Theta \cos^2\varphi. \tag{13}$$

Integration is carried out with respect to the angles Θ and ϕ, which characterize the orientation of the dipole moments of the excited molecules. Substituting the value of n_3 from (5) into (10) and (11) and completing the integration, we obtain

$$W_{21}^z = \frac{9}{8\pi} nh\nu_{21} (p_{21} + p_{23}) A_{21} B_{13} s\Delta\Omega' \frac{1}{K} \times\left[\frac{1}{3b} - \frac{1}{b^{3/2}}\left(1 - \frac{1}{b^{1/2}}\arctan b^{1/2}\right)\right], \tag{14}$$

$$W_{21}^x = \frac{9}{16\pi} nh\nu_{21} (p_{21} + p_{23}) A_{21} B_{13} s\Delta\Omega' \frac{1}{K} \times\left[-\frac{1}{3b} + \frac{1}{b}\left(\frac{1}{b} + 1\right)\left(1 - \frac{1}{b^{1/2}}\arctan b^{1/2}\right)\right], \tag{15}$$

where

$$b = \frac{L}{K} = \frac{3B_{13} s\Delta\Omega' (2p_{21} + 2p_{23} + p_{32})}{(A_{31} + d_{31})(p_{21} + p_{23}) + p_{21} p_{23}}. \tag{16}$$

The degree of polarization of the luminescence is

$$P = \frac{W_{21}^z - W_{21}^x}{W_{21}^z + W_{21}^x} = \frac{(3 + b)\arctan b^{1/2} - 3b^{1/2}}{\frac{4}{3} b^{3/2} - b^{1/2} + (1 - b)\arctan b^{1/2}}. \tag{17}$$

For b = 0, P = 0.5; for b = 1, P = 0.425. When b goes to infinity, the polarization tends toward zero. If $b < 1$, then P can be represented in the form of a series

$$P = \frac{1}{2}\left(1 - \frac{3}{14} b + \ldots\right). \tag{18}$$

A graph of the polarization as a function of the

parameter b is shown in Fig. 2 (curve 1). Formula (17) differs from Feofilov's formula[5,6] for systems of particles with two energy levels, only in the value of the parameter b. In the latter case

$$b = b_0 = \frac{6B_{12}s\Delta\Omega'}{A_{21}+d_{21}} = \frac{3c^3}{4\pi h\nu_{21}^3}\frac{A_{21}}{(A_{21}+d_{21})}s\Delta\Omega'. \qquad (19)$$

For a system of particles with three levels,

$$b = b_0\beta, \qquad (20)$$

where

$$\beta = \frac{2p_{21}+2p_{23}+p_{23}}{p_{21}+p_{23}+\frac{p_{21}p_{23}}{A_{21}+d_{21}}}. \qquad (21)$$

With the usual intensities used for exciting radiation, the value of b_0 is small and the degree of polarization of the luminescence a system of particles with two energy levels is therefore close to ½. For a system of particles with three levels, the value of the constant b increases enormously, which can lead to a marked depolarization of the luminescence, even with comparatively weak excitation. Let us assume that in a given system and for a given temperature only α-phosphorescence is observed. In this typical case $p_{21} \ll p_{23} < p_{32}$, and consequently,

$$\beta \approx \frac{p_{23}+2p_{32}}{p_{23}}.$$

Experiment shows[7,8] that the transition probability from a metastable state to a labile one can be approximated by the formula

$$p_{23} = pe^{-\frac{E_2-E_3}{kT}},$$

in which p and p_{23} are equal in order of magnitude. Thus,

$$\beta \approx e^{\frac{E_2-E_3}{kT}}.$$

If, as for example in fluorescence, $E_2 - E_3 \approx 3000$ cm^{-1}, then at room temperature $\beta \approx 10^6$. In order to attain the same depolarization of luminescence in a system of particles with two energy levels, it would be necessary to increase the intensity of the incident radiation at least 10^6 times. In many molecules which have metastable levels, the dependence of the degree of polarization of luminescence on the intensity of the incident light is already evident at ordinary intensities. It is extremely probable that the departure of the value of polarization of luminescence from ½ must be explained by the presence of a metastable state and by a high value for the constant β. In these cases, the temperature dependence of P may be due not only to thermal motion, but also to a significant change in the probability p_{23}.

3. The depolarization of luminescence occurring in a system of particles with three energy levels is directly connected with the sharp decrease in the number of unexcited particles. When the exciting radiation is weak, the angular distribution of unexcited molecules is almost uniform, and the distribution of excited particles is therefore determined by the value of $\cos^2\Theta$ (which corresponds to P = ½). With an increase of excitation intensity, the number of particles in the lower level decreases, chiefly at the expense of molecules with dipole moments oriented along the z-axis. As a result of this, there is a decrease in the absorption coefficient for the incident radiation (a violation of Bouguer's Law) and at the same time a decrease in the degree of orientation of the excited molecules. In the limit, with very high intensities of external radiation, the excited molecules completely lose their orientation (see Eqs. (5)-(7) for $L \gg K$) and the luminescence becomes depolarized. This depolarization is entirely independent of the fact that the molecules remain in a metastable state, since according to the original hypothesis, the probabilities p_{32} and p_{23} are independent of the direction of the electric vector of the incident radiation, and are determined solely by the internal properties of the molecule. The role of the metastable state in depolarizing luminescence merely comes down to an accumulation in the state of a significant quantity of oriented molecules and a corresponding decrease in the number of unexcited molecules.

From formulas (5)-(9) and (16) it is not difficult to obtain a simple relation connecting the number of oriented molecules n_1, n_2, and n_3 with the parameter b characterizing the degree of depolarization of the luminescence

$$b = \frac{L}{K} = \frac{n_2+2n_3}{(n_1-n_2)\cos^2\Theta} \approx \frac{n_2}{n_1\cos^2\Theta}. \qquad (22)$$

The connection of luminescence depolarization with the accumulation of excited particles in a metastable state appears in a particularly graphic manner if one expresses the total number of particles in the second level as a function of the parameter b. For this, integrating Eq. (6) with respect to angle, we obtain

$$N_2(b) = \int_\Omega n_2(\Omega)\,d\Omega = n\frac{p_{23}}{2p_{21}+2p_{23}+p_{21}}\left(1-\frac{1}{b^{1/2}}\arctan b^{1/2}\right) = N_2(\infty)\left(1-\frac{1}{b^{1/2}}\arctan b^{1/2}\right), \qquad (23)$$

where $N_2(\infty)$ is the value of $N_2(b)$ for $b \to \infty$, i.e., for complete saturation by light. If $b < 1$, Eq. (23) takes the form

$$N_2 = N_2(\infty)\left(\frac{1}{3}b - \frac{1}{5}b^2 + \ldots\right), \qquad (24)$$

and, consequently, for small values of b the number of particles N_2 is proportional to the value of b. The dependence of N_2 on b is presented in Fig. 2 (curve 2). Comparing the graphs of $N_2(b)$ and P(b), it is easily seen that an accumulation of particles in the metastable state is accompanied by depolarization of the luminescence.

From the preceding considerations, and also from Eqs. (22)-(24), it follows that luminescence depolarization should be observed simultaneously with other phenomena connected with the accumulation of particles in a metastable state and the decrease in the number of particles in the ground (unexcited) state. Among these phenomena are: a decrease in absorption coefficient, the occurrence of dichroism, and an intense, long-lived phosphorescence. It is easy to show that all these phenomena depend directly on the same parameter b, which is determined both by the excitation intensity and by the relations between the transition probabilities within the molecule.

4. The absorptive power of the exciting radiation is equal to

$$W_{abs.} = h\nu_{21}\int_\Omega [n_1(\Omega)-n_2(\Omega)]\,3B_{12}s\Delta\Omega'\cos^2\Theta\,d\Omega = \frac{3nB_{12}s\Delta\Omega'h\nu_{21}}{b}\left(1-\frac{1}{b^{1/2}}\arctan b^{1/2}\right) = W_{abs.}(\infty)\left(1-\frac{1}{b^{1/2}}\arctan b^{1/2}\right), \qquad (25)$$

where $W_{abs.}(\infty)$ is the limiting absorptive power as $b \to \infty$. From Eqs. (23) and (25) it is not difficult to see that for any given system (p_{ij} = const.) the absorptive power and the total number of particles in the metastable level depend in like manner on the intensity of the incident radiation.

Knowing the absorptive power, one can easily calculate the absorption coefficient χ,[9]

$$\varkappa = \frac{1}{c\sigma\Delta\Omega'} W_{abs.} = \frac{3n}{c} B_{12}h\nu_{21} \frac{1}{b}\left(1 - \frac{1}{b^{3/2}} \arctan b^{1/2}\right). \quad (26)$$

For small values of b, it is

$$\varkappa = \frac{1}{c} B_{12} n h\nu_{21} \left(1 - \frac{3}{5} b + \ldots\right). \quad (27)$$

From comparison of Eqs. (27) and (18) it follows that the decrease in absorption coefficient begins at somewhat smaller values of b (intensities of the exciting radiation $s\Delta\Omega'$) than the decrease in the polarization of luminescence, and consequently the value of the absorption coefficient is more sensitive to saturation by light. (Fig. 2, curve 3).

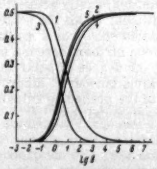

Fig. 2. The various spectral characteristics (in rel. units) of a system of particles with three energy levels as functions of the parameter b. 1—polarization of luminescence P; 2—number of particles in the metastable state $N_2/2N_2(\infty)$; 3—absorption coefficient $\chi c/2B_{12}nh\nu_{21}$; 4—dichroism D/2; 5—light sum of α-phosphorescence $S_t/2S_t(\infty)$.

5. The anisotropy of angular distribution of the excited molecules, caused by the interaction with polarized light, also appears in the dichroism.** For the experimental study of this phenomenon one can make use of two beams of linearly polarized light. The first beam should be fairly powerful, and should create an anisotropy in the orientation of the excited molecules. It is expedient to make the second beam of variable light polarization comparatively weak, otherwise it will evoke additional anisotropy of the molecules, which will make the comparison of theory with experiment more difficult.

We shall assume that the second beam of radiation falls on the system in the direction of the y-axis. The direction of the electric vector coincides in one case with the z-axis, in the other with the x-axis. The absorption of these beams will be different. The probabilities of transition with absorption are, respectively,

$$\left.\begin{aligned} B'_{12}(\Omega)\, s_1 \Delta\Omega'' &= 3B_{12}s_1\Delta\Omega'' \cos^2\theta, \\ B''_{12}(\Omega)\, s_1 \Delta\Omega'' &= 3B_{12}s_1\Delta\Omega'' \sin^2\theta \cos^2\varphi, \end{aligned}\right\} \quad (28)$$

where s_1 is the radiation density of the second beam, computed for unit solid angle ($\Delta\Omega''$ is the solid angle of the incident beam). The frequency of the beam corresponds, as before, to the transition 1 → 3. The absorptive powers for the steady state, which is determined by the distribution functions (5)-(7), correcting for induced emission, are

$$W'_{abs.} = 3B_{12}s_1\Delta\Omega''h\nu_{21}\int_\Omega [n_1(\Omega) - n_3(\Omega)]\cos^3\theta\, d\Omega$$

$$= 3nB_{12}s_1\Delta\Omega''h\nu_{21}\frac{1}{b}\left(1 - \frac{1}{b^{3/2}}\arctan b^{1/2}\right), \quad (29)$$

$$W''_{abs.} = 3B_{12}s_1\Delta\Omega''h\nu_{21}\int_\Omega [n_1(\Omega) - n_3(\Omega)]\sin^2\theta\cos^2\varphi\, d\Omega$$

$$= \frac{3}{2} nB_{12}s_1\Delta\Omega''h\nu_{21}\left[-\frac{1}{b} + \left(\frac{1}{b^{3/2}} + \frac{1}{b^{5/2}}\right)\arctan b^{1/2}\right]. \quad (30)$$

It follows from Eqs. (29) and (30) that the absorptive powers of the system for beams directed along the y-axis depend on the intensity of the first beam, which causes the anisotropy of the system (through the parameter b). For b = 0, as expected, $W'_{abs.} = W''_{abs.}$, corresponding to the absence of dichroism. For b = 0, the absorptive powers for light polarized in different planes are different—$W''_{abs.}$ tends to zero more rapidly than $W'_{abs.}$, for $b < 1$

$$W'_{abs.} = nB_{12}s_1\Delta\Omega''h\nu_{21}\left(1 - \frac{3}{5}b + \frac{3}{7}b^2 - \ldots\right), \quad (31)$$

$$W''_{abs.} = nB_{12}s_1\Delta\Omega''h\nu_{21}\left(1 - \frac{3}{15}b + \frac{3}{35}b^2 - \ldots\right). \quad (32)$$

Following Feofilov,[10] we shall take as a measure of the dichroism

$$D = \frac{\varkappa'' - \varkappa'}{\varkappa'' + \varkappa'} = \frac{W''_{abs.} - W'_{abs.}}{W''_{abs.} + W'_{abs.}}, \quad (33)$$

where χ'' and χ' are the absorption coefficients of the second beam, polarized along the x-axis or the z-axis, respectively. Substituting Eqs. (29) and (30) into (33), we obtain

$$D = \frac{(b+3)\arctan b^{1/2} - 3b^{1/2}}{(b-1)\arctan b^{1/2} + b^{1/2}}. \quad (34)$$

When $b < 1$, Eq. (34) can be represented in the form

$$D = b\frac{\sum_{k=0}^{\infty}(-1)^k b^k \frac{k+1}{(2k+3)(2k+5)}}{\sum_{k=0}^{\infty}(-1)^k b^k \frac{k+1}{(2k+1)(2k+3)}} = \frac{1}{5}b - \frac{16}{175}b^2 + \ldots \quad (35)$$

According to Eqs. (34) and (35), as b increases from zero to infinity, D increases from zero to one* (Fig. 2, curve 4).

6. Let us look quite briefly at the afterglow phenomenon, which arises after the cessation of a previously steady excitation.* It is also connected with the accumulation of particles in a metastable level. Solution of the corresponding system of differential equations yields

$$n_3 = R_1 \frac{s\Delta\Omega'\cos^2\theta}{K + L\cos^2\theta} e^{-\frac{t}{\tau_1}} + R_2 \frac{s\Delta\Omega''\cos^2\theta}{K + L\cos^2\theta} e^{-\frac{t}{\tau_2}}. \quad (36)$$

Here τ_1 and τ_2 are the corresponding durations of

---

*The calculation performed by Cherdyntsev[3] applies rigorously only to a system of particles with two levels and does not describe the properties of particles with three energy levels.

**Sometimes dichroism is characterized by the difference of the absorption coefficients.[3] In our case it equals

$$D' = \varkappa'' - \varkappa' = \frac{3}{2\sigma} nB_{12}h\nu_{21}\frac{1}{b^{3/2}}[(3+b)\arctan b^{1/2} - 3b^{1/2}].$$

At first D′ increases with increasing b up to some maximum value (for $b \approx 7.5$), and then it begins to decrease rapidly; in the limit, when $b \to \infty$ and all nonlinear effects attain their highest values, it tends toward zero. The magnitude of D′ does not reflect that the fact that the ratio χ''/χ' becomes infinite as $b \to \infty$. Hence the selection of D′ to characterize dichroism seems to us unfortunate.

*A similar theoretical investigation of this phenomenon was performed by Sveshnikov.[7,8] The present calculation takes into account several details (dependences on intensity and the angles θ, φ).

fluorescence and the phosphorescence; R_1 and R_2 are constants that depend on the transition probabilities. Substituting (36) into (10) and (11), one obtains without difficulty the time dependence of the afterglow power. The first term of (36) determines the power of short-lived afterglow; the second, the power of α-phorphoresecence.

The dependence of the power of α-phosphorescence on the time has the form

$$W_t^{\alpha} + W_t^{\alpha} = \frac{A_{21} h\nu_{21} s\Delta\Omega'}{K b} R_2$$

$$\left[1 - \frac{3}{4b} + \frac{3}{4}\left(\frac{1}{b^{3/2}} - \frac{1}{b^{1/2}}\right)\arctan b^{1/2}\right] e^{-\frac{t}{\tau_2}}. \quad (37)$$

The light sum of the α-phosphorescence equals

$$S_t = \int_0^{\infty} \left[W_t^{\alpha} + W_t^{\alpha}\right] dt =$$

$$\frac{A_{21} h\nu_{21} s\Delta\Omega'}{K b} \tau_2 R_2 \left[1 - \frac{3}{4b} + \frac{3}{4}\left(\frac{1}{b^{3/2}} - \frac{1}{b^{1/2}}\right)\arctan b^{1/2}\right]. \quad (38)$$

Like the integral number of particles in the metastable level, the light sum attains a very high value as $b \to \infty$. For $b < 1$, the expression has the form

$$S_t(b) = S_t(\infty)\left(\frac{2}{5} b - \frac{9}{35} b^2 + \ldots\right), \quad (39)$$

where

$$S_t(\infty) = \frac{A_{21} h\nu_{21} \tau_2 R_2}{3B_{13}(2p_{21} + 2p_{23} + p_{23})}. \quad (40)$$

The dependence of S_t on b (intensity of exciting radiation) is presented in Fig. 2 (curve 5). It almost coincides with the dependences of N_2 and D on b.

Thus, all of the nonlinear effects arise under such intensities of the exciting radiation as are necessary to develop phosphorescence. The presence of observable α-phosphorescence is always accompanied by a nonlinear dependence of the absorption coefficient, the degree of polarization, and the dichroism on $s\Delta\Omega'$. The converse is not so. The occurrence of nonlinear effects (at some intensity of incident light) is not always accompanied by phosphorescence. This can come about, for example, if $2 \to 3$ transitions are forbidden, and the excited particles can go from the metastable state to a normal one because of the existence of radiationless transition probabilities d_{21}. For sufficiently large d_{21}, not only is the afterglow quenched, but all nonlinear effects also decrease (are "quenched") since in this case the accumulation of excited molecules in the second level is not possible.

The calculations also show that the polarization of the afterglow is the same as the polarization for steady-state illumination and does not change with time. The decline in the degree of polarization of α-phosphorescence compared to the degree of polarization of the total light which was observed in reference 11 is obviously connected with the presence of depolarizing factors (e.g., rotation of the molecules in the excited state), which are not taken into account in the present paper.

In conclusion, we should note the desirability of experimental study of all of nonlinear optical effects on one and the same sample. With molecules which can be represented as a system of particles with three energy levels, these effects should appear at relatively small exciting light intensities, easily accessible under actual experimental conditions. Of all the nonlinear phenomena, the first to be detected should be a marked deviation from Bouguer's Law. Upon further increase in the density of the incident beam, the degree of polarization will begin to decrease, and, simultaneously, dichroism will appear. All of the results of the preceding calculation are accessible to direct experimental test.

REFERENCES

1. S. I. Vavilov. "Mikrostruktura sveta." (The Micro-Structure of Light), Izd. Akad. Nauk SSSR, Moscow, 1950.
2. B. Ya. Sveshnikov. Doklady Akad. Nauk SSSR 51, 675 (1946).
3. S. V. Cherdyntsev. Zhur. Eksptl. i Teoret. Fiz. 18, 352 (1948).
4. P. P. Feofilov. Kand. diss. (Candidate's dissertation), Gosudarst. Opt. Inst., 1944.
5. P. P. Feofilov. "Polyarizovannaya liuminestsentsiya atomov, molekul i kristallov." (The Polarized Luminescence of Atoms, Molecules, and Crystals), Fizmatgiz, Moscow, 1959.
6. V. P. Gribkovskii and B. I. Stepanov. Opt. i Spektr. 8, 176 (1960).
7. B. Ya. Sveshnikov. Zhur. Eksptl. i Teoret. Fiz. 18, 878 (1948).
8. B. Ya. Sveshnikov. Izvest. Akad. Nauk SSSR, Ser. Fiz. 13, 67 (1949).
9. B. I. Stepanov. "Liuminestsentsiya slozhnykh molekul." (Luminescence of Complex Molecules), Izd. Akad. Nauk Byeloruss. SSR, Minsk, 1956; S. E. Frish. Uspekhi Fiz. Nauk 53, 512 (1951).
10. P. P. Feofilov. Uspekhi Fiz. Nauk 36, 417 (1948).
11. V. A. Pilipovich. Kand. diss. (Candidate's dissertation), Minsk, 1958.

INVESTIGATION OF REFLECTANCE AND LUMINESCENCE SPECTRA OF COPPER HALIDES AT LOW TEMPERATURE*

*This report was based on the results of the graduate work of B. S. Razbirin and R. I. Shekhmamet'ev, carried out at the Zhdanov Leningrad State University in 1955-1957.

E. F. Gross, B. S. Razbirin, and R. I. Shekhmamet'ev

Received 3 June 1959

The optical absorption of copper halide crystals was studied for the first time by Fesefeldt and Gyulai,[1] by observing in the spectra of films sublimed into a vacuum at room temperature the maxima located in the long wavelength region of natural absorption, and lying at λ372 mμ for CuCl, at λ395 mμ for CuBr, and at λ406 mμ for CuI. These authors, and also Seitz,[2] associated this structure with the fundamental absorption of the lattice of a substance. The absorption of CuCl films in the far ultraviolet region was studied by Schneider and O'Bryan.[3] Later Kokhanenko[4] and Shalimova,[5] who interpreted this structure as the absorption of excess copper atoms occurring in the field of the crystalline lattice, studied the discrete structure of the long wavelength absorption region of CuI and CuCl films at low temperatures (−180°C).

In the luminescence spectra of copper halides, broad emission bands in the visible region of the spectrum,[6,8] and also narrow emission lines[7-9] in the area of the absorption region of crystals, associated with lines of discrete structure of the absorption region, are known. In the works of Nikitine and co-workers,[7] who studied the absorption, reflectance, and luminescence spectra of copper halides at low temperatures, the narrow lines in the absorption and emission regions in this range are associated with the formation and annihilation of the excitonic states.

Some results of the investigation of diffuse reflectance and luminescence spectra of CuI, CuBr, and CuCl crystals in the spectral range close to the region of natural absorption of these substances are presented in this report.*

*Some of these results were reported earlier.[8]

The crystals were studied as coatings, sublimed in vacuo onto a glass backing, and also as finely crystalline powders. We obtained polycrystalline copper halide films of different thicknesses by sublimation of the appropriate powder (analytical reagent grade) at a temperature of 400-500°C onto the wall of a glass test tube, with continuous evacuation to a pressure of 5×10^{-3} mm Hg. Luminescence was excited by the ultraviolet radiation of a SVDSh-1000 mercury lamp in the λ3660 A region for CuI and CuBr and in the shorter wavelength region (λ3100-3500 A) for CuCl. A continuous spectrum source (incandescent lamp) was used in the study of reflectance spectra. Examination of the reflectance and luminescence spectra was made on the same sample. The spectra were photographed with a Q-12 quartz spectrograph with a dispersion of about 50 A/mm in the 4000 A region.

1. CuI. According to the works cited in references 4, 5, 7-9, the structure of the absorption region of CuI at low temperatures consists of narrow lines in the λ3990-4150 A region. At the temperature of liquid nitrogen (77°K), in the diffuse reflectance spectrum of the CuI film which we studied, a series of narrow reflectance maxima was observed: a strong one at λ4050 A, and weaker ones at about λ4065 and 4095 A (Fig. 1, c), two

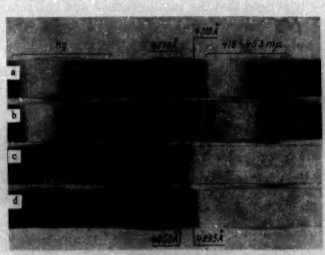

Fig. 1. Variation in the reflectance and luminescence spectra of CuI coating with the action of iodine vapors on it (T = 77°K). a—Luminescence of coating before interaction of iodine and after its removal; b—luminescence of coating after interaction of iodine; c—reflectance of coating before interaction of iodine and after its removal; d—reflectance of coating after interaction of iodine.

of which (4050 and 4065 A) coincided in position with the corresponding absorption lines of the CuI coating.[4,7] From the short wavelength side of the major reflectance maximum of λ4050 A, a sharp reflectance minimum was located at λ4045 A. Only one narrow minimum at about λ4050 A and a sharp reflectance minimum at λ4050 A, and also a weaker broad minimum at about λ4060-4130 A (Fig. 2, b) was observed in the reflectance spectrum of CuI powder at T = 77°K.

In the luminescence spectrum of the CuI coating at T = 77°K, a group of narrow lines at λ4045, 4063, 4078 (line has the form of the doublet 4071-4078 A), 4107, 4118, 4132, 4143 A,* and two broad emission bands were

*As was reported previously,[8,9] some of these emission lines displayed resonance with respect to the corresponding absorption lines.

observed in the λ418-453 mμ region (Fig. 1, a). The

Fig. 2. Luminescence (a) and reflectance (b) spectra of CuI powder at T = 77°K.

4045 and 4063 A emission lines were not very intense.

The short wavelength broad emission band has an equidistant structure (λ4250, 4282, 4315 A). The difference in frequencies among lines having this structure amounts to about 170 cm^{-1}. (The structure is not visible in the figure because of over-exposure).

In the luminescence spectrum of CuI powder at T = 77°K three faint lines at λ4045, 4058, and 4076 A and a broad intense band in the λ4080-4530 A region were observed where, in contrast to the corresponding emission band of the CuI coating, no equidistant structure was observed (Fig. 2, a).

We observed that the luminescence and reflectance spectra of the CuI coating varied greatly with the action of iodine vapors or oxygen on the coating. The test tubes with the CuI coating (first evacuated to a pressure of $p \approx 5 \times 10^{-3}$ mm Hg) were filled with iodine vapor or oxygen at room temperature. Examination of the spectra at the temperature of liquid nitrogen was made 20-30 min after the introduction of iodine or oxygen.

After admission of iodine vapors into the test tube with the CuI coating, the luminescence spectrum changed in the following way:

(a) the group of emission lines in the λ4070-4150 A region was strongly diffused forming two bands of λ4071-4112 A and 4118-4150 A;

(b) with the action of iodine, the broad bands in the 4180-4530 A region were preserved, but the equidistant structure of their short wavelength side (λ4180-4320 A) disappeared.

The reflectance spectrum of the CuI coating also varied under the influence of iodine vapors. The λ4095 A reflectance maximum disappeared (the λ4050 and 4065 A maxima were preserved). These changes in the luminescence and reflectance spectra are presented in the spectrogram (Fig. 1, b, d). On removal of iodine by evacuation with a vacuum pump, with simultaneous heating of the sample at T = 100°C for 30-60 min, the initial form of the emission and reflectance spectra was restored (Fig. 1, a, c).

The form of the luminescence and reflectance spectra of CuI also changed in such a way with the action of oxygen on the coating for 20-30 min at room temperature. However, in the emission spectrum of the sample at T = 77°K, the narrow lines in the λ4070-4150 A region are diffused to a lesser extent than with the action of iodine. The appearance of an emission line at about λ4098 A which was not detected before the action of oxygen, can also be observed. In the reflectance spectrum the maximum at about λ4095 A disappears. These variations in the spectra, as in the case of the interaction of iodine also, are completely reversible, and with removal of oxygen by evacuation (vacuum pump) with simultaneous heating of the CuI coating at T = 100°C for 1.5-2 hr, the luminescence and reflectance spectra reversibly acquire the same form as before the interaction with oxygen. On subsequent repetition of this cycle, the reflectance and emission spectra vary reversibly as stated above.

Investigation of the relationship of the emission and reflectance spectra of CuI powder, with interaction of iodine or oxygen, led to no definite results.

2. CuBr. In the spectrum of thin films and coatings of CuBr, at low temperatures, in the long wavelength absorption region, there is[7-9] a series of narrow absorption lines located in the λ3970-4170 A range.

In the reflectance spectrum of CuBr coatings at T = 77°K, we have observed two reflectance maxima at λ3970 and 4163 A, coinciding in wavelength with the absorption lines. The emission spectrum of the CuBr coating at T = 77°K consists of a group of narrow lines of different intensity at λ4154, 4174 (strongest), 4196, 4224, and

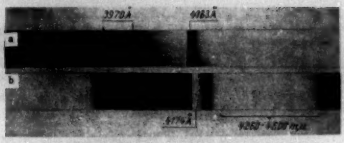

Fig. 3. Absorption (a) and luminescence (b) spectrum of CuBr coating at T = 77°K.

4250 A, and a band of λ4260-4600 A (Fig. 3, a, b). A similar group of narrow lines and a broad band are observed in the emission spectrum of CuBr powder, but the relative intensity of the lines is different (Fig. 4, b).

Under the action of evacuation with heating (by method described above) the emission spectrum of CuBr powder varied considerably,* thus:

*Variability in the emission spectrum of CuBr powder was observed also in Shvist's work.[10]

(a) the intensity of the λ4174 and 4196 A lines was much weakened;

(b) new intense equidistant emission lines of λ4216, 4242, 4271, 4300, and 4330 A appeared. The distance between these lines amounts to 30 A (Fig. 5, b).

Fig. 4. Reflectance (a) and luminescence (b) spectrum of CuBr powder at T = 77°K.

If oxygen is introduced into the evacuated test tube with the CuBr powder, the effect of the evacuation is annihilated, and the emission spectrum acquires its original form (Fig. 5, a). On subsequent repetition of evacuation and the action of oxygen, a complete reversibility in the form of the spectrum was observed.

Fig. 5. Variability in the luminescence spectrum of CuBr powder at T = 77°K. a—Luminescence of the powder before heating in vacuum; b—luminescence of powder after heating in vacuum.

The emission spectrum of the CuBr coating varied with the interaction of oxygen, but we were unable to establish a definite relationship in the variation of the spectrum.

3. CuCl. The discrete structure of the absorption

region of CuCl at T = 77°K was located in the λ3760-3850 A range.[4, 5, 7, 8] In the reflectance spectrum of the sublimed coating and of the finely crystalline CuCl powder, two reflectance maxima were observed at λ3765 and 3850 A,[7] which corresponded to the strong absorption lines (Fig. 6, a, b).

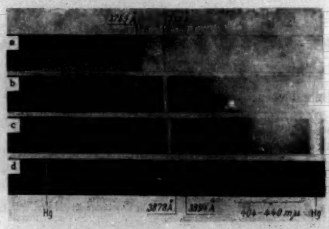

Fig. 6. Absorption, reflectance, and luminescence spectra of CuCl at T = 77°K. a—Absorption spectrum of coating; b—reflectance spectrum of coating; c—luminescence spectrum of coating; d—luminescence spectrum of powder.

The emission spectrum of the CuCl coating, as with the emission of CuI and CuBr also, consists of a group of narrow lines at λ3840, 3850, 3878 A,[8] and 3894 A (width of 20 A) and a λ4040-4400 A band. The emission spectrum of finely crystalline CuCl powder is distinguished by the fact that the λ3878 A line, very sparp in the emission of the coating, is diffused in the case of the powder (Fig. 6, c, d).

With evacuation, the action of oxygen or chlorine on the emission and reflectance spectra of CuCl coating and powder, revealed no appreciable variations.

Summarizing the results obtained, the following can be noted:

1. We turn our attention to the general similarity of the reflectance and luminescence spectra of the copper halides studied.* Actually, the long wavelength absorption regions of CuCl, CuBr, and CuI do not differ greatly as to their positions in the spectrum. In all of these substances, in the range of the long wavelength absorption region there are reflectance maxima coinciding with absorption lines. In the luminescence spectrum of CuCl, CuBr, and CuI a group of narrow emission lines is also observed, the shortest wavelength of which coincides with the corresponding absorption lines. Longer wavelength broad bands are also present in the emission spectra of all three halides.

2. A substantial influence of gases on the line spectrum structure was observed. In the luminescence spectrum of CuI (coating), with the action of gases on the sample, a portion of the lines is diffused. Moreover, in the reflectance spectrum of the coating the maximum of about λ4095 A disappeared; at the same time, the weak short wavelength emission lines did not change appreciably.

On evacuation with simultaneous heating, the emission lines in the luminescence spectrum of CuBr were much weakened, and new lines, shifted somewhat toward the long wavelength side, appeared.

3. Attention should be called, first, to the capacity of the emission and reflectance spectra of CuI and CuBr to revert to their initial form after removal of the gas from the surface of the substance; secondly, to the fact that this process of variation of the spectrum and its return to the initial condition can be reproduced repeatedly on the same sample. These two facts indicate that the changing portion of the luminescence spectrum can be caused by a gas adsorbed by the surface of the substance.

4. A group of equidistant emission lines is present in the luminescence spectrum of CuI and CuBr. Most authors associate the similar equidistant structure also observed in the emission spectra of a number of different semiconductor crystals (CdS, CdSe, ZnS, ZnO, etc) with lattice vibrations. Although this phenomenon appears to be general for semiconductor crystals, in a number of cases no equidistant structure was observed (particularly for CuCl). It seems, therefore, that certain conditions are required (for example, low temperature, presence of impurities, lattice defects, surface condition, etc.) for the appearance of this structure in the luminescence of a crystal.

Thus, the results obtained apparently make it possible to conclude that the short wavelength weak emission lines of CuI, CuBr, and CuCl, coinciding with the absorption lines and not changing appreciably with interactions on the surface, are associated with the fundamental lattice of the substance.

At the same time, the variable long wavelength strong emission lines, very sensitive to the treatment of the surface of the sample, can be more readily associated with phenomena occurring on the surface of the substance. It should be noted that the variability in the copper halide spectra appears to an even greater extent than the well-known variability in the strong narrow emission lines in the spectra of CdS crystals.[12]

The facts described in this work indicate that surface phenomena exert a substantial effect on the structure of the emission spectra of crystals.

*Kokhanenko[4] indicated some similarity in the absorption spectra of CuCl and CuI. The general similarity of the reflectance and luminescence spectra of the copper halides was also noted in the recent work of Nikitine.[11]

REFERENCES

1. H. Fesefeldt and Z. Gyulai. Gött. Nachr. 226 (1929).
2. F. Seitz. Revs. Modern Phys. 23, 328 (1951).
3. E. G. Schneider and H. M. O'Bryan. Phys. Rev. 51, 293 (1937).
4. P. N. Kokhanenko. Izvest. Akad. Nauk SSSR, Ser. Fiz. 15, 685 (1951); Zhur. Eksptl. i Teoret Fiz. 26, 120 (1954); Zhur. Eksptl. i Teoret. Fiz. 30, 30 (1956); P. N. Kokhanenko and V. D. Gol'tsev. Doklady Akad. Nauk SSSR 85, 543 (1952).
5. K. V. Shalimova. Dokt. Diss. (Doctor's dissertation), 1952;
K. V. Shalimova and N. S. Mendakov. Zhur. Eksptl. i Teoret. Fiz. 26, 247 (1954).
6. J. T. Randall. Trans. Faraday Soc. 35, 1 (1939); Nature 142, 113 (1938).
7. S. Nikitine and R. Reiss. Compt. rend. 242, 1003 (1956); Compt. rend. 245, 52 (1957); J. phys. radium 17, 1017 (1957);
S. Nikitine, R. Reiss, and G. Perny. Compt. rend. 242, 1588 (1956); Compt. rend. 242, 2540 (1956);
S. Nikitine. J. Chimie Phys. 55, 621 (1958).
8. E. F. Gross and A. A. Kaplyanskii. Opt. i Spektr. 2, 204 (1957);
A. A. Kaplyanskii. Izvest. Akad. Nauk SSSR, Ser. Phys. 21, 531 (1957).
99. B. S. Razbirin. Diplomnaya rabota. (Diploma Report), Leningrad. Gosudarst. Univ., 1956.

10. P. Shvist. Opt. i Spektr. 4, 801 (1958).
11. S. Nikitine. J. phys. radium 19, S21 (1958).
12. E. F. Gross and M. A. Yakabson. Doklad na I Vsesoyuznom soveshchanii po fotoelektricheskim i opticheskim yavleniyam in poluprovodnikakh. 20-26 noyabrya 1957, Kiev. (Proceedings of the First All-Union Congress on Photoelectric and Optical Phenomena in Semiconductors, November 20-26, 1957, Kiev).

A PHOTOGRAPHIC METHOD OF MEASURING THE OPTICAL CONSTANTS OF METALS

I. N. Shklyarevskii and A. I. Sharapov

Received 5 June 1959

A method of measuring the optical constants of metals in the visible and ultraviolet regions of the spectrum is described. Measurements of the optical constants of antimony in the visible region of the spectrum are reported.

INTRODUCTION

The polarization method of measuring the optical constants of metals in the visible[1] and infrared regions of the spectrum[2,3] based on the use of multiply reflected light from two uniform samples in parallel arrangement was developed earlier. This method, generally speaking, is useful in the ultraviolet region of the spectrum; naturally, suitable polarizing prisms and radiation receivers must be used in the apparatus.

By the use of the same principle as in the method mentioned above, and in a somewhat modified form of measurement and calculation, it is possible to measure the optical constants of metals more simply. Our proposal of a photographic method of measuring the optical constants of metals in the visible and ultraviolet regions of the spectrum is certainly preferable by comparison with the well known methods of Voigt[4,5] and Pfestorf,[6] since it does not require the use of compensators.

METHOD OF MEASUREMENT

A sketch of the equipment is shown in Fig. 1. Here O is the light source, P the polarizer, A the analyzer, 1 and 2, samples mounted on the table of a goniometer, S the spectrograph slit, L_1 and L_2 achromatic lenses.

Collimated white light passes through the equipment at an angle of 45° with the plane of incidence of the polarizer, is reflected from the samples and passes through the analyzer and is focused on the spectrograph slit. If the angle of incidence of light φ_1 on the sample is chosen reasonably, then for some wavelength λ_1 in the whole spectrum the phase difference $m\Delta$ for m-tuple light reflection from samples will be equal to $-180°$. In order to extinguish this at these wavelengths the analyzer must be rotated by the angle ψ' which is connected with

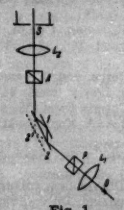

Fig. 1

the azimuth of the restored polarization angle ψ by the relation

$$\tan\psi = \sqrt[3]{\tan\psi'}. \qquad (1)$$

The remaining wavelengths at a given incidence angle and a given position of the analyzer pass through the polarizer-sample-analyzer system. In this way the whole spectrum is photographed on the plate, with the exception of a narrow band at λ_1. If the comparison spectra are photographed side by side, then with their help it is easy to locate λ_1, the middle of the suppressed band.

It should be noted that if the analyzer is not accurately rotated through the angle ψ' (the error tolerance 5° to 6°), then instead of complete extinction of the spectrum at λ_1 the light will be partially extinguished. Naturally, the location of the minimum in the spectrum (λ_1) does not depend on the position of the analyzer. Since complete extinction of light in the photographic method of recording intensities is very difficult to distinguish from partial extinction, the accurate determination of the azimuth of restored polarization is impossible. Nevertheless, the fact that λ_1 may be determined for a given angle of incidence φ_1 by a rather coarse setting of the analyzer is an advantage of this method. This rough analyzer position is easily found, needing only a few test prints.

To determine the wavelength λ_1 corresponding to a given angle of incidence φ_1, the spectrum at the angle of incidence φ_2, was again photographed and the wavelength of the middle of the successor extinguished band was found. It is easy in this case to take into consideration where the analyzer should be rotated in the measurement of the angle of incidence of light in order to observe practically complete extinction of light of wavelength λ_1. Fifteen photographs are sufficient to encompass the whole of the visible and ultraviolet regions of the spectrum.

A series of photographs made in the indicated manner allows the plotting of the relation $\varphi = f_1(\lambda)$ for $\Delta_1 = -60°$ (triple reflection). The analogous relation $\varphi = f_2(\lambda)$ is plotted on the same graph from fivefold reflection from samples where $\Delta_2 = -36°$. With the help of these curves for any wavelengths it is possible to determine two pairs of values φ_1, $\Delta_1 = -60°$ and φ_2, $\Delta_2 = -36°$.

The photographic method of measuring optical constants of metals, in contrast to the majority of known methods, does not demand a stabilized light source. In the ultraviolet region the line spectrum of the iron spark is perfectly useful in place of a continuous spectrum. The minimum blackening on the spectrogram was found best with the aid of an MF-2 or MF-4 microphotometer.

COMPUTATION OF THE OPTICAL CONSTANTS

The phase difference Δ and the incidence angle φ are connected with the quantities a and b (see formula (6) in reference 1) through the following equation

$$\tan\Delta = \frac{2b\sin\varphi\tan\varphi}{\sin^2\varphi\tan^2\varphi - a^2 - b^2}. \qquad (2)$$

The quantities a and b in their turn are related to the optical constants μ and $\mu\chi$ of a metal and the angle of incidence by the equations

$$\left.\begin{aligned}\mu &= \left[\frac{1}{2}(a^2 - b^2 + \sin^2\varphi) + \frac{1}{2}\sqrt{(a^2 - b^2 + \sin^2\varphi)^2 + 4a^2b^2}\right]^{1/2}\\ \text{and}\\ \mu\chi &= \left[-\frac{1}{2}(a^2 - b^2 + \sin^2\varphi) + \frac{1}{2}\sqrt{(a^2 - b^2 + \sin^2\varphi)^2 + 4a^2b^2}\right]^{1/2}.\end{aligned}\right\} \qquad (3)$$

From the two Eqs. (2) written for φ_1, Δ_1 and φ_2, Δ_2, respectively, it is found that

$$b = \frac{\tan\Delta_1\tan\Delta_2(\sin^2\varphi_1\tan^2\varphi_1 - \sin^2\varphi_2\tan^2\varphi_2)}{2(\tan\Delta_2\sin\varphi_1\tan\varphi_1 - \tan\Delta_1\sin\varphi_2\tan\varphi_2)} \qquad (4)$$

and

$$a = \sqrt{\sin^2\varphi_1\tan^2\varphi_1 - b^2 - 2b\cdot\cot\Delta_1\sin\varphi_1\tan\varphi_1}. \qquad (5)$$

In the computation of the index of refraction μ and the absorption coefficient $\mu\chi$ from Eq. (3) it is necessary to substitute

$$\sin^2\varphi = \frac{1}{2}(\sin^2\varphi_1 + \sin^2\varphi_2). \qquad (6)$$

If $\sin^2\varphi_1 \approx \sin^2\varphi_2 \ll |\mu^2 - (\mu\chi)^2|$, then $\mu = a$ and $\mu\chi = b$.

The computation of the optical constants of a metal may be carried out by a graphical method. Actually, Eq. (2) after a simple transformation may be written in the form

$$a^2 + (b - \sin\varphi\cdot\tan\varphi\cdot\cot\Delta)^2 = \left(\frac{\sin\varphi\cdot\tan\varphi}{\sin\Delta}\right)^2. \qquad (7)$$

But (7) is the equation of a circle. Plotting the two circles for φ_1, Δ_1 and φ_2, Δ_2, respectively, and finding the coordinates of their points of intersection, determines the quantities a and b.

MEASUREMENT OF THE OPTICAL CONSTANTS OF ANTIMONY IN THE VISIBLE REGION OF THE SPECTRUM

For the experimental testing of our proposed method, measurements of the optical constants of antimony were made in the visible region of the spectrum. The lack of suitable polarizing prisms prevented us from making corresponding measurements in the ultraviolet region.

In Fig. 2, by way of illustration, two photographs are shown in which the decreasing density in certain parts of the spectrum, at a wavelength for which λ_{min} at the given angle of incidence on the sample gives a phase difference $m\Delta = -180°$, is very easily seen. Below each photograph the comparison spectrum is shown. Microphotometric traces allow enough accuracy to determine the wavelength λ_{min}. Corresponding photographs were made in the spectrum of the iron spark.

Through the plot of the curves $\varphi = f(\lambda)$ for three- and fivefold light reflection from metal surfaces, respectively, two pairs of values of φ and Δ were found, which were used for the calculation of the optical constants of antimony.

Fig. 2

The results of measurements of the optical constants of antimony are shown in the Table. The values of wavelength, light incidence angles φ_1 and φ_2 on the samples corresponding to $\Delta_1 = -60°$ and $\Delta_2 = -36°$, the index of refraction μ, and coefficient of absorption $\mu\chi$ of antimony are given in appropriate columns.

The optical constants of antimony were determined by polarization methods[1] in three- and fivefold reflection on the same pair of samples. The optical constants computed from measurements of the values of φ, ψ, and Δ agreed with great accuracy with the μ and $\mu\chi$ shown in the Table. The optical constants of antimony measured on different pairs of samples agreed well (within the accuracy of 3-5%) between themselves.

λ (mμ)	φ_1	φ_2	μ	$\mu\chi$
650	72°24′	63°27′	2.89	3.92
600	71 24	61 57	2.31	3.89
550	70 9	60 18	2.01	3.69
500	68 36	58 21	1.75	3.44
450	66 41	56 3	1.46	3.14

Some discrepancies between our measurements of the optical constants of antimony and those of Quincke[7] are noted. However, results of our measurements of the optical constants of antimony in the visible and infrared[8] regions of the spectrum agree very well among themselves.

N. Ya. Seraya and L. Ya. Seraya shared in the measuring of the optical constants of antimony.

The authors take this occasion to express their profound appreciation to K. D. Sinel'nikov for his consideration and interest in the work.

REFERENCES

1. I. N. Shklyarevskii and V. K. Miloslavskii. Opt. i Spektr. 3, 361 (1957).
2. I. N. Shklyarevskii, I. G. Starunov, and V. G. Padalka. Opt. i Spektr. 4, 792 (1958).
3. I. N. Shklyarevskii and V. G. Padalka. Opt. i Spektr. 6, 78 (1958).
4. W. Voigt. Physik. Z. 2, 303 (1901).
5. R. S. Minor. Ann. Physik. 10, 581 (1903).
6. Pfestorf. Ann. Physik. 81, 906 (1926).
7. Landolt-Bornstein, Physikalisch-Chemische Tabellen.
8. I. N. Shklyarevskii, A. A. Avdeenko, and V. G. Padalka. Opt. i Spektr. 6, 527 (1959).

THE DETERMINATION OF THE SIZE OF PARTICLES BY SCATTERING OF LIGHT
II. DETERMINATION OF THE SIZE OF GLOBULES OF THE POLYCHLOROPRENE LATEX BY MEANS OF OPTICAL AND ELECTRON-MICROSCOPE METHODS

I. Ya. Slonim, N. M. Fodiman, and Z. M. Ustinova

Received 28 April 1959

1. THE INFLUENCE OF POLYDISPERSION ON DETERMINATION OF THE SIZE OF PARTICLES BY THE SCATTERING OF LIGHT.

The formulas[1] formerly derived for calculating the radius of a particle from the measurements of light scattering, pertain to a monodispersed system. Should we apply this formula to a polydispersed system, we would obtain a certain effective mean value (a) of the radius of particles of a monodispersed system which scatters the light in the same manner as the system under investigation.

It is expedient for the characterization of a polydispersed system to use two kinds of the mean values of the radius; one is the mean-numerical a_n and the other is the mean-weighed a_w defined by the following formulas:

$$a_n = \left(\frac{\sum \nu_i a_i^2}{\sum \nu_i}\right)^{1/2} \tag{1}$$

and

$$a_w = \left(\frac{\sum \nu_i a_i^6}{\sum \nu_i a_i^3}\right)^{1/3}, \tag{2}$$

where ν_i is the number of particles of radius a_i.

Using these definitions, we obtain, as is customary in studies of polymers, the mean-numerical and the mean-weighed weight of the particles as given, respectively, by the products $(4/3)\pi a_n^3 d$ and $(4/3)\pi a_w^3 d$ (d is the specific gravity).

For particles relatively smaller than the wavelength of the incident light, the Rayleigh equation is applicable. Then the intensity of scattering, with a constant weight concentration, is directly proportional to the third power of the radius. In this case, as is known,[2] the value a_w is determined from the scattering measurements.

If the size of particles is greater than $\lambda/10$, the intensity of scattering does not become directly proportional to the third but to some lower power of the radius. In this case, the formulas derived on the basis of the Shifrin theory are valid in the first approximation:

$$\tau = \frac{\alpha^2}{\lambda} c_{vol} \varphi(z) \tag{3}$$

and

$$\frac{I_{45}}{I_0} = \frac{\alpha^2}{\lambda} c_{vol} \psi(z), \tag{4}$$

where τ is the turbity, I_{45} is the intensity of light scattered at an angle of 45°, I_0 is the intensity of the incident light, $\alpha = 3(m^2 - 1)/4\pi(m^2 + 2)$, m is the relative index of refraction of the particle, $z = 8\pi a/\lambda$, c_{vol} is the volume concentration, and $\varphi(z)$ and $\psi(z)$ are the functions whose values are given in reference 1.

The character of the mean values of the radius of the particle, obtained as the result of computation, depends on the form of the function of the size distribution of particles. The problem of light scattering by a polydispersed system with spherical particles commeasurable with wavelength presents great difficulties; in so far as we know, this problem has been solved only for the case of a specially selected distribution function.[3]

By transforming Eqs. (3) and (4) as shown below, one may obtain some idea about the nature of the mean values that may result:

$$\tau = k_1 c_{vol} a^{n_\varphi} \tag{5}$$

and

$$\frac{I_{45}}{I_0} k_2 c_{vol} a^{n_\psi}, \tag{6}$$

where k_1 and k_2 are constants, and the exponents n_φ and n_ψ are by themselves functions of the size of particles. Taking into consideration that, at low concentrations of suspensions, the intensities of light scattered by separate particles add up, that is:

$$\tau = \sum \tau_i = k_1 \sum c_{vol\,i} a_i^{n_\varphi}, \tag{7}$$

and the volume concentration is equal to the sum concentration of the fractions:

$$c_{vol} = \sum c_{vol\,i} \tag{8}$$

and

$$c_{vol\,i} = \nu_i \cdot \frac{4}{3} \pi a_i^3, \tag{9}$$

we find that the mean value a_τ of the radius, obtained from the measurements of the optical density, is determined by the following expression:

$$a_\tau = \left(\frac{\sum \nu_i a_i^{n_\varphi+3}}{\sum \nu_i a_i^3}\right)^{\frac{1}{n_\varphi}}. \tag{10}$$

Analogously, for the mean value a_I, determined from the intensity of scattering at an angle of 45°, we have:

$$a_I = \left(\frac{\sum \nu_i a_i^{n_\psi+3}}{\sum \nu_i a_i^3}\right)^{\frac{1}{n_\psi}}. \tag{11}$$

For small particles, n_φ and n_ψ are equal to 3, and Eqs. (10) and (11) reduce to (2) ($a_\tau = a_I = a_w$). For large particles, n_φ and n_ψ are less than 3. The following expressions can be used for computing n_φ and n_ψ:

$$n_\varphi = \frac{\Delta[\log \varphi(z)]}{\Delta \log z} \tag{12}$$

and

$$n_\psi = \frac{\Delta[\log \psi(z)]}{\Delta \log z}, \tag{13}$$

These expressions are obtained by substituting $a = z\lambda/8\pi$ in (5), equating (5) and (3), and then taking the logarithms of both sides.

Using the values of $\varphi(z)$ and $\psi(z)$ computed in reference 1, we find that when $z = 2$, $n_\varphi = 2.81$ and $n_\psi = 2.95$; and when $z = 8$, $n_\varphi = 1.33$ and $n_\psi = 2.04$. The values n_φ and n_ψ decrease as z increases; furthermore, in the whole interval from $z = 2$ to $z = 8$, $n_\psi > n_\varphi$, which is phys-

ically conditioned by the forward spreading of the indicatrix of dispersion when the size of particles increases. When z changes from two to eight, the exponent of a_1 in the numerator of Eq. (10) diminishes from 5.81 to 4.33 and in Eq. (11) from 5.95 to 5.04; while in Eq. (2) for computation of a_w this exponent is equal to 6. It is obvious that the computation of a from τ and from I_{45} will yield the mean values of radii which are intermediate between the mean-numerical and mean-weighed; furthermore, a_1 is nearer to the mean-weighed than a_r. The value of ratio a_1/a_r may serve as a measure of the degree of polydispersion of the system.

2. EXPERIMENTAL PART

In this work measurements were made of the size of the globules of the polychloroprene latex.

Using as a base the latex with a dry residual of 45.3%, we prepared several dilutions for measuring the light scattering. To avoid coagulation, 1% solution of ammonia was added to the dilutions. The optical density was determined for dilutions from 1:3,333 to 1:10,000 using photoelectrocolorimeter-nephelometer FEK-N-54 and cells 5 cm long for four wavelengths. Nephelometer NFM with a turbid prism etalon was used for determining the intensity of the light scattered at an angle of 45°; the measurements were made for dilutions from 1:5,000 to 1:40,000.

Photographs of the latex were made by means of a Zeiss electrostatic electron microscope D-2, using a magnification of 8000 times. The sizes of the globules on the photographs were determined by means of measuring microscope MIR-12; 690 particles were measured.

3. THE RESULTS OF MEASUREMENTS AND THE DETERMINATION OF THE SIZE OF PARTICLES.

The results of the measurements of the optical density and of the light scattering are presented in Fig. 1 and in the Table.

λ (A)	[τ] (cm^{-1})	[I_{45}] (cm^{-1})	z	a (A)	Mean value (A)
2710	8500	—	5.97	644	a_r = 630
3110	5500	—	5.07	628	
3410	4150	—	4.81	624	
4020	2450	—	3.90	624	
4140	—	525	4.95	816	a_1 = 816

As can be seen from Fig. 1, the values $I_{45}/I_0 s_{vol.}$ and $\tau/s_{vol.}$ decrease with increasing concentration—as a result of the secondary scattering. In the second and third columns of the Table are given the values of the turbity $\tau = \lim (\tau/s_{vol.})$, and of the characteristic intensity of scattering:

$$[I_{45}] = \lim \frac{I_{45}}{I_0 c_{vol}}$$

for $s_{vol.} \to 0$, obtained through the graphic extrapolation toward $s_{vol.} = 0$. The values of parameter z and of the radius of the particles are given in the fourth and fifth columns; they were computed using the formulas and tables given in reference 1. In the computation, the following values were used for polychloroprene: the specific gravity d = 1.23,[4] the index of refraction = 1.558.[5]

A change of optical density D with wavelength corresponds to the value of the exponent in the equation $D = \text{const} \cdot \lambda^{-n}$; equal to n = 3.15, which yields a = 590 A.

As a result of the measurements on the electron microscope photographs, a curve was constructed (Fig. 2) of the weight distribution, and, in accordance with Eqs. (1) and (2), the values were computed, a_n = 590 A and a_w = 919 A.

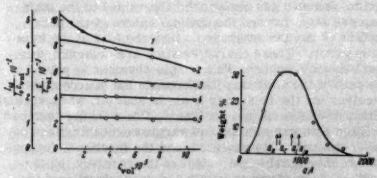

Fig. 1

Fig. 2

Fig. 1. The extrapolation toward the zero concentration, of the measurements of the light scattering by the latex. ●—$I_{45}/I_0 s_{vol.}$; —$\tau/s_{vol.}$. Wavelengths (in A): curve 1—4140, curve 2—2710, curve 3—3110, curve 4—3410, curve 5—4020.

Fig. 2. The curve of weight distribution of the globules of the latex.

The arrows in Fig. 2 indicate the mean-numerical and the mean-weighed radius of the particles; these values were obtained by means of the electron microscope method; the values a_r and a_1 were found by the optical method. In accordance with the theory, $a_n < a_r < a_1 < a_w$. Thus, the determination of the size of particles of the latex from light scattering, using the theoretical formulas for particles whose optical properties do not deviate much from those of the medium, gives results which are in satisfactory agreement with the results of electron microscope measurements.

REFERENCES

1. I. Ya. Slonim. Opt. i Spektr. 8, 98 (1960).
2. "Fizicheskie metody organicheskoi chimii." Vol. 4, IL, Moscow, 1955.
3. I. Rocard. Rev. Opt. 2, 97 (1930).
4. N. L. Catton. "Neopreny." (Neoprenes), Gosudarst. Nauch. Tekh. Izd. Khim. Lit., Moscow, 1958.
5. "Sinteticheskii kauchuk." (Synthetic Rubber), Gosudarst. Nauch. Tekh. Izd. Khim. Lit., Leningrad, 1957.

GAS CHARACTERISTICS OF AN OPTICO-ACOUSTIC GAS ANALYZER

A. O. Sall

Received 29 May 1959

The relationship between the signal from the gas and the signal from the total radiation flux, and the determination of their ratio by means of gas characteristics of a gas analyzer have each been investigated in detail.

One can obtain from the gas characteristics of an optico-acoustic gas analyzer[1, 2] the values of the main sources of error, and the optimal values of the parameters of the gas analyzer that correspond to the minimum error.[3] These characteristics are determined in the following manner. The sample chamber is placed in the path of the radiation flux between the source and the receiver (or the reference beam is shut off, when working with a double beam gas analyzer). The working chamber is filled with gas mixtures of varying concentrations of the component to be analyzed, and the functional dependence of the signal in the output of the receiver, on the product of the chamber length and concentration of the component is determined. As an example, such curves are depicted in Figs. 1 and 2 for an optico-acoustic gas analyzer used for the analysis of carbon dioxide and methane.* Here u is the product of concentration of the component in the mixture to be analyzed, and of the length of the sample chamber; w is the product of the concentration of the component in the beam-receiving cylinder, and the light path. The ordinate is the signal value in relative units.

*The path length in the beam-receiving cylinder of the optico-acoustical radiation receiver was 50 mm, the frequency of interruption 6 hz.

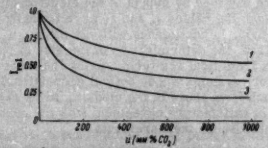

Fig. 1. Gas characteristics of an optico-acoustic gas analyzer for CO_2. Values of w: curve 1—5×10^2; curve 2—2.5×10^{-3}; curve 3—5×10^2.

Without the component to be analyzed in the sample chamber, the signal in the output of the receiver of an ordinary double beam gas analyzer is zero. After the mixture with the component is introduced into the sample chamber, a signal is produced in the receiver.

One of the main parameters which determine the error of an absorption gas analyzer is the quantity F—the ratio of the signal produced in the receiver by changing the concentration of the component in the mixture, to the signal produced in the receiver by the total radiation flux.[3] The value of F can be determined by means of the gas characteristics of the absorption analyzer. The radiation absorption by the gas in the beam-receiving cylinder of the radiation receiver is not uniform; it is strong near the chamber window and is weaker in the central parts of the chamber volume.[3] The heat produced in the thin flat layer in the vicinity of the chamber window is

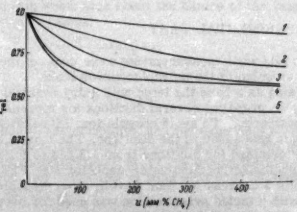

Fig. 2. Gas characteristics of an optico-acoustic gas analyzer for CH_4. Values of w: curve 1—5×10^2; curve 2—1.5×10^3; curve 3—5×10^2; curve 4—25; curve 5—100.

transferred to the window and does not participate in the excitation of sound vibrations. Let us call it the passive layer. The radiation corresponding to the part of the gas spectrum most intensively absorbed, is absorbed near the chamber window. The heat evolved thereby is transferred to the window. Because of this, at low frequency of interruption the sensitivity of the receiver has "deeps" in those spectral regions where the gas absorption of radiation is very intensive. The depth of these deeps depends on the thickness of the passive layer near the window of the beam-receiving chamber. This layer thickness depends on the depth of penetration of the thermal vibrations. The deeps in the spectral sensitivity curve disappear with increased frequency of interruptions. It should be mentioned that the presence of these deeps at increased frequency of interruptions results in a smaller decrease of the signal than would follow from the inverse proportionality between the signal and the frequency of interruptions (in some cases the signal is decreasing inversely proportional to the square root of the frequency).

Because of these "deeps," the gas characteristics depend not only on the values of u and w, but also on the thermal constants of the gas mixture, on the frequency of interruptions, and so forth. It can be assumed, in the first approximation, that the gas characteristics are determined by the values of u, w, and by the ratio η of the thickness of the passive layer to the path length in the beam-receiving chamber. In other words, in the first approximation it can be assumed $F = F(u, w, \eta)$. Let us consider this function in some detail. Assuming that the depth of the beam-receiving cylinder is considerably larger than the depth of penetration of thermal vibrations, and solving the generalized equation of heat transfer,[3] we obtain

$$F \simeq \frac{\int_0^\infty I\,(1-e^{-2\sigma u})(1-e^{-2\sigma w})\,d\nu - (1-Mi)\int_0^\infty I\,(1-e^{-2\sigma u})(1-e^{-2\sigma w\eta})\,d\nu}{\int_0^\infty I\,(1-e^{-2\sigma u})\,d\nu - (1-Mi)\int_0^\infty I\,(1-e^{-2\sigma u\eta})\,d\nu}$$

where k is the absorption coefficient and ν is the frequency.

Both the numerator and the denominator of the above expression are given by a difference of two integrals. The first integrals (minuends) represent the quantity of heat evolved in the volume of the beam-receiving cylinder, and the second integrals (subtrahends) represent, up to the factor (1 − Mi), the quantity of heat evolving in the thin passive layer at the window of the beam-receiving cylinder. The numerical value of M changes, as calculations show, from 1 to 0.4, in the transition from the ideal absorption (uniform throughout the chamber volume), when $kw \ll 1$, to the absorption following the square root law. The thickness of the passive layer changes thereby only little. A significant decrease of the thickness of the passive layer at the window of the beam-receiving chamber commences only when the nonuniformity of heat evolution in the gas volume is so great that practically all the radiation is absorbed in a layer which is smaller than the depth of penetration of the thermal vibrations. However, this case is seldom encountered in practice.

The imaginary unit in the above expression indicates that the signal produced in the receiver when the sample chamber is filled with the component to be analyzed, leads (in phase) the signal produced by the total radiation flux by an angle

$$\arctan\left[\frac{M\int_0^\infty I\,(1-e^{-kw})\,(1-e^{-kw\eta})\,d\nu}{\int_0^\infty I\,(1-e^{-kw})\,(e^{-kw\eta}-e^{-kw})\,d\nu}-\frac{M\int_0^\infty I\,(1-e^{-kw\eta})\,d\nu}{\int_0^\infty I\,(e^{-kw\eta}-e^{-kw})\,d\nu}\right].$$

The explanation is as follows. The difference of the sound pressures produced in the beam-receiving cylinders, after filling the chamber with the mixture to be analyzed and acting on the membrane of the microphone, is caused mainly by the change of radiation absorption in the spectral ranges where the maxima are located of the absorption lines of the component. Since the absorption coefficient in these spectral ranges is relatively large, the change of the radiation absorption inside the cylinder which is receiving the sample beam, occurs essentially near the window. However, the signal from the total flux is caused by the absorption of radiation by the whole line, including the wings, where the coefficient of absorption is relatively small. The radiation absorption in the latter case, is more uniformly distributed throughout the whole volume of the beam-receiving cylinder. Therefore the influence of the heat conduction will be smaller, and the phase shift between the overtone of the periodic change of the intensity of the radiation flux and the overtone of the acoustic pressure will have a different value.

With an increase in the mixture of the component to be determined, the phase shift between the signals decreases.

The phase shift between the signals will be negligible only in the two limiting cases: (1) when the depth of penetration of thermal vibrations is considerably larger than the length of the beam-receiving cylinder, and (2) when, to the contrary, the length of the beam-receiving cylinder and the window radius are considerably larger than the penetration depth of thermal vibrations.

Denoting by $F_0 = F_0(u, w)$ the ratio of signals for the limiting ideal case when the passive layer is absent ($\eta = 0$), we have for the signal ratio $F(u, w, \eta)$ for the real case (assuming $u \ll w$ and $0 < \eta \ll 1$)

$$F(u, w, \eta) = F_0(u, w)\left\{1-(1-Mi)\left[\frac{\int_0^\infty I\,(1-e^{-kw})\,(1-e^{-kw\eta})\,d\nu}{\int_0^\infty I\,(1-e^{-kw})\,(1-e^{-kw})\,d\nu}-\frac{\int_0^\infty I\,(1-e^{-kw\eta})\,d\nu}{\int_0^\infty I\,(1-e^{-kw})\,d\nu}\right]\right\}\simeq F_0(u, w)\,[1-(1-Mi)\,F_0(w_\xi\,\eta, u)],$$

where $F_0(w\eta, u)$ is the signal ratio when the product of the concentration of the component in the mixture and of the length of the sample chamber is $w\eta$, and the product of the concentration of the component in the beam-receiving cylinder and of the path length in the latter is equal u.

If, for instance, the absorption of radiation follows the square root law, then

$$F(u, w, \eta) = \sqrt{\frac{u}{w}}\left[1-(1-Mi)\sqrt{\frac{w\eta}{u}}\right]\simeq\sqrt{\frac{u}{w}}-\sqrt{\eta}+Mi\sqrt{\eta}.$$

Taking $M \approx 0.4$, we obtain a complete agreement with the expression given earlier.[3] On decreasing the ratio η, the gas characteristics become somewhat lower (the same values of u and w correspond to somewhat higher values of F).

Figures 1 and 2 depict the dependence of the quantity (1 − F) on the value of u, for different values of w. By using these curves one can find the ratio F = F (u, w). When the latter is expressed graphically, we obtain straight lines F = F (u, w) = const., given in Fig. 3 (for CO_2) and Fig. 4 (for CH_4).

If the radiation absorption by the component would follow strictly the square root law, then the values of u and w which correspond to the condition F = const. would be cinnected by the relationship u = f (F) · w for $\eta = 0$, that is, the straight lines F = const. would go through the origin of coordinates. In practice, the radiation absorption deviates from the square root law, and in addition $\eta \neq 0$. The curves F (u, w) = const. in the real case can be presented, in a fairly wide range of u and w, by the straight lines segments $u = u_0 + Hw$. The numerical values of u_0 and H (which depend on F) can be easily found by means of the gas characteristics for each design of the gas analyzer, and for each particular component to be determined.

The phase shift between the signals produced by the

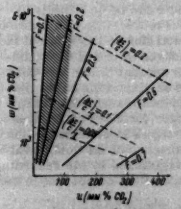

Fig. 3

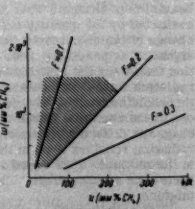

Fig. 4

Fig. 3. The range of permissible values for u and w in an optico-acoustic gas analyzer for CO_2.

Fig. 4. The range of permissible values for u and w in an optico-acoustic gas analyzer for CH_4.

sample and the reference beams, may in some cases be as high as several degrees. In the result for the gas analyzers with optical compensation (with a shutter in one of the radiation beams) or with electrical compensation in the source circuits[2] there is a residual signal in the output of the radiation receiver when the recording system is balanced. Let us denote the ratio of this signal to the signal from the total flux by $(\Delta F)_f$. This signal shifted 90° relative to the signal from the total flux may in many cases be a source of error. The error caused by the phase shift between the signals is largest at the end of the scale of the gas analyzer, because changes in concentration of the component in the mixture cause the smallest changes of the signal at the end of the scale, compared with other ranges of the scale. Let us denote by $(\Delta c)_f$ the change of concentration of the component in the mixture which produces at the end of the scale a signal, the absolute value of which is equal to the residual uncompensated signal. The phase shift can be evaluated quantitatively by the relative concentration change

$$\frac{(\Delta c)_f}{c} = \frac{(\Delta F)_f}{\frac{dF}{du} \cdot u},$$

where c is the concentration of the component in the mixture which corresponds to the end of the gas analyzer scale; $(\Delta F)_f$ is the ratio of the residual uncompensated signal corresponding to this concentration, and the signal from the total radiation flux.

The values of $(\Delta F)_f$ and of u(dF/du) for various values of u and w were experimentally determined for an optico-acoustic gas analyzer, and then the values of $(\Delta c)_f/c$ calculated. The dashed lines in Fig. 3 connect points with equal values of $(\Delta c)_f/c$, i.e. with an equal influence of the phase shift. It can be seen from these data that there is a considerable influence of the phase shift only in the gas analyzers with an optical or an electrical compensation. In the apparatus with gas compensation, the phase shift between the signals from the working and the comparison beams is considerably smaller, and the error caused by the residual uncompensated signal is negligible.

For the optico-acoustic gas analyzers with electrical compensation made in GSKB for construction of analytical instruments,[2] the ranges for u and w used in gas analyzers with various measurement limits correspond to the shaded parts of Figs. 3 and 4.

During the time between the periodical checkings of the zero adjustment of the gas analyzer, the signal from the total radiation flux (in the sample or in the reference beams) may change.[3] This change can be quantitatively evaluated by the quantity α equal to the ratio of a possible change of the signal from the total flux to the value of the signal. It is precisely these changes of one of the radiation fluxes (or the simultaneous unequal changes of both radiation fluxes) that determine in almost all cases the threshold sensitivity of a double-beam analyzer. When one of the radiation fluxes changes (or when both fluxes change in different amounts), a signal is produced in the radiation receiver even in the absence of the component in the mixture. This signal is registered by the recording system as a concentration change of the component in the mixture.

Let us define the threshold sensitivity Δc of a gas analyzer as such a change in concentration of the component which produces in the receiver a signal of the same magnitude. For the ratio of the signal produced in the receiver with the concentration change Δc, to the signal from the total radiation flux, we obtain

$$\left(\frac{dF}{du}\right)_{u=0} L\Delta c,$$

where L is the optical path length in the sample chamber, and $(dF/du)_{u=0}$ is equal to the absolute value of the tangent of the slope of the gas characteristics at u = 0. For a numerical evaluation of Δc this expression must be equated to α, that is,

$$\left(\frac{dF}{du}\right)_{u=0} L\Delta c = \alpha.$$

Thus the sensitivity of a gas analyzer with respect to a certain component can be expressed by the product $L\Delta c\alpha^{-1}$. The numerical value of this product which depends on the optical selectivity of the beam-receiving cylinder is equal to the absolute value of the cotangent of the slope. From the inspection of the gas characteristics of an optico-acoustic gas analyzer for methane it can be seen (Fig. 2) that the absolute values of the cotangent of the slope first decreases with the decrease of methane concentration in the beam-receiving cylinder, reaches a minimum value at w ≈ 100 mm%, and increases again with a further decrease of w. The minimum value of $L(\Delta c)\alpha^{-1}$ is approximately equal 100 mm% (i.e., for $\alpha = 10^{-3}$, and L = 100 mm, one obtains $\Delta c = 10^{-3}$%).

The sensitivity can be considerably increased by increasing the selectivity of the beam-receiving cylinder[3] (by decreasing the radiation absorption by the cylinder walls and by the chamber windows, by filtering off from the total flux those spectral ranges in which the admixtures of the gases in the beam-receiving cylinder are absorbing, etc.).

When the sensitivity of a gas analyzer is determined by the noise level in the radiation receiver (for instance, in a one-beam absorptiometer with a modulation of the number of molecules of the component in the path of the beam), for the determination of the sensitivity threshold it is necessary, instead of α, to use γ—the ratio of the noise signal to the signal caused by the total radiation flux.

Remeasuring the gas characteristics permits checking of the proper gas filling of the chamber of an optico-acoustic receiver.

The gas characteristics given in this paper were obtained with a gas analyzer constructed in GSKB for the construction of analytical instruments.[2] The gas characteristics for gas analyzers of a different design may differ somewhat from those given above.

REFERENCES

1. M. L. Veingerov. Doklady Akad. Nauk SSSR 19, 687 (1938); Doctor dissertation, Gosudarst. Opt. Inst., 1940; Zav. Lab. No. 4, 426 (1947).
2. B. A. Pavlenko. Sbornik Novye termoenergeticheskie proisvodstvennye pribory i regulatory (Collection: New Thermoenergetic Industrial Instruments and Regulators), Mashingis, 1953; Zav. Lab. No. 7, 868 (1954).
3. A. O. Sall. Priborostroenie, No. 6, 14 (1956); Zhur. Tekh. Fiz. 29, 33 (1959); Opt. i Spektr. 5, 316 (1958); Opt. i Spektr. 7, 432 (1959).

SHORT COMMUNICATIONS

RELATIONS BETWEEN THE INFRARED BAND INTENSITIES OF ISOTOPIC MOLECULES

L. M. Sverdlov

Received 25 May 1959

1. In previous investigations[1-6] relations between the vibrational frequencies of isotopic molecules were derived. It can be shown that similar rules hold also for the intensities of the infrared bands of a system of isotopic molecules.

As is well known,[6,7] the integrated intensity of the infrared band corresponding to the normal coordinate Q_l is given by the expression,

$$I_l = \int K_\nu d\nu = \frac{\pi N_1}{3c}\left(\frac{\partial P}{\partial Q_l}\right)^2. \qquad (1)$$

where K_ν is the absorption coefficient, ν the frequency, N_1, the number of molecules per unit volume, and c the velocity of light. The derivative of the dipole moment with respect to the normal coordinate, $\partial P/\partial Q_l$, can be expressed in terms of the derivatives of the dipole moment with respect to the natural vibrational coordinates, $\partial P/\partial S_k$, or with respect to the symmetry coordinates, $\partial P/\partial S_k^{(\chi)}$ ($S_k = \sum L_{k,l} Q_l$):

$$\frac{\partial P}{\partial Q_l} = \sum_k L_{kl}\frac{\partial P}{\partial S_k}. \qquad (2)$$

From this it follows that

$$\left(\frac{\partial P}{\partial Q_l}\right)^2 = \sum_{kj} L_{kl}L_{jl}\frac{\partial P}{\partial S_k}\cdot\frac{\partial P}{\partial S_j}.$$

Summing over all the n normal coordinates we obtain

$$\sum_{l=1}^{n} I_l = \frac{\pi N_1}{3c}\sum_{kj}\frac{\partial P}{\partial S_k}\cdot\frac{\partial P}{\partial S_j}\sum_{l=1}^{n} L_{kl}L_{jl} = \frac{\pi N_1}{3c}\sum_{kj}\frac{\partial P}{\partial S_k}\cdot\frac{\partial P}{\partial S_j}A_{kj}; \qquad (3)$$

taking into acount the fact that $\sum_{a=1}^{n} L_{kl}L_{jl} = A_{kj}$, where the A_{kj} are the kinematic coefficients which are linear functions of the reciprocals of the atomic masses, $\varepsilon_\alpha (\varepsilon_\alpha = m/m_\alpha)$.

In the case for which the molecule has no permanent dipole P_0, or for which, if P_0 is not equal to zero, the vibrations belong to symmetry species which do not include a rotation; the quantities $\partial P/\partial S_k$ (or $\partial P/\partial S_k^{(\chi)}$ are the same for all isotopic molecules. Thus $\sum_l I_l$ is a linear function of ε_α, and any power k of $\sum_l I_l$ will be a homogeneous polynomial of degree k in ε_α.

2. In reference 3 the following theorem was formulated. If we have a function of the type

$$\Phi_k^l(a_\alpha a_\beta \ldots a_\lambda) = \sum_j c_j [f_{j1}(m_{a_1}) f_{j2}(m_{a_2}) \ldots f_{jk}(m_{a_k})]$$

where the c_j are coefficients independent of the masses, $f_{jl}(m_l)$ is an arbitrary function of the mass of the l-th atom, the index k indicates the number of factors, and the index i is the number of substituted atoms which are specified in the brackets, then the function satisfies the following identity:

$$\sum_{i=0}^{k+1}(-1)^i C_{k+1}^i \Phi_k^i(a_\alpha a_\beta \ldots a_\lambda) = 0. \quad (k = 1, 2, \ldots, N-1). \qquad (4)$$

Here C_{k+1}^i denotes the number of different functions Φ_k^i which correspond to the molecules with i substituted atoms, and N is the number of atoms in the molecule.

Putting $\Phi_k^l = \left(\sum_l I_l\right)^k$, we obtain

$$\sum_{i=0}^{k+1}(-1)^i C_{k+1}^i \left(\sum_l I_l\right)^k (a_\alpha a_\beta \ldots a_\lambda) = 0. \quad (k = 1, 2, \ldots, N-1) \qquad (5)$$

We will call (5) the sum rule for powers of the sum of the intensities.

For k = 1 we obtain the intensity sum rule derived by Decius[8] by another method,

$$\sum_l I_l + \sum_l I_l(a_\alpha a_\beta) = \sum_l I_l(a_\alpha) + \sum_l I_l(a_\beta). \qquad (6)$$

In the derivation of (5) we have neglected the mechanical and electrical anharmonicities.[9] Moreover, one must take into account the conditions on the applicability of (5) which were referred to in paragraph 1. The rule in (5) can be applied, for example, to the isotopic molecules of methane, ethane, ethylene, benzene, and all other nonpolar molecules.

The rules derived for the intensities of isotopic molecules will be useful for checking the accuracy of a determination of the integrated intensities of a system of isotopic molecules and for calculating unknown intensities of infrared bands. In recent years a considerable number of investigations have been concerned with the experimental evaluation of absolute integrated intensities in infrared spectra, and in the next years the number of detailed investigations will quickly increase; the relations obtained above will then have a wide application in the analysis of these data. Finally, the relations (5) can serve as a control on the accuracy of theoretical calculations of the intensities of isotopic molecules. In this case they should be strictly fulfilled. If the systems of isotopic molecules have the same symmetry, relations (5) should be fulfilled for the vibrations of each symmetry species separately. In the opposite case it is necessary to take into account the rules for the correlation of the symmetry species of the point groups, and then the relations (5) will be fulfilled only for those species whose symmetry is retained; otherwise, it is necessary to use the general relations.

3. As examples we will consider the methane and ethane molecules and their deuterated species:

$$(\Sigma I_l)^3(CH_4) + 3(\Sigma I_l)^3(CH_3D_2) = 3(\Sigma I_l)^3(CH_3D) + (\Sigma I_l)^3(CHD_3);$$

$$(\Sigma I_l)^3(CH_4) + 6(\Sigma I_l)^3(CH_2D_2) + (\Sigma I_l)^3(CD_4) = 4(\Sigma I_l)^3(CH_2D) + 4(\Sigma I_l)^3(CHD_3);$$

$$(\Sigma I_l)^3(C_2H_6) + (\Sigma I_l)^3(i\text{-}C_2H_4D_2) + (\Sigma I_l)^3(s.\text{-}C_2H_4D_2) + (\Sigma I_l)^3(a.\text{-}C_2H_4D_2) = 3(\Sigma I_l)^3(C_2H_5D) + (\Sigma I_l)^3(\text{unsymm.-}C_2H_3D_3);$$

$$(\Sigma I_i)^3(C_6H_6) + 3(\Sigma I_i)^3(s\text{-}C_6H_4D_2) + 3(\Sigma I_i)^3(s.\text{-}C_6H_4D_2)$$

$$+ (\Sigma I_i)^3(s\text{-}C_6H_3D_3) = 4(\Sigma I_i)^3(C_6H_5D) + (\Sigma I_i)^3(1, 2, 3\text{-}C_6H_3D_3)$$

$$+ (\Sigma I_i)^3(s\text{-}C_6H_3D_3) + 2(\Sigma I_i)^3(\text{unsymm.-}C_6H_3D_3)$$

and so on. The following designations have been used here: t-$C_6H_4D_2$, s-$C_6H_4D_2$, a-$C_6H_4D_2$ are the isomers belonging to the point groups C_{2h}, C_{2v} and C_s, respectively; 1,2,3-$C_6H_3D_3$ to the group C_{3v}, s-$C_6H_3D_3$ to C_s; unsymm.-$C_6H_3D_3$ possesses no symmetry.

4. In conclusion it should be noted that relations similar to (5) are applicable also to the sum of the intensities in the Raman spectrum,* $\sum_{i=1}^{n} I_i'$, and also to the quantities* $\sum_{i=1}^{n} b_i'^2$ and $\sum_{i=1}^{n} g'^2$, since these are linear functions of the reciprocals of the atomic masses.[9] However, the applicability of these rules is more restricted. For their application it is necessary that the static polarizability tensor of the molecule possess spherical symmetry or, if this condition is not satisfied, that the vibrations refer to those symmetry species which do not include a rotation.

*$I_i' = I_i\{[1-\exp(-h\nu_i/kT)]\nu_i/(\nu - \nu_i)^4\}$, where ν is the frequency of the exciting line, ν_i the frequency of the vibration and I_i the intensity of the Raman line.

*$b_i'^2$ and $g_i'^2$ are the trace and the anisotropy, respectively, of the optical polarizability tensor.

REFERENCES

1. L. M. Sverdlov. Doklady Akad. Nauk SSSR 78, 1115 (1951).
2. L. M. Sverdlov. Doklady Akad. Nauk SSSR 86, 513 (1952).
3. L. M. Sverdlov. Doklady Akad. Nauk SSSR 88, 249 (1953).
4. L. M. Sverdlov. Doklady Akad. Nauk SSSR 94, 451 (1954).
5. L. M. Sverdlov. Opt. i Spektr. 8, 36 (1960).
6. M. V. Vol'kenshtein, M. A. El'yashevich, and B. I. Stepanov. "Kolebaniya molekul." (Vibrations of Molecules), Gosudarst. Izd. Tekh.-Teoret. Lit., Moscow, 1949.
7. E. B. Wilson, J. C. Decius, and P. C. Cross. "Molecular Vibrations." McGraw-Hill, New York, 1955.
8. J. C. Decius. J. Chem. Phys. 20, 1039 (1952).
9. B. L. Crawford. J. Chem. Phys. 20, 977 (1952).

A NOMOGRAM FOR CALCULATING THE DIAMETER OF PARTICLES FROM TURBIDITY BY MEANS OF THE MIE EQUATION

I. Ya. Slonim

Received 1 June 1959

In previous communications,[1] formulas were derived for determining the size of particles in suspensions by light scattering, and nomograms were constructed on the basis of the approximate equations of Shifrin's theory. The accuracy of these formulas is of the order of 5% when the ratio of the index of refraction of the particle to that of the medium is $m \leq 1.50$ and the diameter of particles is not greater than 0.64 of the wavelength of the light. An increase in the accuracy and range of particle sizes can be obtained by using the light scattering tables based on the Mie theory.[2] As was shown for the case of synthetic latexes,[3] the sizes of latex globules determined by the turbidity of suspensions agree to within 0.33% with the values obtained by the electron microscopy method. The Tables[2] give the values of the coefficient of light scattering K, defined by

$$\tau = K\pi a^2 N_1, \qquad (1)$$

where τ = turbidity of suspension (cm^{-1}), a = radius of the particles (cm) and N_1 = the number of particles per unit volume of suspension ($1/cm^3$). The values of K correspond to various m and a number of values of the parameter ρ.

$$\rho = \frac{2\pi a}{\lambda} = \frac{\pi D}{\lambda}, \qquad (2)$$

where D is the diameter of particles and λ is the wavelength of light in the medium, which is equal to the wavelength in vacuum divided by the index of refraction of the medium. By measuring the optical density at several concentrations it is possible, by means of a graphical extrapolation, to obtain the characteristic turbidity τ.

$$[\tau] = \lim\left(\frac{\tau}{C_v}\right)_{C_v \to 0}, \qquad (3)$$

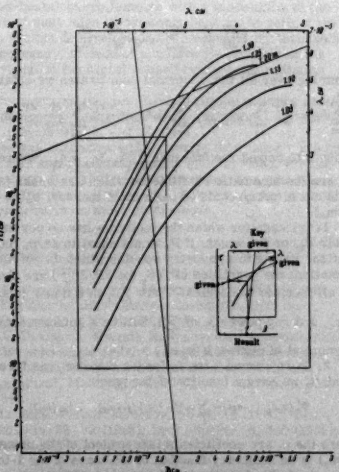

Nomogram for determining the diameter of particles from turbidity. Example: Given $[\tau]$ = 2550 cm^{-1}; $\lambda = 6.28 \times 10^{-5}$ cm; m = 1.20. Answer: $D = 2 \times 10^{-3}$ cm.

where C_v is the partial volume of particles in suspension.

Substituting the value of $N_1 = 3C_v/4\pi a^3$ into (1), we obtain the formula:

$$[\tau] = \frac{3K}{4\pi}, \quad (4)$$

showing that the turbidity of the suspension can easily be determined if the size of particles is known.

The reverse problem—the determination of the particles size from $[\tau]$—is easily solved with the aid of the equation

$$\frac{K}{\rho} = \frac{2[\tau]\lambda}{3\pi}, \quad (5)$$

obtained from (2) and (4). For the computation it is necessary to have a table of $K/\rho = f(m,\rho)$.

For facilitating computation in the region of m = 1.05 to 1.30, which is particularly important in studying dispersions of polymers, a nomogram has been constructed, the use of which is clear from the key and example (see the illustration). The lower limit of values of ρ for which the nomogram was constructed is 0.2 for all m. For $\rho < 0.2$, one may use the Rayleigh equation with an error of less 0.4%. The upper limit of values of ρ is from 5 (for m = 1.30) to 15 (for m = 1.10 and 1.05). For still greater values of ρ, the turbidity vs particle diameter curve passes through a maximum; in this case the unique determination of D is impossible. The accuracy of computation by means of the nomogram is of the order of 1 to 2%.

REFERENCES

1. I. Ya. Slonim et al. Opt. i Spektr. 8, 98, 243 (1960).
2. N. J. Pangonis, W. Heller, and A. Jacobson. "Tables of Light Scattering Functions for Spherical Particles." Detroit 2, Michigan, 1957.
3. P. M. Tabibian, W. Heller, and J. W. Epel. J. Colloid Sci. 11, 195 (1956).

INFRARED ABSORPTION SPECTRA OF A MICROPOROUS GLASS DURING ADSORPTION OF METHANOL AND PHENOL FROM SOLUTIONS IN CARBON TETRACHLORIDE

A. M. Bogomolny and Yu. A. Lyubimov

Received 16 June 1959

Spectroscopic investigations of the adsorption of molecules both from vapors[1-4] and from solutions[5,6] on silica gel, microporous glass, and alum silicates showed that a gradual weakening in intensity of the first overtone band of surface OH-groups occurred with increasing coverage of the adsorbent surface. The discovery of steps in adsorption isotherms and the extreme changes in the isotherms of integral heats of adsorption of phenol from a heptane solution on silica gel[7] indicate that the adsorption process is complex.

In the present investigation, a detailed study was carried out of intensity changes of the first overtone band of the surface OH-groups (and several other bands) of microporous glass during adsorption of methanol and phenol from dilute solutions in carbon tetrachloride. In the work a double-beam infrared spectrometer IKS-2 with a quartz prism (F-1) was used. The spectral slit-width in the 7000 and 5000 cm^{-1} region was 44 and 30 cm^{-1}, respectively. The magnitude of the band intensity was reproducible within 5%. Samples of microporous glass, 8.5 mm wide, obtained by a method described previously,[1] were used as the adsorbent. The specific surface of the samples was 275 m^2/gm. Before each series of experiments, in order to reduce the surface, the samples were subject to etching in nitric acid vapors for 10 hr with subsequent thorough washing in distilled water, and then were annealed at a temperature of 300°C for 12 hr, in vacuum. After this, the samples were placed in a cell with solutions of various concentrations and were left there for 12-15 hr in order to establish an adsorption equilibrium.

In the absorption spectrum of a sample annealed at 300° in vacuum and then placed in pure carbon tetrachloride, the following bands were observed: a narrow, strong band at 7250 cm^{-1}, a weak band at 5290 cm^{-1}, and a band average in intensity with a maximum at about 4470 cm^{-1}.

The first band near 7250 cm^{-1}, according to literature data,[4,8] is the first overtone of the stretching vibration of the surface OH-groups. The decrease of its frequency by 75 cm^{-1}, according to Filimonov,[8] can be explained by the influence of the vehicle (CCl_4). After annealing in vacuum at 500°C its intensity decreased twofold, and at 700°C it completely disappeared. The more rapid decrease in intensity of this band in comparison with that described by Yaroslavskii[4] may possibly be explained by the fact that our sample was very porous and therefore sintered at a lower temperature.

The second band near 5290 cm^{-1} disappears after annealing the sample at 500°C. This band evidently corresponds to the 5250 cm^{-1} band which was interpreted by Yaroslavskii[4] as a combination of fundamental stretching and bending vibrations, $\nu_{OH} + \delta_{OH}$, of adsorbed water. The shift of the band by 40 cm^{-1} is probably explained by the influence of the vehicle.

The third band, near 4470 cm^{-1}, according to our data, possesses the following properties: (1) the shape of the band observed in the spectrum of a sample annealed in vacuum at 300°C has a distinct asymmetry; (2) annealing the sample at 500° causes splitting of the band with the appearance of absorption maxima at about 4400 and 4500 cm^{-1}; (3) a band is retained after annealing the sample in vacuum at 700°C; (4) during adsorption of phenol and methanol the band intensity is noticeably changed.

At this time a convincing interpretation of this band is not available in the literature. It is possible that it consists of two independent bands—the second overtone of the bending vibration of the surface OH-groups and one of the overtones of vibrations of the atoms in SiO_4 tetrahedrons. This interpretation makes it possible to explain, on the one hand, the susceptibility of the band to adsorption and, on the other hand, its presence in the spectrum of a sample annealed at 700°C.

During analysis of the absorption spectra of microporous glass which contained different amounts of the adsorbing molecules of methanol and phenol the following regularities in the behavior of the bands discussed above were observed: (1) with an increase of solute concentration the band intensity changed extremely; it peri-

odically increased and decreased (see the Figure); (2) in the case of methanol, the maxima and minima of all three bands coincide, i.e., are found at the same concentrations,* in the case of phenol, this coincidence is also found for the 7250 and 4470 cm^{-1} bands; (3) the indicated effect of alternate increase and decrease of band intensity occurs approximately within the range of a monolayer, within which, as the solute concentration increases, the effect becomes less noticeable.

*In the figures the abscissae show the concentration C of the resulting solutions.

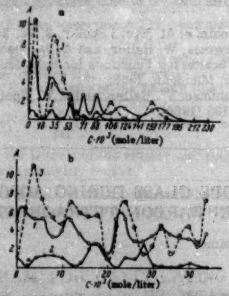

The dependence of relative intensities A of absorption bands of microporous glass on the adsorption of methanol (a) and phenol (b) from solutions of different concentrations in CCl_4. Frequency of the absorption bands (in cm^{-1}): 1—7250; 2—5290; 3—4470.

The results presented above were obtained from two different series of measurements carried out both for methanol and for phenol. This ensured the reproducibility of the observed effects. Previous data on the infrared adsorption spectra of microporous glass during adsorption of methanol vapor, obtained by one of the present authors, also attests to the extreme character of change of all the observed bands in dependence on the relative pressure of the vapor, P/P_0. Also, in the case of solutions, the indicated change in intensity becomes smooth as the coverage approaches a monolayer. Thus, this effect cannot be caused by the interaction of adsorbing molecules with the molecules of the vehicle.

If the effects of the intensity changes of bands observed by us were compared with those described by Kiselev and Krasilnikov[5,6] in terms of the adsorption isotherm and heat of adsorption from solutions, then it is probable that the indicated effect of intensity changes of the bands observed by us has a general origin. At the present time it is too early to give an interpretation of this effect. Possibly it is connected with changes in the orientation of the adsorbing molecules as a function of surface coverage.

The authors express appreciation to A. S. Predvoditelev, V. F. Kiselev, and K. G. Kracilnikov for contributions to this work.

REFERENCES

1. N. G. Yaroslavskii. Zhur. Fiz. Khim 24, 68 (1950).
2. N. G. Yaroslavskii and A. N. Terenin. Doklady Akad. Nauk SSSR 66, 885 (1949).
3. L. N. Kurbatov and G. G. Neuimin. Doklady Akad. Nauk 68, 341 (1949).
4. A. N. Terenin. Sb.: "Poverkhnostnie Khimicheskie Soedineniya i ikh Rol' v Yavleniyakh Adsorbtsii." (Surface Chemistry of Compounds and their Role in Adsorption Effects), p. 206, Izd. Moskov. Gosudarst. Univ., 1957.
5. V. N. Filimonov. Ph.D Thesis, Leningrad University, 1955.
6. A. N. Terenin. Nauchnaya Sessiya LGU, Tezisi. (Scientific Session, Leningrad U., Thesis), Izd. Leningrad. Gosudarst. Univ., 1950.
7. V. F. Kiselev and K. G. Kransilnikov. Doklady Akad. Nauk SSSR 86, 111 (1952).
8. V. F. Kiselev and K. G. Kransilnikov. Zhur. Fiz. Khim. 32, 1435 (1958).

ON THE CAUSES OF THE LUMINESCENCE OF LIQUIDS UNDER THE ACTION OF HARD RADIATION

L. I. Al'perovich, I. D. Sherbaf, and R. Marupov

Received 24 July 1959

In order to interpret their experiments on the measurement of the concentration dependence of the intensity of luminescence in a series of organic solutions under the action of γ-rays, Kallman and Furst[1] proceeded from the concept of an intermolecular excitation energy transfer from solvent molecules to impurity molecules. The luminescence of "pure" solvents is attributed by these authors to impurities which could not be eliminated by distillation.*

*Compare with the results of reference 5.

Terenin,[2] arguing against such an interpretation, indicates that the luminescence of solvents such as CCl_4, heptane, etc., whose molecules have unstable upper electronic levels, cannot be explained by energy migration from the solvent to the impurity.[2] Galanin[3] also pointed out the possibility of a strong influence of the Vavilov-Cerenkov effect on the results of reference 1. This latter statement does not, however, completely agree with the statement of the authors of reference 1, who indicate that the main part of the luminescence fell in the spectral region around 4000 A.

To investigate this question, we compared the luminescence intensities of a number of aromatic and non-aromatic solvents and solutions upon excitation with X-rays. The tube voltage was varied from 30 to 200 kv. (The Vavilov-Cerenkov effect does not take place under such conditions.) Moreover, measurements were made

on the same samples in an apparatus similar to the one described in reference 1, using a 10 mC preparation of Co^{60} for the excitation of luminescence. The intensity of luminescence was determined with an FEU-19M photomultiplier. The exciting X-ray beam was collimated by lead diaphragms and was directed from the side onto an aluminum cell containing the liquid under investigation. The photomultiplier was located above the cell. The influence of secondary and scattered X-ray radiation was corrected for. The errors in the measurement of intensity usually did not exceed 7-10%.

Measurements were made on the concentration dependence of the luminescence intensity of anthracene, naphthalene, β-naphthylamine, phenantrene, and stilbene solutions in various solvents (see Figure). The shape of the curves and the value of the optimum concentrations were found, with rare exceptions, to be very close to those listed in reference 1 for the case of excitation by γ-radiation. In agreement with the results of reference 1, no increase in the intensity of radiation with increasing concentration was observed on dissolving naphthalene and anthracene in ether, alcohol, chloroform, or other solvents. The only exception among all of the nonaromatic solvents employed was dioxane. A similar effect is also observed in the case of dioxane upon γ-excitation. These results point to a considerable similarity in the excitation processes of the luminescence of solutions with X-ray and γ-ray excitation.

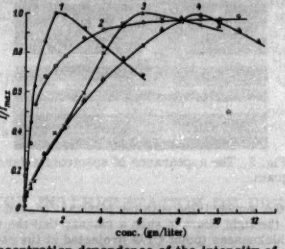

Concentration dependence of the intensity of luminescence upon excitation with X-rays. Curve 1—anthracene in xylene, U = 55 kv; curve 2—naphthalene in benzene, U = 55 kv; curve 3—naphthalene in toluene, U = 200 kv; curve 4—anthracene in dioxane, U = 38 kv.

Measurements were also made with "pure" liquids. Commercial reagents were used hereby, the majority being of grades Ch (pure) and ChDA (analytical reagent grade). Benzene, toluene, xylene, and water were subjected to an additional purification by distillation. In the case of benzene (chemically pure) the change in luminescence intensity after distillation was negligible. On the other hand, in the case of xylene and of toluene, distillation leads to a considerable increase in the intensity of luminescence. It follows from this that the luminescence resides mainly in the molecules of the solvent and not in those of the impurities.*

*This conclusion is also confirmed by control experiments with a filter cutting out radiation with $\lambda < 3500$ A.

The results of the investigation of "pure" solvents are listed in the Table. It is easy to see from these data that sharp differences can be observed between the luminescence intensities of "pure" solvents upon excitation with X-ray and λ-radiation. In the first case, the luminescence intensity of aromatic compounds exceeds that of nonaromatic solvents by at least one or two orders of magnitude. On the other hand, all nonaromatic solvents show equal intensity of luminescence upon γ-excitation (within 5-7%), while aromatic solvents (benzene, toluene, and xylene) have an intensity which is 1.5-2 times greater. Upon addition of KI to water or methyl alcohol, no change in luminescence intensity under γ-ray excitation was observed up to a KI concentration of 8 gm/liter. At the same time, according to data in reference 4, the intensity of the "blue" luminescence of methyl alcohol excited by ultraviolet radiation is decreased 3 times for the same KI concentration.

Luminescence Intensities of "Pure" solvents with Different Modes of Excitation

Solvent	Type of excitation		
	X-rays U=50 kV	γ-rays (Co^{60})	γ-rays[1] (Ra)
Ortho-xylene	1.0	1.0	0.53
Ortho-xylene (non-distilled	0.77	0.82	0.8 —1.0*
Toluene	0.45	0.78	0.67—0.8
Benzene	0.35	0.69	0.67—0.8
Dioxane	0.03	0.44	0.33
CCl_4	0.01	0.46	0.40—0.47
Methyl alcohol	0.00	0.45	0.60**
Water	0.00	0.47	0.60

*Data for a nonpurified mixture of xylenes.
**Data for ethyl alcohol.

Thus pure nonaromatic liquids show practically no luminescence under X-rays, whereas their luminescence under γ-rays is explained by Vavilov-Cerenkov radiation. In aromatic solvents, a superposition of luminescence and Vavilov-Cerenkov radiation takes place.

The authors express their deep gratitude to M. D. Galanin for a discussion of the results.

REFERENCES

1. H. Kallman and M. Furst. Phys. Rev. 79, 857 (1950); Phys. Rev. 81, 883 (1951); M. Furst and H. Kallman. Phys. Rev. 85, 816 (1952); Phys. Rev. 94, 503 (1954).
2. A. N. Terenin. Uspekhi Fiz. Nauk 43, 347 (1951); A. N. Terenin and V. L. Ermolaev. Uspekhi Fiz. Nauk 48, 37 (1956).
3. M. D. Galanin. Izvest. Akad. Nauk SSSR, Ser. Fiz. 20, 396 (1956).
4. S. I. Vavilov and L. A. Tumerman. Z. Physik 54, 270 (1929).
5. V. A. Kizel and M. N. Rakhmatov. Uchenye Zapiski Tomsk. Gosudarst. Univ. 4, 71 (1955).

THE DETERMINATION OF THE ORDER OF INTERFERENCE BANDS BY MEANS OF A MONOPRISM AND A PLATE

V. G. Khomazuk

Received 26 June 1959

One of the most important problems in interference measurements of the index of refraction of transparent media is the determination of the order of a band at least for one wavelength. A wide application of these methods to the research practice is greatly impeded by the necessity of employing, in addition to a spectrograph, a monochromator,[1] and also a goniometer of high precision (angular readings of one minute of arc[2,3]). To avoid the necessity for using these instruments, we have developed[4] a method of four plane-parallel plates which permits the determining of the order of interference bands in practically all known cases.

In addition to these methods, the determination of the order of interference bands may also be carried out, of course, by other methods. In particular, one of them developed by us is described in this paper. For the method suggested here, a monoprism is used, which is similar to the one employed by us previously for obtaining interference of light,[5] and also a plane-parallel plate made of the same material (fused quartz). By a monoprism we mean a plane-parallel plate with one face cut at 5 deg, so that a refracting angle of about 175 deg is obtained (ABC, Fig. 1).

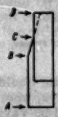

Fig. 1. The monoprism with the plate (side view).

As an example, the following dimensions may be used for this arrangement (Fig. 1): the thickness of the plane-parallel part of the monoprism is 1 mm, its length, AB is 5 mm; the thickness of the monoprism in the D region is about 0.95 mm; the length of the beveled face BD is about 10 mm. The width of the monoprism is 5 mm, and its length 15 mm; the thickness of the plane-parallel plate is equal to 0.9 mm, its width 5 mm, and its length 12 mm.

The plate and the prism are in direct contact along their polished sides (which are normal to the direction of thickness). Obviously, at some point C the thicknesses of the prism and of the plate will be exactly the same.

The thickness of the prism (in its plane-parallel part) and of the plate are assumed to be previously known with a high degree of accuracy. The thickness measurement may be done, for example, by the methods investigated by Obreimov.[1]

With this monoprism and plate (of exactly known thicknesses) made of fused quartz and used as an etalon, one may conduct interference measurements of indices of refraction of liquid media for any value of the index. The measurement is conducted in the following manner. The monoprism and plate are placed in the cell containing the liquid under investigation. The cell is illuminated by a collimated beam of light produced from a pinhole placed in the focal point of the collimator lens. The image of some intense light source (for example, the quartz-mercury lamp SVDSh-250) is focused on the pinhole (produced by piercing a metallic foil with a needle). The face along which the monoprism and the plate are in contact is placed vertically, that is, parallel to the slit of the spectrograph (we used ISP-22), and in such a manner that the center of the geometrical shadow of the face is projected exactly on the slit. It is clear that the plane-parallel plate as well as the unbeveled face of the monoprism must be perpendicular to the beam of the incident light. In the region of the geometrical shadow, one will observe a Fresnel diffraction pattern which will have, upon passing the spectrograph, the form shown in Fig. 2a or 2b.

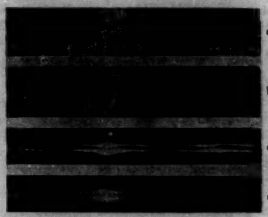

Fig. 2. The appearance of spectrointerferogram.

If the monoprisms with the plate are placed in the path of the light beam in such a manner that the region of equal thicknesses (point C) is projected at the center of the slit, at the level of which a metallic thread is strung across the slit, then at the spectrograph exit the pattern shown in Fig. 2a will be observed. In this case, the interference band of the zero order (achromatic) is spread on the spectrointerferogram along the image of the metallic thread (the dark line across the spectrum). Above and below this band are distributed the interference bands of higher positive and negative orders. When the monoprism with the plate is shifted so that the region of point B is projected at the center of the spectrograph slit, an image similar to the one shown in Fig. 2b is obtained. While the monoprism with the plate is being shifted, the interference bands crossing the reference line (the image of the thread) in the region of some intense spectral lines emitted by lamp SVDSh-250 are counted. The fractional part of the band can be frequently estimated with an accuracy of from 0.2 to 0.3 of the band. (It is not necessary to photograph the image.) After this, it is necessary to rotate the arrangement by 90 deg about the optical axis of the assembly and, instead of the illuminated small opening, use a slit which, in the same way as the boundary line between the monoprism and the plate, is set across the slit of the spectrograph.

The plane-parallel plate in the region of 0.1 mm thickness is projected on the center of the spectrograph; then the interference pattern and the iron spectrum ad-

jacent to it are photographed, the latter being used as a reference scale of wavelengths (Fig. 2c). Then, in a similar manner, a photograph is taken of the 1 mm step of the plane-parallel part of the monoprism near point A (Fig. 2d).

The previously obtained approximate order of the interference band for a selected spectral line of the lamp is determined more accurately from measuring the spectrointerferogram (Fig. 2c) by means of comparator IZA-2. With this measuring procedure, the accuracy of determining the order of the bands is usually considered to be equal to ±0.02 of the band. As we now know exactly the order of the bands for the step quartz-liquid of 0.1 mm thickness, it is obvious that for a similar step of 1 mm thickness (Fig. 2d) the order will be ten times greater. Consequently, the accuracy of the results will be equal to ±0.2 of the band. This accuracy is sufficient for easy and entirely reliable finding the computed interference band on the spectrointerferogram Fig. 2d. Now, by measuring the order of the bands on a comparator with an accuracy up to 0.02 of the band, it is possible to determine the refraction index n_l of the fluid under investigation for any wavelength, in accordance with the well-known formula:

$$(n_l - n)d = N\lambda \qquad (1)$$

or

$$n_l = n + N\frac{\lambda}{d}, \qquad (2)$$

where n is the index of refraction of the plate material, d is the thickness of the plate, and N is the order of the interference band corresponding to the wavelength λ.

It is obvious that when the monoprism and the plate are in the air, it should be possible to determine the index of refraction of the material from which they are made.

Using the arrangement described, it is also possible to conduct investigations of the anomalous dispersion of liquids, solutions, gases, and solid substances. As a very important advantage of the method, we consider the fact that the interference band of zero order (achromatic), for all the substances, is a straight line which coincides with the reference line. This particular circumstance permits an errorless absolute determination of the order of the interference bands.

It also may be noted that the use of the instrumentation described here permits interference measurements of light dispersion in any transparent medium, using only a spectrograph; other methods[1-5] require, however, additional instruments such as a monochromator and a goniometer.

The amount of the liquid needed for the measurement does not exceed one to two drops; this permits considering this method as belonging to the class of microanalytical ones. This may be particularly important in investigations of rare or expensive liquids or solutions as well as in many other simpler cases.

REFERENCES

1. I. V. Obreimov. "O prilozhenii frenelevoi difraktsii dlya fizicheskikh i tekhnicheskikh izmerenii." (On the Application of the Fresnel Diffraction for Physical and Technical Measurements), Izd. Akad. Nauk SSSR, Moscow, 1945.
2. D. V. Chepur and A. A. Shishlovskii. Izvest. Akad. Nauk SSSR, Ser. Fiz. 17, 761 (1953).
3. I. S. Gorban' and A. A. Shishlovskii. Zhur. Tekh. Fiz. 25, 1297 (1955).
4. V. T. Khomaziuk. Vestnik Moskov. Gosudarst. Univ., Ser. Mat., Mekh., Astron., Fiz., Khim., No. 3, 161 (1958).
5. V. T. Khomaziuk. Vestnik Moskov. Gosudarst. Univ., Ser. Mat., Mekh., Astron., Fiz., Khim., No. 3, 125 (1957).

ON THE INTERPRETATION OF PRESSURE-INDUCED INFRARED SPECTRA OF GASES

E. E. Nikitin

Received 2 July 1959

A number of investigations[1-4] have been concerned with the interpretation of the infrared spectra of nonpolar molecules. Up to the present, however, no explanation has been given for the linear dependence of the splitting of the Q branch on the density of the perturbing gas, which has been observed experimentally.[5] Since the residual splitting at low pressures is caused by rotation of the induced moment directed along the line joining the two colliding molecules,[5,6] the linear dependence of the separation of the Q_P and Q_R components of the Q branch on the density must be an effect of ternary collisions. In the framework of the theory developed previously[3] it is possible to give the following qualitative interpretation of this splitting.

The intensity of the Q branch is proportional to the square of the modulus of the Fourier component of the matrix element of the dipole moment for the vibration transition, where the time dependence of the dipole moment is determined by the characteristics of the relative motion of the colliding molecules.[3] If the collisions are sufficiently rare, interference of the corresponding probability amplitudes can be neglected; the total intensity is then proportional to density of the perturbing gas, the intensity distribution being independent of the density. At high densities it is necessary to take account of interference between the probability amplitudes for the different collisions. The total probability amplitude $I(\omega)$ has the form

$$I(\omega) = \sum_{k=1}^{Z} I_k(\omega). \qquad (1)$$

where the index k numbers the successive collisions and takes values from 1 to Z, and $I_k(\omega)$ is the probability amplitude of absorption for the kth collision (Z is the number of collisions of absorbing and perturbing molecules per sec). For definiteness, we will consider the Q_R component, and we will assume the frequency ω to be measured from the position of the Q_R maximum at low pressures; the Q_P component is obtained by a reflection of the Q_R component through the vibrational transition frequency. If we neglect differences in the relative velocities of individual pairs of colliding molecules, all the terms in $I_k(\omega)$ become equal except for the complex factors a_k, which characterize the geometrical configuration of the collisions (in reference 3, a_k =

$\exp(i\varphi_k)$, where φ_k is the azimuthal angle of the induced dipole at the moment of the collision), and the factors $\exp(i\omega t_k)$ which arise from the retardation of the kth collision with respect to the first by the time t_k. In the following we will consider the case in which the concept of isolated collisions is applicable, that is, we will assume that the time between collisions, $1/Z$, is considerably greater than the collision time, $\tau \approx 1/\alpha\bar{V}$, where $\bar{V}$ is the relative velocity of the colliding molecules and α^{-1} is the range of the exchange forces. Thus, the product $Z\tau$ appears as a small parameter.

In the evaluation of the intensity, $A(\omega) \sim |I_0(\omega)|^2$, it is sufficient to take into account the interference only between collisions which are separated by a very short time interval, since the probability of overlapping m-fold collisions decreases proportionally with $(Z\tau)^m$. We then obtain

$$A(\omega) \sim Z\,|I_0(\omega)|^2 + 2Z\tau \sum_{k=1}^{\infty} |a_k e^{i\omega t_k} + a_{k+1} e^{i\omega t_{k+1}}|^2\,|I_0(\omega)|^2, \quad (2)$$

where $I_0(\omega) = I_k(\omega) |a_k \exp(i\omega t_k)|$. Let us consider the simplest case of two successive collisions in the same plane. We have $a_k = \exp(i\varphi_k)$, and expression (2) takes the form

$$A(\omega) \sim Z\,|I_0(\omega)|^2 \left\{1 + 2\tau \sum_{k=1}^{\infty} |1 + \exp(i\Delta\varphi_k + i\omega\Delta t_k)|^2\right\}, \quad (3)$$

where $\Delta\varphi_k = \varphi_k - \varphi_{k+1}$ and $\Delta t_k = t_k - t_{k+1}$. Expression (3) must be averaged over the different values of the geometrical collision parameter $\Delta\varphi_k$ and of the time Δt_k. The latter average can be easily obtained since the probability of successive collisions is given by the simple expression $W(\Delta t) \sim \exp(-Z\Delta t)$. Carrying out the averaging, we obtain

$$A(\omega) \sim Z\,|I_0(\omega)|^2 \left\{1 + 4Z\tau \left[1 + \frac{Z^2\,\overline{(\cos\Delta\varphi_k)} - Z\omega\,\overline{(\sin\Delta\varphi_k)}}{Z^2 + \omega^2}\right]\right\}. \quad (4)$$

In averaging over $\Delta\varphi_k$ one must take account of the fact that different values of $\Delta\varphi_k$ make different contributions to the intensity. Since the magnitude of the induced moment increases with increasing relative energy of the colliding molecules, the maximum contribution is made by those collisions which are characterized by opposite orientation of the moments of molecular pairs formed in two successive collisions. On the basis of the classical picture of the collision it can be concluded that $\Delta\varphi_k$, corresponding to the maximum induced moment, must lie in the interval $-\pi < \Delta\varphi_k < 0$, and probably should be close to $-\pi/2$. The negative sign of $\Delta\varphi_k$ corresponds to the negative phase difference of the two rotations in opposite directions, which characterize the two successive collisions.

We will introduce the designations $(-\overline{\sin\Delta\varphi_k}) = \sin\gamma$ and $\overline{(\cos\Delta\varphi_k)} = \cos\gamma$. These designations are not strictly consistent; however, this does not change the qualitative conclusions. In order to find the maximum in (4), we will represent $|I_0(\omega)|^2$ for $\omega\tau \ll 1$ in the form

$$|I_0(\omega)|^2 \approx 1 - \omega^2\tau^2, \quad (5)$$

in which $1/\tau$ represents the half-width of the Q_R component. Relation (4) then takes the form

$$A(\omega) \sim Z\,(1 - \omega^2\tau^2) \left\{1 + 4Z\tau \left(1 + \frac{Z^2\cos\gamma + Z\omega\sin\gamma}{Z^2 + \omega^2}\right)\right\}. \quad (6)$$

It is easy to show that the frequency dependence of the second factor in this expression is unimportant in the region of variation of ω which interests us. The third factor has its maximum, in fact, at the point

$$\omega_m = Z\,\frac{1 + \cos\gamma}{\sin\gamma}. \quad (7)$$

The condition that the variation of the second factor is slow in comparison with the third can then be written in the form

$$Z\tau \ll \frac{2\,(\sin\gamma)^2\,(1 + 2\cos\gamma)}{(1 + \cos\gamma)^2}. \quad (8)$$

It is not difficult to see that this inequality is fulfilled over a reasonably large range of possible values of γ close to $\pi/2$, if the basic restriction $Z\tau \ll 1$ is taken into consideration. It is necessary, however, to keep in mind that this inequality may actually be unnecessarily restrictive, as follows, for example, from the results of the investigation of Van Kranendonk.[4]

We thus reach the following conclusion: the shift in the frequency of the maximum of the Q_R component with increasing density is directly proportional to the number of collisions, and the constant of proportionality is a small number. The separation $\Delta\omega$ of the maxima of the Q_P and Q_R components, omitting the constant residual splitting, is twice as great as the magnitude of the shift ω_m.

We will now compare this result with the experimental data. Chisholm and Welsh[5] have studied the infrared spectrum of hydrogen in mixtures with various gases. At a density of 200 Amagat units and T = 298°K, the experimental value of the splitting of the Q branch of hydrogen in a mixture with helium is equal to 6×10^{12} sec^{-1}, which corresponds to $\omega_m = 3 \times 10^{12}$ sec^{-1}. Under the same conditions, the number of collisions Z is approximately equal to 10^{12} sec^{-1}; thus, relation (7) is fulfilled with adequate accuracy.

It is natural to assume that the basic temperature dependence of ω_m depends on the factor Z, so that the splitting at any given density is proportional to $\sqrt{T}$. In this case the ratio of the splittings for the temperatures 298 and 80°K should be 1.93. The experimental value, determined from the data in reference 5 is somewhat smaller (1.7). Thus, a qualitative agreement between theory and experiment is evident also in this respect.

I wish to thank Professor N. D. Sokolov for discussions of this research.

REFERENCES

1. J. Van Kranendonk. Physica 23, 825 (1957).
2. J. Van Kranendonk. Physica 24, 347 (1958).
3. E. E. Nikitin. Opt. i Spektr. 7, 744 (1959).
4. J. Van Kranendonk. Physica 25, 337 (1959).
5. D. A. Chisholm and H. L. Welsh. Can. J. Phys., 32, 291 (1954).

ON THE CORRECTION FOR THE SIZE OF EXIT DIAPHRAGM IN THE PHOTOELECTRIC RECORDING OF INTERFERENCE BANDS OF EQUAL INCLINATION

Yu. P. Efremov and Yu. P. Kanevskii

Received 3 June 1959

All the arrangements for photoelectric registration of interference rings of equal inclination contain a diaphragm separating a certain part of the ring pattern (usually the central part). The light flux, transmitted by this diaphragm, is directed to the photoreceiver connected with an amplifier and autorecorder. When the thicknesses of the Fabry-Perot etalon are small, a change of the order of interference and, consequently, of the light flux transmitted by the diaphragm, is achieved most easily by changing the air pressure between the mirrors of the etalon.[1-3] Then the autorecorder registers a series of successive orders of interference. However somewhat larger values, i.e., $N + \delta\varepsilon$, not the whole values N, of the order of interference correspond to the maxima on the record (the interference bands will appear to be shifted in the direction of the higher order). This results in a lowering of the measured order of interference (ε') in comparison with the actual value (ε); the difference between these two values is equal to the shift. Therefore, the taking of $\delta\varepsilon$ into account becomes necessary for measurements intended for a highest possible accuracy in determination of the order of interference (measurements of wavelengths of light, and of the lengths of the Fabry-Perot etalons). The value $\delta\varepsilon$ of the shift depends on the size and form of the diaphragm separating a part of the interference rings. The simplest case of determining $\delta\varepsilon$ is that by means of a ring or a circular diaphragm. Chabbal and Jaffe have shown that a circular diaphragm, the center of which coincides with the center of the rings of equal inclination, transmits a flux determined by the following expression with an accuracy within constant factors:

$$\Phi_{cir}(\varepsilon, \Delta) = \arctan\sqrt{F+1}\tan\pi\varepsilon - \arctan\sqrt{F+1}\tan\pi(\varepsilon-\Delta). \quad (1)$$

Here: ε and $\varepsilon - \Delta$ are the fractional parts of the order of interference at the center and the margins of the diaphragm, respectively; $\Delta = td^2/4\lambda f^2$, where t is the length of the etalon, d is the diameter of the diaphragm, λ is the wavelength, f is the focal length of the objective; and $F = 4R/(1-R)^2$, where R is the coefficient of reflection of the mirrors of the etalon. Obviously, $\Phi = \Phi_{max}$ when $\varepsilon = 0.5\Delta$. Consequently, for a circular diaphragm $\delta\varepsilon = 0.5\Delta$ and

$$\varepsilon = \varepsilon' + 0.5\Delta. \quad (2)$$

A diaphragm of the shape of a narrow slit was explored and used by Rank and his co-workers.[5,7] It follows from the tables given in reference 7 that $\delta\varepsilon = 0.325\Delta$, for a narrow slit.

In the same paper, a square diaphragm was used when registering the bands of equal inclination. It was found that correction $\delta\varepsilon$ for a square diaphragm is equal to correction $\delta\varepsilon$ for a circular opening inscribed in the given square, that is, $\delta\varepsilon = 0.5\Delta_1 = 0.25\Delta$, if Δ is calculated along the circle circumscribing the square ($\Delta = 2\Delta_1$).

In this communication, the results are given of an investigation aiming at determining the correction $\delta\varepsilon$ for rectangular diaphragms with various ratios of the sides. The results obtained by us differ from the Rank results, given above, for corresponding diaphragms.

The value of correction for a rectangular diaphragm may be computed in the following manner.

The light flux passing through a rectangular diaphragm with sides a and b, the center of which coincides with the center of interference rings, is given by the following expression with an accuracy within constant factors:

$$\Phi_{rect}(\varepsilon, \Delta) = \arctan\sqrt{F+1}\tan\pi\varepsilon - \frac{2}{\pi}\int_0^{\varphi_0}\arctan\sqrt{F+1}\tan\pi\left(\varepsilon + \frac{\Delta\cos^2\varphi_0}{\cos^2\varphi}\right)d\varphi - \frac{2}{\pi}\int_0^{\varphi_0}\arctan\sqrt{F+1}\tan\pi\left(\varepsilon - \frac{\Delta\sin^2\varphi_0}{\cos^2\varphi}\right)d\varphi, \quad (3)$$

where $\varphi_0 = \arctan(a/b)$, $\Delta = t\sqrt{a^2+b^2}/4\lambda f^2$.

In the case of a square diaphragm (a/b = 1),

$$\Phi_{sq}(\varepsilon, \Delta) = \arctan\sqrt{F+1}\tan\pi\varepsilon - \frac{4}{\pi}\int_0^{\frac{\pi}{4}}\arctan\sqrt{F+1}\tan\pi\left(\varepsilon - \frac{\Delta}{2\cos^2\varphi}\right)d\varphi. \quad (4)$$

Using the theorem of the mean value, we obtain

$$\Phi_{sq}(\varepsilon, \Delta) = \arctan\sqrt{F+1}\tan\pi\varepsilon - \arctan\sqrt{F+1}\tan\pi\left(\varepsilon - \frac{2}{\pi}\Delta\right). \quad (5)$$

The expression above is analogous to Eq. (1) for the light flux passing through a circular diaphragm, that is,

$$\Phi_{sq}(\varepsilon, \Delta) = \Phi_{cir}\left(\varepsilon, \frac{2}{\pi}\Delta\right).$$

Consequently, the following condition must be fulfilled:

$$k_3 = 0.5\,\frac{2}{\pi}\,\Delta \approx 0.32\Delta.$$

An analogous transformation of Eq. (3) results in the following form

$$\Phi_{rect}(\varepsilon, \Delta) = k_1\Phi_{cir}(\varepsilon, k_2\Delta) + (1-k_1)\Phi_{cir}(\varepsilon, k_3\Delta), \quad (6)$$

where the coefficients $k < 1$ depending on the ratio a/b, and the functions Φ_{cir} have the form of (1). Thus, for example, when a/b = 0.5, (6) has the form

$$\Phi(\varepsilon, \Delta) = 0.705\Phi_{cir}(\varepsilon, 0.38\Delta) + 0.295\Phi_{cir}(\varepsilon, 0.88\Delta). \quad (7)$$

Each of the terms of the right side of (7) has the maximum value when $\varepsilon_1 = 0.18\Delta$ and $\varepsilon_2 = 0.43\Delta$, respectively. The maximum value of the whole expression must obviously be reached for ε_1 lying between ε_1 and ε_2, but nearer to ε_1. For $a \leq 0.1\,b$, the computation results in $0.1\Delta < \delta\varepsilon < 0.3\Delta$.

The experimental determination of correction $\delta\varepsilon$ for

a rectangular diaphragm was conducted in the following manner. The fractional part of the order of interference at the center of the rings of equal inclination ε' was measured consecutively for a series of diaphragms of various forms and sizes. The true fractional part $\varepsilon = \varepsilon' + \delta\varepsilon$, must naturally be the same (within the limits of accuracy of measurements) for all the diaphragms; moreover, for the circular ones, (2) must hold. For example, let us denote by ε_0' the fractional part measured by means of a circular diaphragm, and by ε', the part measured by means of a rectangular one; then correction $\delta\varepsilon$ for a rectangular diaphragm may be found if $\delta\varepsilon_0$ for a circular diaphragm is known:

$$\delta\varepsilon = \delta\varepsilon_0 + \varepsilon_0' - \varepsilon'.$$

The instrumentation, by means of which the measurements were made, and the method for determining the values ε' are described in references 8 and 9. The measurements were made using the yellow and the yellow-green lines of Kr^{86} (λ = 5870 A and 5649 A), the Fabry-Perot etalons 47 and 100 mm in length, and two pairs of mirrors (R = 55% for one pair, and R = 85% for the other).

The results of the investigation are presented in the Figure as a graph (the solid curve) showing the dependence of $\delta\varepsilon/\Delta$ on the ratio a/b of the shorter side of the rectangular diaphragm and its longer side. The values Δ used above were determined for the circular diaphragm circumscribing the given rectangular diaphragm:

$$\Delta = \frac{\varepsilon\sqrt{a^2+b^2}}{4\lambda f^2}.$$

The values Δ used in this investigation were in the region from 0.014 to 0.616 of the order of interference. The circles on the graph correspond to the experimental values.

For a square diaphragm (a/b = 1), we obtained $\delta\varepsilon/\Delta$ = 0.32 which is in good agreement with the computed value. For a rectangular diaphragm whose one side is twice as long as the other (a/b = 0.5), $\delta\varepsilon/\Delta$ = 0.22. The extrapolation from the graph for a narrow slit (a/b → 0), gives the value $\delta\varepsilon/\Delta$ = 0.16. Both these values lie also within the computed intervals.

REFERENCES

1. P. Jacquinot and Ch. Dufour. J. rech., Centre nat. rech. scient. 6, 91 (1948).
2. N. R. Batarchukova. Trudy Vseyouz. Nauch.-Issledovatel. Inst. Metrol. 7 (67), 47 (1949).
3. N. I. Kalitevskii and M. P. Chaika. Vestnik Leningrad. Gosudarst. Univ., 1 Chim 1, No. 4, 9 (1956).
4. R. Chabbal. J. recherches centre nat. recherch sci., Lab. Bellevue (Paris) 24, 138 (1953).
5. J. H. Jaffe. J. Opt. Soc. Am. 43, 1171 (1953).
6. D. H. Rank and J. M. Bennett. J. Opt. Soc. Am. 45, 46 (1955).
7. D. H. Rank, J. M. Bennett and H. E. Bennet. J. Opt. Soc. Am. 46, 477 (1956).
8. Yu. P. Efremov. Izmeritelnaya tekh. i Poverochnol Delo No. 6, 15 (1958).
9. Yu. P. Efremov. Trudy Vseyouz. Nauch.-Izzledovatel. Inst. Metrol. 40 (100), 18 (1959).

ON THE SEMI-EMPIRICAL CALCULATION OF THE IONIZATION POTENTIALS OF ALIPHATIC COMPOUNDS

V. M. Baranov and T. K. Rebane

Received 6 July 1959

Using the Fock-Hartree method of self-consistent fields,[1] Hall proposed in 1951 a semi-empirical method for the calculation of ionization potentials of related molecules.[2] The method is more simple in its application to aliphatic molecules. The structure of the latter is assumed to be such that all carbon atoms lie in the same plane. Calculations are greatly simplified if assumption is made that the ionized molecular orbitals are antisymmetric with respect to the plane of symmetry of the molecule. With this assumption it becomes possible to describe separate groups of atoms in the molecule (such as CH_2, for example) with the aid of parameters, which may be calculated from the experimentally obtained ionization potentials. For normal aliphatic compounds C_nH_{2n+2}, Hall[2] obtained the following formula for the calculation of the first ionization potentials

$$I(n) = -a - 2b\cos\frac{\pi n}{n+1}, \qquad (1)$$

where a is a parameter describing CH_2 groups and terminal CH_3 groups (all such groups are taken to be equivalent), and b is a parameter describing interaction of neighboring groups (the long-range interactions being neglected).

Parameters a and b were obtained by Hall from the experimental values of the ionization potentials of the aliphatic compounds. Similar computations, but with different values of these parameters, were made by Franklin.[4]

It must be pointed out that a sufficiently significant discrepency exists between the calculated and experimental values obtained by these authors.

We made analogous calculations with different values of a and b parameters, and found it impossible to approximate satisfactorily by means of formula (1) the ionization potentials of the whole set of the aliphatic molecules. The situation is not changed if a correction in the parameter a is introduced, taking into consideration the nonequivalence of the CH_2 and CH_3 groups, located respectively in the middle and at the terminals of the molecule. However, if one assumes that the ionization potentials of methane and ethane do not have to be correctly described, for some reason, by formula (1), then for the remaining members of the aliphatic series

there is found a good agreement with experiment, taking the parametric values a = −14.06 ev and b = −2.02 ev, obtained from the experimental ionization potentials of propane and butane. The ionization potential values calculated for the normal aliphatic compounds are listed in Table 1, where they are compared with the values calculated by other authors and the experimental values.

Table 1. The Ionization Potentials of the Normal Aliphatic Compounds

Molecule	$I_{calculated}$			$I_{exptl.}$
	Present work (a = −14.06, b = −2.02 ev)	Ref. 4 (a = −13.31, b = −1.55 ev)	Ref. 3 (a = −13.126, b = −1.493 ev)	
CH_4	14.06	13.31	13.14	13.12
C_2H_6	12.04	(11.76)	11.65	11.65
C_3H_8	(11.21)	11.12	11.03	11.21
C_4H_{10}	(10.80)	(10.80)	10.73	10.80
C_5H_{12}	10.56	10.63	10.56	10.55
C_6H_{14}	10.42	10.52	10.45	10.43
C_7H_{16}	10.33	10.43	10.38	10.35
C_8H_{18}	10.27	10.39	10.34	10.24
C_9H_{20}	10.22	—	10.30	10.21
$C_{10}H_{22}$	10.19	10.33	—	10.19

The experimental ionization potentials of the molecules C_nH_{2n+2} (n = 3, 4, 5, ..., 10) were taken from Honig,[5] and those of the remaining molecules were obtained by taking averages of values reported by several other authors (cf. for example, reference 6).

The possible explanation for the exception of methane and ethane from the general pattern may lie in the deviation of the experimental ionization potentials of these molecules from the vertical ionization potentials calculated with the halp of the semi-empirical method. For these molecules such deviation may be relatively large, which follows from the theorem of Yahn-Teller, according to which the symmetric configurations of the ions with degenerate electronic states are unstable. In as much as CH_4^+ and $C_2H_6^+$ are just this kind of ions, there must follow a lowering in their energy resulting from the deformation of the symmetry of their nuclear skeleton, which may affect the magnitude of ionization potential.

Making use of the parametric values a and b found for the normal aliphatic compounds, we calculated ionization potentials I of some aliphatic free radicals. For the description of a group with a free valence and of its interaction with neighboring groups, we introduced two additional parameters, obtained from the average[5] experimental values:

$$I_{CH_3} = 9.96 \text{ ev and } I_{C_2H_5} = 8.72 \text{ ev.}$$

The results of these calculations are given in Table 2. For the series of aliphatic free radicals investigated by us, Stevenson[5] made analogous calculations (but using different values for the parameters). The results of both calculations are in agreement, within the experimental error.

Table 2. Ionization Potentials of the Aliphatic Free Radicals (ev)

Radical	$I_{calculated}$		$I_{exptl.}$	$W_{calc.}$
	Present work	Ref. 6		
CH_3	(9.96)	(9.96)	9.96	1.00
C_2H_5	(8.72)	(8.67)	8.72	0.98
$n-C_3H_7$	8.51	8.48	7.57 — 7.94	0.95
$n-C_4H_9$	8.47	8.47	8.3	0.94
$sec-C_4H_9$	7.76	7.81	7.45 — 7.90	0.85
$sec-C_5H_{11}$	7.67	7.76	8.0	0.85
$tert-C_4H_9$	6.94	7.11	6.9	0.82
$n-C_5H_{11}$	8.49	—	—	0.94
$sec-C_6H_{13}$	7.86	—	—	—
$CH(C_2H_5)_2$	7.58	—	—	0.82
$CH(C_3H_7)_2$	7.56	—	—	0.81
$C_2H_5C(CH_3)_2$	6.94	—	—	—

In the last column are listed the probabilities of localization (W) of the unpaired electron on the group with free valence, which may be useful in the interpretation of the electron paramagnetic resonance of free radicals.

REFERENCES

1. V. A. Fock. Z. Physik 61, 126 (1930).
2. G. G. Hall. Proc. Roy. Soc. A202, 541 (1951).
3. G. G. Hall. Trans. Faraday Soc. 50, 319 (1954).
4. J. L. Franklin. J. Chem. Phys. 22, 1304 (1954).
5. R. F. Honig. J. Chem. Phys. 16, 105 (1948).
6. F. H. Field and J. L. Franklin. "Electron-Impact Phenomena and the Properties of Gaseous Ions." New York, 1957.

CHANGE IN THE INFRARED ABSORPTION OF CERTAIN SEMICONDUCTING ADSORBENTS UNDER ULTRAVIOLET ILLUMINATION

V. N. Filimonov

Received 8 July 1959

In a previous note[1] we showed that under ultraviolet illumination ZnO and TiO_2 absorb radiation in the infrared part of the spectrum, and that after the illumination is stopped the absorption decreases slowly when the specimen is in vacuum, but rapidly in the presence of air or oxygen. A similar change in the infrared absorption of ZnO was found by Miloslavskii and Kovalenko.[2] Since the ultraviolet illumination of zinc oxide is accompanied by desorption of oxygen from the surface of ZnO, as determined by measurements of photo-emf[3] and photoconductivity[4] and also by direct manometric methods,[5] it is natural to assume that the infrared absorption is due to an increase in the concentration of free electrons with photodesorption of oxygen, and is connected with transitions of electrons from the donor levels into the conduction band or with transitions within this band. To extend the previous experiments we have now investigated the infrared absorption which appears with illumination of WO_3 and SnO_2 which, like ZnO and TiO_2, show a sharp increase in electrical conductivity when illuminated in vacuum.[6]

The tungsten trioxide used in our investigation was obtained by decomposing H_2WO_4 at 500°C. In order to investigate the absorption, the powdered WO_3 was transferred as an alcohol suspension onto a plate of NaCl. The specimens of SnO_2 were prepared by transferring a mixture of $SnCl_4$ and ethanol onto a plate of NaCl and heating to 500°C. The thickness of the specimens was

2-3 mg/cm². We used the IKS-14 infrared spectrometer with NaCl, LiF, and F-1 prisms.

Figure 1 shows the variation of transmission T of the specimens of WO_3 and SnO_2 for 5000 and 1300 cm^{-1} when the specimens are illuminated by radiation from an SVD-250 mercury lamp passing through glass and water filters. It is evident from the figure that the illumination of the specimens in vacuum causes infrared absorption which slowly decreases after the illumination ceases. The admission of air (or O_2) rapidly increases the transmission of WO_3 to its initial value. In the case of SnO_2, only a partial restoration of the transmission of the specimen takes place. The variation of the infrared absorption of WO_3 and SnO_2 thus resembles the variation of the electrical conductivity of these semiconductors.[6]

The absorption spectrum due to the illumination of WO_3 and SnO_2 in vacuum is shown in Fig. 2. The figure also shows a corrected absorption curve for TiO_2 which differs somewhat from the curve in reference 1, which was obtained with thick, highly scattering specimens. The ordinates give the ratio of the transmission of the specimen after illumination to its transmission before illumination. The absorption band of WO_3 has a broad maximum in the region 0.3-0.9 ev. The absorption maximum of SnO_2 is in the neighborhood of 0.16 ev. In the case of TiO_2, a gradual increase in absorption is observed in the region of low frequencies, as in ZnO,[1] although a uniform absorption extends from 3000 cm^{-1} towards the higher frequencies.* The infrared absorption of WO_3 and SnO_2 is apparently connected with the transition of electrons from the donor levels into the conduction band.

*Investigation of the absorption of TiO_2 above 7000 cm^{-1} was hindered by intense scattering of light by the specimens.

Since the powdered specimens used in our experiments scattered light quite strongly, we did not investigate the infrared absorption of the original specimens themselves, but only measured the changes of absorption under illumination. In connection with this it should be observed that the appearance of absorption with the illumination of ZnO, TiO_2, WO_3, and SnO_2 does not mean that the specimens themselves did not exhibit any absorption in this spectral region. On the contrary, since adsorption of oxygen only partially decreases the concentration of electrons in the donor levels and in the conduction band, it is possible to assume that even in the absence of illumination these semiconductors still exhibit absorption in this spectral region. Investigations published recently indicate that single crystals of ZnO[7] and rutile TiO_2[8] have approximately the same absorption spectra as we observed after illuminating corresponding samples.

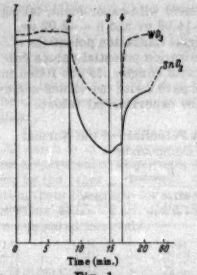

Fig. 1

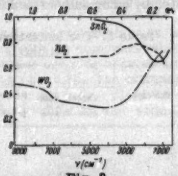

Fig. 2

Fig. 1. Variation of transmission of WO_3 and SnO_2. 1—evacuation (to 10^{-4} mm Hg); 2—beginning of illumination; 3—end of illumination; 4—admission of air (760 mm Hg).

Fig. 2. Infrared absorption of WO_3, SnO_2, and TiO_2 under illumination of specimens in vacuum.

The author wishes to express his deep gratitude to A. N. Terenin for advice and interest in this work.

REFERENCES

1. V. N. Filimonov. Opt. i Spektr. 5, 709 (1958).
2. V. K. Miloslavskii and N. A. Kovalenko. Opt. i Spektr. 5, 613 (1958).
3. E. K. Putseiko and A. N. Terenin. Doklady Akad. Nauk SSSR 101, 645 (1955).
4. I. A. Myasnikov and S. Ya. Pshezhetskii. Doklady Akad. Nauk SSSR 99, 125 (1954).
   D. A. Melnik. Phys. Rev. 94, 1438 (1954).
5. A. N. Terenin. "Problemy kinetiki i kataliza." (Problems in Kinetics and Catalysis) Vol. 8, Izd. Akad. Nauk SSSR, Moscow, 1955.
   Iu. P. Solonitsyn. Zhur. Fiz. Khim 32, 2142 (1958); Y. Fujita and T. Kwan. Bull. Chem. Soc. Japan 31, 379 (1958);
   D. B. Medved. J. Chem. Phys. 28, 870 (1958).
6. B. P. Kryzhanovskii and A. Ya. Kuznetsov. Optiko-Tekh. Prom. No. 4, 20 (1959).
   G. A. Korsunovskii. Zhur. Fiz. Khim (in press).
7. R. Arneth. Naturwissenschaften 45, 282 (1958); D. G. Thomas. J. Phys. Chem. Solids 10, 47 (1959).
8. D. C. Cronemeyer. Phys. Rev. 113, 1222 (1959).

SUPERLINEARITY IN LUMINESCENCE AND PHOTOCONDUCTIVITY PHENOMENA AND THE ROSE-BUBE THEORY

N. A. Tolstoi and A. I. Ryskin

Received 10 July 1959

Among the phenomena and rules of luminescence and photoconductivity which serve as "touchstones" for a theory, the superlinear dependence of steady luminescence I_∞ and photoconductivity $\Delta\sigma_\infty$ on the density E of luminous excitation play a special role. Experiments indicating the parallel manifestation of superlinearity in luminescence and photoconductivity[1] make it desirable to find a somewhat unified explanation of both phenomena. Since the possible number of ways of explaining superlinear photoconductivity is somewhat more limited, it is advisable to start with them.

In the most general case, the photoconductivity $\Delta\sigma_\infty$ is proportional to the quantity

$$\Delta\sigma_\infty \sim E\beta\tau u, \qquad (1)$$

independently of any theory. Here β is the quantum yield of electron transitions into the conductivity band (CB), τ the lifetime of a carrier in the CB, and u the electron mobility.

In order to explain superlinear photoconductivity, it is necessary to assume that at least one of the three quantities (β, τ, or u) increases with an increase in E. Accordingly, three types of theory of photoconductivity are possible, which will explain superlinearity.

1. The barrier theory,[2] based on the assumption that u increases with E. This theory has no relation to luminescence and is meaningless in the case of single crystals. It is therefore superfluous to consider it here.

2. Theories based on the assumption that β increases with E. Among these is the two-step theory[3,4] according to which the transition of the electrons into the CB does not proceed directly, but from an intermediate nonphotoactive excited state whose population under ordinary conditions increases with E. Thus the process of excitation of photocarriers becomes more efficient with increasing E; i.e., the yield β increases.

3. Theories based on the assumption that τ increases with E; i.e., on the increase of the lifetime of a carrier in the CB. The theory developed by Rose and Bube[5,6] belongs in this group. According to this theory, the number of free levels through which the recombination of electrons proceeds may decrease with increasing E. Such a "blocking" of the recombination channels increases the lifetime of a carrier in the CB.

We shall show that there is a direct experiment which indicates the erroneousness of the point of view defended by the American authors mentioned. Let us recall that this point of view is based on the following initial assumptions: (1) the absorption of the exciting quantum results only in the transition of an electron from the valence band (or from an "activator" level close to it) into the CB. (2) This process has a constant quantum yield equal to 1. (3) The electrons trapped in the intermediate levels do not absorb the exciting light; therefore the percentage occupancy of these levels by electrons can be infinitely close to 100. (4) The electron recombination process must proceed through intermediate local levels (the band – band recombination has low probability), i.e., it is essentially a two-step process.

It follows from these assumptions that the equilibrium concentration of electrons in the CB is achieved through a balance between: (a) the direct single-step influx into the CB of "optical" electrons from the valence band or from activator levels, and (b) the resulting departure of electrons from the CB. This resulting departure is in turn composed of the totality of all "nonoptical" processes (recombination, trapping, and thermal return to the CB from the trapping levels). No matter how complex these processes, the decrease of electrons in the CB which they determine is exactly equal to the influx of "optical" electrons.

For a given set of conditions, however, the rate of the resulting decrease process is determined only by the concentration of excited electrons. Therefore an instantaneous turning off of the exciting light cannot influence the initial phases of the process of electron decrease, which now proceed in an "unbalanced" form. Therefore the initial rate of the resulting decrease of electrons or, in other words, the initial rate of photoconductivity decrease* must, according to the Rose-Bube theory be

*The initial stage of photoconductivity decay is naturally taken to be the process measured in a time during which photoconductivity does not vary appreciably.

strictly proportional to the intensity E of excitation (see reference 7), i.e.,

$$\Delta\sigma'(0) \sim E. \qquad (2)$$

To check relation (2), we performed experiments with superlinear CdS photoresistors. The experiments were carried out by the method of electric differentiation.* A single light modulation was achieved by interrupting the focused light beam by the bullet of a small caliber rifle. The differentiated signal was registered (photographically) by means of triggered oscilloscope.*

*A detailed description of the experiments will be given in a subsequent paper.

Experiments have shown that relation (2) is not satisfied rigorously and that $\Delta\sigma'0$ depends superlinearly on E for superlinear photoresistors. It is not difficult to see that since

$$\tau = \frac{\Delta\sigma_\infty}{\Delta\sigma'(0)}, \qquad (3)$$

and

$$\beta = \frac{\Delta\sigma'(0)}{euE}, \qquad (4)$$

a knowledge of the dependence of $\Delta\sigma_\infty$ and $\Delta\sigma'(0)$ on E allows us to establish the dependence of $\tau(E)$ and $\beta(E)$. Experiment has shown that for superlinear CdS, $\tau(E)$ not only does not increase, but as a rule decreases slightly with an increase in E. The quantum yield, on the other hand, increases sharply with E, being thus responsible for the superlinearity of photoconductivity.

The results described, namely, the failure of relation (2) to be satisfied, and the decrease in τ with increasing E (and hence an increase of β with E) indicate that the basic assumptions of the Rose-Bube theory are erroneous.

On the other hand, the established dependence is in agreement with the basic ideas of the two-step theory.

It is interesting to note that the work of Lashkarev and collaborators[9] has established the yield, and not the lifetime, as the basic factor responsible for the spectral response of the photoconductivity of CdS and CdSe. This in turn contradicts the premises of the Rose-Bube theory.

REFERENCES

1. N. A. Tolstoi, B. T. Kolomiets, O. I. Golikov, and M. Ya. Tsenter. Zhur. Eksptl. i Teoret. Fiz. 30, 575 (1956).
2. J. C. Slater. Phys. Rev. 103, 1631 (1956).
3. V. E. Lashkarev and G. A. Fedorus. Izvest. Akad. Nauk SSSR, Ser. Fiz. 16, 81 (1952).
4. N. A. Tolstoi. Zhur. Eksptl. i Teoret. Fiz. 30, 171 (1956).
5. A. Rose. Proc. I.R.E. 43, 1850 (1955).
6. R. Bube. Phys. Chem. Solids 1, 234 (1957).
7. N. A. Tolstoi. Radiotekh. i Elektron. 1, 1135 (1956).
8. N. A. Tolstoi. Izvest. Akad. Nauk SSSR, Ser. Fiz. 15, 712 (1951).
9. V. E. Lashkarev, E. A. Sal'nov, G. A. Fedorus, and M. K. Sheinkman. Doklady Akad. Nauk SSSR 114, 1203 (1957).

ISOTOPIC EFFECT OF THE CENTRAL ATOM IN THE VIBRATIONAL SPECTRUM OF METHANE

R. R. Shvangiradze and Sh. Z. Jamagidze

Received 14 July 1959

The isotopic effect of the central atom in the vibrational spectrum of a tetrahedral molecule of the type XY_4 has not, to our knowledge, been studied experimentally. Examination of this problem is of considerable interest from the viewpoint of ascertaining the nature of the vibrational motion of atoms in such molecules.

Of the four fundamental frequencies of a tetrahedral molecule of the XY_4 type, the central atom is mobile only in two threefold degenerations of the f_2 class. Consequently, one may expect phenomena, caused by changes in mass of the central atom X, only at these infrared-active frequencies.

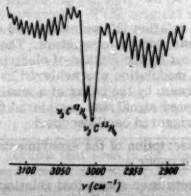

In the present work, the infrared spectrum of natural methane and of methane containing 70-90% of C^{13} is studied. The investigation was carried out using an IKS-6 infrared spectrometer which was calibrated in the appropriate spectral region by a procedure described in reference 1. The studied gases, at a pressure of 100 mm Hg, were placed in a cell 15 cm in length having windows of KBr. The spectrum was studied in the region from 2 to 15μ, using prisms of LiF and NaCl.

The experimental values of the infrared-active fundamental frequencies (ν_3 and ν_4) and certain compound frequencies and their isotopic displacements, are tabulated. The maximum experimental error in the determination of isotopic displacement is 1 cm^{-1}.

The absorption band near 4650.7 cm^{-1}, marked with an asterisk in the table, we initially assigned to methane. It has an isotopic displacement approximately twice that of the fundamental frequency ν_3. On the basis of the extent of the isotopic displacement we consider the combination $2\nu_3 + \nu_2 - \nu_1$ to be the most probable interpretation of this band. The band at 4280 cm^{-1} also shows an isotopic displacement, equal to 9 cm^{-1}. However, its interpretation was difficult.

Infrared Frequencies of Molecules $C^{12}H_4$ and $C^{13}H_4$ (in cm^{-1})

Frequency	$\nu_{exp.}$		$\Delta\nu_{exp.}$	$\Delta\nu_{theor.}$	
	$C^{12}H_4$	$C^{13}H_4$		Lechner's formulas	Teller-Redlich rule
ν_3	3015.9	3007.8	8.1	12.7	12.3
ν_4	1300.5	1292.8	7.7	7.3	7.3
$2\nu_4$	2601.8	2586.2	15.6	—	—
$\nu_3 + \nu_4$	4245.0	4206.3	8.7	—	—
$\nu_3 + \nu_4$	2817.0	2808.7	8.3	—	—
$\nu_3 + \nu_4$	4316.5	4299.6	16.9	—	—
$2\nu_3 + \nu_2 - \nu_1$	4650.7*	4634.0	16.7	—	—
—	4280.0	4271.0	9.0	—	—

Values of the isotopic displacements of the fundamental frequencies ν_3 and ν_4, calculated from formulas derived by Lechner in a suggestion about valence forces, are presented in the fifth column of the table, and values determined on the basis of the Teller-Redlich[2] rules are given in the sixth column. For very small isotopic displacements the agreement between experimental and theoretical values is considered to be satisfactory.

The small magnitude of the isotopic effect at frequencies ν_2 and ν_4 indicates that the central atom of a tetrahedral molecule of the XY_4 type takes a small part in the vibrations of the f_2 class.

A record of the absorption band corresponding to the frequency ν_3, for methane containing 75% $C^{13}H_4$, is shown in the figure. It should be noted that the magnitude of the isotopic displacement of the central minimum ν_3 is of single order, the distance between adjacent rotary lines being in cm^{-1}. Therefore, the lines of $C^{12}H_4$, with a rotational quantum number J, practically coincide with the lines of $C^{13}H_4$ with a quantum number $J \pm 1$. The isotopic effect in the vibrational spectrum during changes of mass of the central atom, as expected, was not observed.

REFERENCES

1. A. N. Aleksandrov and V. A. Nikitin. Uspekhi Fiz. Nauk 56, 3 (1955).
2. G. Herzberg. "Kolebatel'nye i vrashchatel'nye spektry mnogoatomnykh molekul." (Vibrational and Rotational Spectra of Polyatomic Molecules), IL, Moscow, 1949.

ON THE POLARIZATION OF THE LUMINESCENCE OF ZnS SINGLE CRYSTALS

V. I. Gribkov and N. D. Zhevandrov

Received 18 July 1959

This note describes an investigation of the polarization of single crystals of ZnS activated with copper (prepared by Panasiuk[1]). The degree of polarization was measured on microcrystals by use of equipment built around a microscope and a Cornu polarimeter.[2] Besides these measurements, our samples included some crystals that were a few millimeters long, which could be investigated without a microscope.

The measurement of the azimuthal dependence of the polarization (that is, the dependence of the degree of polarization on the angle of rotation of the crystal about an axis perpendicular to its surface, and coinciding with the direction in which the polarization of the luminescence was measured) made it possible to find a crystal orientation for which the degree of polarization was a maximum. This value was found to be about the same for different samples and was approximately 20%. The results obtained agree with the data of reference[3].

Both the azimuthal dependence and the maximum value of the degree of polarization were found to be the same for luminescence excited by light of different wavelengths—436, 405, 365, and 313 mμ.

It is obvious that the absolute values of the positive and negative extrema of the azimuthal dependence should be the same. However, the data of reference 3 do not agree with this conclusion. (For polarized excitation, the degree of polarization was –3% at the negative extremum and +20% at the positive extremum; for natural excitation, the degree of polarization was 12%.) The cause of this phenomenon is not yet known. This might be a consequence of imperfection of the crystal, or the result of the dependence of polarization of luminescence on the polarization of the exciting light.

We undertook a special investigation of the dependence of the polarization of the luminescence of single crystals of ZnS on the orientation of the electric vector of the exciting light. In this case, the orientation of the crystal was kept constant, and the Nicol through which the exciting light was passed was rotated about its own axis. The results of the measurement are presented in Fig. 1 (the two straight lines correspond to two different orientations of the crystal). As is evident from the figure, the polarization of the luminescence does not depend on the polarization of the exciting light. In this case, the degree of polarization was shown to be the same as for excitation by natural light. At first glance this appears to disagree with Antonov-Romanovskii's assumption[4] that in excitation by polarized light, centers of only a particular orientation are ionized, so that electrons can recombine only with those centers (their orientation is determined, apparently, by the orientation of the electric vector of the exciting light), and consequently the polarization of the luminescence should depend on the polarization of the excitation. However, if one takes into account the fact that in addition to the migration of electrons in a crystallophosphor, holes also migrate (in other words, ionization states may migrate from center to center), this disagreement disappears.

The independence of the polarization of the luminescence of single crystals of ZnS on the polarization of the exciting light can thus be interpreted as the result of the migration of energy of excitation through the crystal. This conclusion cannot of itself resolve the question of the mechanism of the migration, however (for example, exciton, or electron-hole migration), just as in molecular crystals it is impossible by means of a single method to differentiate between localized and free excitons.

Measurement of the degree of polarization in the luminescence spectrum (on a spectro-polarimeter, the basic parts of which are a monochromator, a double image prism, and two photomultipliers, recording two mutually perpendicular components of the electric vector of the luminescence) showed that, within the limits of experimental error, the degree of polarization is practically the same over the entire spectrum (Fig. 2). Further qualitative observations led to the conclusion that phosphorescence has the same degree of polarization as luminescence under excitation.

Fig. 1

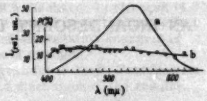

Fig. 2

Fig. 1. Dependence of the degree of polarization of the luminescence P of single crystals of ZnS on the orientation (χ°) of the electric vector of the exciting radiation ($\lambda_{exc.}$ = 365 mμ). Straight lines 1 and 2 correspond to two different orientations of the sample.

Fig. 2. Dependence of the degree of polarization of the luminescence P of single crystals of ZnS on the wavelength of the luminescent light. a—spectrum of luminescence; b—degree of polarization.

We extend our thanks to E. I. Panasiuk for his kindness in furnishing the crystals for the investigation.

REFERENCES

1. M. N. Alentsev and E. I. Panasiuk. Opt. i Spektr. 5, 207 (1958).
2. N. D. Zhevandrov. Doklady Akad. Nauk SSSR 83, 677 (1952).
3. A. Lempicki. Phys. Rev. Letters 2, 155 (1959).
4. V. V. Antonov-Romanovskii. J. Phys. rad. 17, 661 (1956).

"ANISOTROPY" OF THE LIGHT PULSE FROM A POLARIZED ELECTROLUMINESCENT CELL

V. L. Rabotkin and V. A. Sokolov

Received 18 July 1959

The present communication describes the properties of a polarized electroluminescent cell prepared in the following manner. A ZnS-Cu, Pb phosphor was suspended in molten paraffin between two electrodes; the metal support served as one electrode, and conducting glass was used for the other. Then a potential of 2000 volts dc was applied to the electrodes and maintained until the paraffin solidified.

Prepared in this fashion and excited by periodic unipolar impulses, the cell possesses a strong anisotropy relative to the direction of the exciting electric field, which shows up as a change of form of the light pulse. Thus, if the original direction of the exciting field coincides with the direction of the field which polarized the cell, then the light pulse has the form pictured in Fig. 1, in which the bottom curve is a time scale (500 cps), the middle one is the exciting voltage with its zero line, and the top curve is the light pulse. Upon applying the exciting voltage in the opposite direction, the light pulse takes on

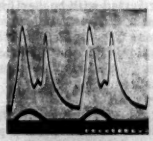

Fig. 1

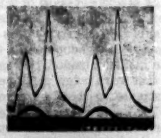

Fig. 2

the appearance shown in Fig. 2.

As follows from a comparison of the oscillograms shown in Figs. 1 and 2, the relative intensity of the principal light pulses changes sharply upon altering the direction of the exciting field.

This anisotropy occurred consistently in both freshly prepared cells and in cells which were stored for several days after preparation.

AN INCANDESCENT LAMP WITH A MICA WINDOW FOR THE INFRARED REGION OF THE SPECTRUM

E. N. Maleyev

Received 25 July 1959

The communication cited in reference 1 described an incandescent lamp with a mica window for the infrared region of the spectrum. The indancescent element of such a lamp may be a tungsten spiral, alternatively, a strip of thin tungsten or tantalum sheet may be used, bent in such a way as to increase the blackness. The blackness of a tungsten helix has now been increased by carburization. The carburization was carried out in the usual manner in benzene vapor under a bell jar. The bases of the lamps with the spirals mounted in them, were attached to the leads. The degree of carburization was controlled by observing the color of the filament.

Tests showed that the carburized filaments vaporized to a considerably lesser extent, thus permitting the lamp to be operated at higher temperatures. A comparison was made between the spectral intensity of the lamp with a carburized conical spiral (employed in STS-62 lamps) and the spectral intensity of a Nernst rod under the usual operating conditions. The brightness temperature of the lamp was 2050°K and that of the rod 1760°K for $\lambda = 0.65\ \mu$.

Wavelength (μ)	Ratio of spectral intensity of lamp to spectral intensity of Nernst rod	Wavelength (μ)	Ratio of spectral intensity of lamp to spectral intensity of Nernst rod
3.0	1.4	6.0	0.4
3.5	1.3	6.5	0.4
4.0	1.2	7.0	0.3
4.5	0.9	7.5	0.2
5.0	0.6	8.0	0.2
5.5	0.4		

The Table gives the averaged comparison results obtained with the aid of an infrared monochromator.

The operation of lamps with carburized spiral filaments has shown that they possess satisfactory mechanical strength.

REFERENCE

1. E. N. Maleyev. Opt. i Spektr. 4, 21 (1958).

THE CHANNEL TEMPERATURE OF A SPARK DISCHARGE IN AIR

A. A. Mak

Received 25 July 1959

Comparison of the results obtained by different workers has led to the hypothesis that the channel temperature in a spark discharge varies little with the rate at which energy is supplied to the spark gap.[1,2]

In the research reported here we studied the variation of the channel temperature with the rate of increase of current for a spark discharge in air; the spark parameters were as follows: $C = 0 \times .05$ μf, U = 3 to 8 kv, $L = 4 \times 10^{-9}$ to 5.4×10^{-3} h, spark gap 5 mm for $L > 4 \times 10^{-9}$ h, 1.5 mm for $L = 4 \times 10^{-9}$ h. For low current increase rates ($U/L \leq 2 \times 10^9$ amp/sec) the temperature was determined by measuring the relative intensities of the lines N II 5535, 5495, and 5045 A. The measurements were made by means of a photoelectric arrangement having a maximum time resolution of 5×10^{-8} sec.[3] At greater current increase rates the temperature was measured by the brightness method,[2,4] using the spectral brightness density in the spark channel for the wavelength corresponding to the center of gravity of the N II line at 5001 A. The absorption of the channel for this wavelength with a current increase rate of $U/L \geq 10^{11}$ amp/sec was assumed to be unity, since it was established that the peak of the N II line at 5001 A was quite flat during the initial stages of the discharge, even at $U/L = 10^{11}$ amp/sec (see the Figure). The Table gives

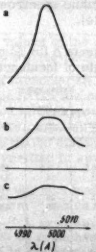

Contour of the N II line at 5001 A at different stages of the discharge. Time (μ sec): a—2.7; b—0.7; c—0.15.

$\frac{U}{L}$ amp/sec	$1.3 \cdot 10^{9}$	$3.2 \cdot 10^{9}$	$6.8 \cdot 10^{9}$	$2 \cdot 10^{10}$	$7.5 \cdot 10^{10}$	$9 \cdot 10^{10}$*
$T \cdot 10^{-4}$ (°K)	2.9	2.9	3.0	2.6	3.1	3.3

*Measurements of the spectral brightness density of the background showed that under these discharge conditions, the channel radiated as a black body at 33,000° K in the visible region of the spectrum.

the results of these measurements. The values of the temperature given in the second line are averages of several measurements of the values of the maximum channel temperature (during the radiation). The scatter in the temperature values lies within the limits of experimental error (the error of measurement for both methods was ~30–35%).

The results obtained show that the channel temperature varies very little with the rate of increase of current in the discharge. Results obtained in the recent work of Sukhodrev and Mandel'shtam, who measured the electrode vapor temperature in a spark discharge,[5] confirm this conclusion.

The channel temperature for the spark in air ($\sim 3 \times 10^{4}$°K) is lower than that of a discharge in nitrogen (4.3×10^{4}°K).[3] This is apparently caused by the cooling effect of oxygen, the ionization and dissociation energies of which are lower than those of nitrogen.[1]

The author is deeply grateful to M. P. Vaniukov for his interest in the work and discussion of the results.

REFERENCES

1. M. P. Vaniukov and A. A. Mak. Usp. Fiz. Nauk 66, 301 (1958).
2. M. P. Vaniukov and A. A. Mak. Doklady Akad. Nauk SSSR 123, 1022 (1958).
3. M. P. Vaniukov, B. A. Ermakov, A. A. Mak, and V. R. Muratov. Vestnik Leningrad Gosudarst. Univ., Ser. Fiz. i Khim. No. 16, 25 (1959).
4. M. P. Vaniukov, A. A. Mak, and N. V. Parazinskaya. Opt. i Spektr. 1, 642 (1956).
5. N. K. Sukhodrev and S. L. Mandel'shtam. Opt. i Spektr. 6, 723 (1959).

REFLEXOMETER FOR THE VACUUM ULTRAVIOLET REGION OF THE SPECTRUM WITH THE USE OF $CaSO_4$:Mn PHOSPHOR

V. A. Arkhangel'skaya, B. I. Vainberg, and T. K. Razumova

Received 25 July 1959

In an earlier work[1] we reported on the possibility of measuring the transmissivity of optical materials in the region 120-145 mμ with the use of phosphor $CaSO_4$:Mn. This possibility is based on the ability of the phosphor to store energy under the action of ultraviolet irradiation with wavelengths $\lambda \leq 1500$ A, and to liberate it in the form of visible radiation during heating (thermoluminescence). The magnitude of the stored energy ("integrated light intensity") within wide limits is linearly proportional to the density of the short wavelength radiation and to the time of irradiation of the phosphor. The phosphor used as a detector is sensitive only to hard ultraviolet radiation, and the utilization of supplementary filters with stepwise displaced short wavelength limits of transmissivity (LiF, CaF_2, etc.) makes it possible to select sufficiently narrow spectral ranges, within which the transmissivity is then measured. In this way the necessity of a vacuum monochromator is avoided, thus simplifying the apparatus and making the method much less laborious.[2]

The present work reports on the possibility of constructing a simple reflexometer based on the phosphor $CaSO_4$:Mn and presents the results of measurement of reflection coefficients for several surfaces in the spectral region 120-145 mμ.*

*I. N. Panova took part in these measurements.

The source of short wavelength ultraviolet radiation was a hydrogen lamp with a lithium fluoride window. The simple setup described earlier[1] was used in recording the thermoluminescence of the $CaSO_4$:Mn phosphor. Sheets of LiF (transmission limit 1050 A), CaF_2 (transmission limit 1250 A) and SrF_2 (transmission limit 1400 A) were used as supplementary filters.

The principal arrangement of the optical, detecting, and recording systems of the reflexometer are presented in the Figure. The optical system consists of a hermetic box with LiF windows and the hydrogen lamp (Figure, a). The reflecting surface is located within the box on a movable axis which has several fixed positions corresponding to various angles of incidence of the radiation. Dry air, as is known,[3] is comparatively transparent in the range 1100-1300 A. However, ozone, carbon dioxide, and particularly water vapor are responsible for strong absorption of ultraviolet radiation. For this reason it is more convenient to carry out measurements with the chamber pumped down to a pressure of 10^{-2}–10^{-3} mm Hg. During the measurements screens covered with the phosphor are placed outside the vacuum chamber so that their surfaces are located in direct proximity to surfaces of the lithium fluoride windows. One of the windows serves in the measurement of the incident beam, the remaining ones for measurement of beams reflected at various angles of incidence. (For simplicity, in the Figure, a, only one window for measurement of reflected radiation is shown.)

As is shown by calculations and control measurements using a vacuum spectrometer, the supplementary

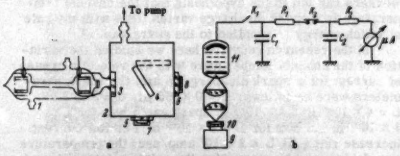

Arrangement of reflexometer. a—optical system of reflexometer; b—detecting and recording system. 1—hydrogen lamp, 2—vacuum chamber, 3—supplementary filter, 4—specimen to be studied, 5, 6—LiF windows, 7, 8, 10—$CaSO_4$:Mn screens, 9—heater, 11—FEU-19 photomultiplier.

filters of LiF, CaF_2, and SrF_2 make it possible to select from the radiation of the hydrogen lamp regions with maxima at 122, 127, and 144 mμ. Reflection coefficients for specula and glass which were measured with the reflexometer in these regions corresponded satisfactorily with the reflection coefficients of these specimens as measured with the vacuum spectrometer for the same wavelengths (see Table).

Reflection Coefficients ρ (in %) of Various Surfaces for Angle of Incidence of 60°

Specimens	Reflexometer			Vacuum spectrometer		
	λ_{max} (mμ)			λ_{max} (mμ)		
	122	127	144	122	127	144
Al specula						
No. 1	8.5	8.5	19	3.5	5.0	20
No. 2	14	14	23	13	16.5	20
No. 3	18	17	26	16	20	26
No. 4	32	28	40	24	31	40
No. 5	34	28	40	23	28	37
Pd specula						
No. 1	9.0	8.0	7.5	9.0	8.5	9.0
No. 2	9.0	7.0	7.0	8.5	8.0	6.5
F-1 glass	13	—	—	15	—	—
Fused quartz	17	—	—	20	—	—

The method described can be recommended for rapid determination of reflection coefficients during mass production of mirrors, and also diffraction gratings, to be used for the vacuum ultraviolet region of the spectrum. The apparatus also can be used in measuring the transmissivity of optical materials in the above-mentioned regions of the spectrum.

REFERENCES

1. V. A. Arkhangel'skaya, B. I. Vainberg, and T. K. Razumova. Opt. i Spektr. 1, 1018 (1956).
2. J. D. Purcell. J. Opt. Soc. Am. 43, 1166 (1953).
3. T. Lyman. Phys. Rev. 48, 149 (1935).

ON THE VIBRATIONAL ANALYSIS OF THE $A^3\Pi - X^3\Sigma^-$ BAND SYSTEM OF THE OH^+ MOLECULE

V. S. Yungman

Received 27 July 1959

In the spectrum of the OH^+ molecule only one band system $A^3\Pi - X^3\Sigma^-$ is known.[1-3] The vibrational constants for both states were calculated twice. From the analysis of 0-0, 0-1, 1-0, and 1-1 bands Loomis and Brandt[3] found $\omega_e'' = 3111$, $\omega''x_e'' = 73$, $\omega_e' = 2387$, and $\omega_e x' = 200$ cm^{-1}. Recently Weniger and Herman,[2] having investigated in addition the 2-2 and 3-3 bands of this system, recalculated the values of the vibrational constants and obtained $\omega_e'' = 3229$, $\omega_e x_e'' = 131$, $\omega_e' = 2202$, and $\omega_e x_e' = 108$ cm^{-1}. In both instances[2,3] the equations used for the computation of ω_e and $\omega_e x_e$ were

$$\Delta G_{v+\frac{1}{2}} = \omega_e - 2\omega_e x_e, \tag{1}$$

$$\omega_e^2 = \frac{4B_e^3}{D_e}, \tag{2}$$

where $\Delta G_{v+\frac{1}{2}}$ is first vibrational quantum, while B_e and D_e are rotational constants obtained from the analysis of fine structure of the bands.

There is another way of calculating the vibrational constants which is better insofar as it guarantees the convergence of the vibrational levels to the dissociation limit. It consists of making use of the equation

$$\omega_e^2 = 4\omega_e x_e D_0,^1 \tag{3}$$

*The use of the zero values of the constants affords a more convenient form for the subsequent calculations.

where D_0 is energy of dissociation. In contrast to Eq. (2), which is derived in the harmonic oscillator approximation, Eq. (3) is derived in the approximation of an anharmonic oscillator, i.e., assuming that the Morse function is applicable to positive diatomic ions. This assumption has been indeed verified in several instances (N_2^+, NO^+, O_2^+, CO^+, etc.).

In our calculation use was made of the values $\Delta G_{\frac{1}{2}}' = 2970$ and $\Delta G_{\frac{1}{2}}'' = 1985$ cm^{-1}, which were found from the zero lines of the 0-0, 0-1, 1-0, and 1-1 bands,[3] obtained by extrapolation of the Q_2 branches of the corresponding bands. In as much as in the case of OH^+ such extrapolation is not reliable, the error in the calculated $\Delta G_{\frac{1}{2}}$ may attain 5 cm^{-1}. The values of $\Delta G_{\frac{1}{2}}$ obtained by the above-mentioned authors[2,3] agree with ours within the limits of this error.

The energy of dissociation D_0 of the OH^+ molecule may be found with great precision by Hess's law from the dissociation energy of OH and the ionization potentials of OH and one of the two atoms.

By making use of the values $D_0(OH) = 35450$,[4] $I_0(H) = 109679$, $I_0(O) = 109837$,[5] and $I_0(OH) = 106310$ cm^{-1},[6] we obtain for $D_0(OH^+, X^3\Sigma^-)$ two values—38819 and 38977 cm^{-1}— depending on whether the products of dissociation of the OH^+ in the ground state are $O(^3P) + H^+$ or $O^+(^4S) + H(^2S)$. Although the difference between these two values is small and is within the permissible computational error for the $D_0(OH^+)$ value, the choice between them is, in principle, significant for the calculation of vibrational constants in both electronic states of OH^+.

If we assume that $OH^+(X^3\Sigma^-) \rightarrow O(^3P) + H^+$, then, in accordance with the correlation rules there must also exist the state $^3\Pi$ with the same dissociation limit. It is natural to suppose that the state $A^3\Pi$, with the excitation energy $\nu_{00} = 27956$ cm^{-1}, may be identified with the above-mentioned state. Then $D_0(OH^+, A^3\Pi) = 10863$, $\omega_0'' = 3030$, $\omega_e x_0'' = 60$, $\omega_0' = 2085$, and $\omega_e x_0' = 100$ cm^{-1}.

If, on the other hand, $OH^+(X^3\Sigma^-) \rightarrow O^+(^4S) + H(^2S)$ then the $^3\Pi$ state can no longer correlate with these atomic states. Assuming that $OH^+(A^3\Pi) \rightarrow O^+(^2D) + H(^2S)$, we obtain $D_0(OH^+, A^3\Pi) = 37837$, $\omega_0'' = 3029$, $\omega_e x_0'' = 59$, $\omega_0' = 2012$, and $\omega_e x_0' = 27$ cm^{-1}.

Thus we have obtained two sets of vibrational constants, which are practically identical for the state $X^3\Sigma^-$, but which are in mutual disagreement for the state $A^3\Pi$.

A criterion for choosing correctly between these two sets may be afforded by comparing the calculated frequencies of the zero lines for the 2-2 and 3-3 bands, based on these two alternatives, with the experimental values obtained by Weniger and Herman.[2] The results of this comparison are listed in Table 1.

Table 1. Comparison Between Calculated and Experimental Values ν_0^{2-2} and ν_0^{3-3} (in cm^{-1})

Band	Experimental value	Calculated value $OH^+(A^3\Pi) \rightarrow O(^3P) + H^+$	Δ	Calculated value $OH^+(A^3\Pi) \rightarrow O^+(^2D) + H(^2S)$	Δ
2—2	26057	25906	151	25050	7
3—3	25189	24761	428	25193	—4

These results indicate that the second set of vibrational constants is undoubtedly more reliable. By the same token the assumption of Loomis and Brandt[3] that the state $A^3\Pi$ dissociates to $O(^3P) + H^+$ is probably incorrect.

Our calculated values for the vibrational constants are listed in Table 2.

Table 2. Vibrational Constants of OH^+ in the States $X^3\Sigma^-$ and $A^3\Pi$ (in cm^{-1})

State	ω_e	$\omega_e x_e$
$X^3\Sigma^-$	3088	59
$A^3\Pi$	3039	27

Thus, the following results were obtained.

1. The vibrational constants of the OH^+ molecule in the states $X^3\Sigma^-$ and $A^3\Pi$ were calculated from experimental data obtained in references 2 and 3, under the condition of convergence of vibrational levels to the dissociation limit.

2. It was shown that the products of dissociation of the OH^+ molecule in the state $X^3\Sigma^-$ must be the atoms $O^+(^4S) + H(^2S)$, and in the state $A^3\Pi$, the atoms $O^+(^2D) + H(^2S)$.

REFERENCES

1. W. H. Rodebush and M. H. Wahl. J. Chem. Phys. 1, 696 (1933).

2. F.W. Loomis and W.H. Brandt. Phys. Rev. 49, 55 (1936).
3. S. Weniger and R. Herman. J. phys. radium 19, 582 (1958).
4. R. F. Barrow. Arkiv Fysik 11, 281 (1956).
5. C. Moore. "Atomic Energy Levels," Vol. I. Washington, 1949.
6. S. N. Foner and R. L. Hudson. J. Chem. Phys. 25, 602 (1956).

CONFERENCE ON THE PHYSICS OF ALKALI-HALIDE CRYSTALS

The Conference on the Physics of Alkali-Halide Crystals took place in Tartu from June 30 to July 4, 1959. The Conference was convened by the Scientific Congress on Luminescence, the Academy of Sciences of the Estonian SSR and the Tartu State University. Over 100 delegates from thirteen cities of the USSR took part in the Conference. Thirty-six lectures were presented during eight meetings.

The subject matter of this Conference differed from that of the other, by now traditional, conferences and meetings on spectroscopy, semiconductors, luminescence, and dialectrics. The Conference was conceived and held in order to obtain a many-sided approach to the study of various optical, electrical, mechanical, dialectric, and other properties of a narrow class of subjects—the alkali-halide crystals. Broad discussion of various physical and physico-chemical problems arising from the study of alkali-halide crystals should have helped to strengthen the bond among the separate investigational approaches, and to broaden the work in the borderline fields where the various approaches had been consolidated.

M. D. Galanin (Moscow) in his introductory talk and F. D. Klement (Tartu) in his concluding talk discussed the basic physical properties of the alkali-halide crystals. It was noted that since the classic papers of Academician A. F. Ioffe in the USSR and Professor Polya in Germany first appeared, the amount of research on alkali-halide crystals has increased very rapidly. The results obtained with these simple ionic crystals became part of the foundation of our present day ideas about the structure of solids and about the mechanism of physical processes occurring in them. In the postwar years, the alkali-halide crystals had very important practical applications as scintillation counters and as dose meters for hard radiation.

A large group of lectures at the Conference dealt with the research on physical processes in crystals connected with the excitation of luminescence. I. A. Parfianovich (Irkutsk) spoke of the optical flash phenomenon in crystals containing color centers which are not uniformly distributed in the crystal. M. L. Kats (Saratov) devoted his lecture to the change in the absorption spectra of crystals after they were acted on by an ionizing radiation. Ch. B. Lushchik, I. V. Yaek, G. G. Liid'ya, and E. S. Tiisler (Tartu), in their lecture, considered the mechanism of electron, hole, exciton, and sensitization processes leading to the luminescence of the alkali-halide crystals. E. I. Shuraleva (Irkutsk) reported on the mechanism of luminescence of NaCl-Ni phosphor. I. V. Yaek (Tartu) cited some data on the excitation spectra of recombination luminescence and on "color center creation spectra" in alkali-halide crystals. G. G. Liid'ya (Tartu) devoted his talk to the interesting problem of the interaction of excitons with the crystal lattice defects. Z. L. Morgenshtern (Moscow) reported on the luminescence of nonactivated CsI crystals, which had received little attention previously.
data were cited by A. Ya. Pae and A. A. Khaav (Tartu). The paper of O. G. Mankin and N. E. Lushchik (Tartu) dealt with the spectrophotometric study of diffusion of

In a number of lectures results of theoretical and experimental studies of luminescence centers in alkali-halide crystals were discussed. The review by M. I. Petrashen' (Leningrad) was devoted to quantum mechanical calculations of the optical properties of the impurity centers in crystals. N. N. Kristofel' (Tartu) and I. V. Abarenkov (Leningrad) carried out a quantum mechanical calculation of the adiabatic potentials and spectral characteristics of some special types of impurity centers (luminescence centers in KCl-Tl, F-centers). The spectroscopy of luminescence centers in crystals activated by several sets of impurity ions (Ga^{+}, Ge^{++}, In^{+}, Sn^{++}, Tl^{++}, Pb^{++}; Cu^{+}, Ag^{+}, Au^{+}, etc.) was discussed in the report of N. E. Lushchik and Ch. B. Lushchika (Tartu). K. K. Shvarts (Riga) made a study of thermal, optical and migrational quenching of luminescence in crystals with mercury-like activators. I. K. Plyavin (Riga) in his talk reported on the temperature dependence of the duration of photoscintillation and its relation to the existence of metastable energy levels in the luminescence centers. Ya. Ya. Kirs and A. I. Laisaar (Tartu) spoke on the influence of hydrostatic pressure on the spectral characteristics of the centers. A very promising new method of studying the anisotropy of luminescence centers by the uniaxial compression of crystals reported by A. A. Kaplyanskii (Leningrad). In the lectures of T. A. Abdusadykov (Alma-Ata) and of A. F. Malysheva (Tartu) spectral characteristics of alkali-halide and alkali-earth-halide phosphors with large activator concentrations and other crystal lattice defects were discussed.

Several lectures dealt with the nature of color centers in alkali-halide crystals. A. A. Shatalov (Kiev) reported on photochemical and thermal transformations of color centers in heated crystals. The report of O. A. Shmit (Riga) dealt with the study of the anisotropy of color centers. A. Kh. Khalilov and collaborators (Baku) reported on the results of research on capture centers in alkali-halide crystals containing various impurity ions. The lecture of I. K. Vitol, Ch. B. Lushchik, I. V. Yaek, and M. A. Elango (Tartu, Riga) dealt with the complex study of the nonisothermal relaxation processes in alkali-halide crystals. L. M. Shamovskii (Moscow) discussed in detail the problem of thermal ionization energy of F-centers.

In recent years it was discovered that many physical properties of crystals depend on special linear defects of the crystal lattice (dislocations). A special session of the Conference was devoted to the study of effects related to the presence of dislocations in alkali-halide crystals. The lecture of M. V. Klassen-Nekliudova and collaborators (Moscow), which aroused a great deal of interest, dealt with the mechanical properties of pure alkali-halide crystals and their connection with the presence and motion of dislocations. The influence of impurities on "etching patterns" in KI crystals was discussed in the lecture of L. M. Shamovskii and A. S. Shibanov (Moscow). R. I. Gindina (Tartu) reported on the masking of dislocations by means of nonisomorphic impurities and on the connection between the masking phenomenon and luminescence. The lecture of A. A. Shatalov

(Kiev) dealt with the "development" of crystal lattice defects with the help of additive coloring.

The physico-chemical properties of alkali-halide crystals were discussed in the papers of physicists of the Tomsk school. A. A. Vorob'eva and collaborators (Tomsk), in their talk, established a connection between the composition of solid solutions NaCl-KCl; KCl-KBr, etc., and their physico-chemical properties. The report of E. K. Zavadovskn, M. S. Ivankina, I. Ya. Melik-Gaikazyan, and M. N. Treskina (Tomsk) dealt with the influence of the dissociation of solid solutions of alkali-halide salts on their various physico-chemical characteristics. Some new data on the structure of alkali-halide phosphors obtained from the X-ray structure analysis impurity ions in crystals. The long paper of L. M. Belyaev and collaborators (Moscow) discussed the methods of obtaining activated lithium fluoride crystals and their luminescent properties.

Interesting papers were devoted to the electrical properties of alkali-halide crystals. A. N. Arsen'eva-Geil' (Leningrad) reported on the external photoeffect in alkali-halide crystals with F-centers. The results of an investigation of photoelectric properties of alkali-halide crystals with defect-gradient layers, using the dynamic condenser method, were cited in the paper of I. K. Vitol (Riga). The long paper of A. A. Vorob'ev and collaborators (Tomsk) reviewed the results of experimental studies on the electrical breakdown of alkali-halide salt crystals.

The Conference on the Physics of Alkali-Halide Crystals was held in an atmosphere of lively discussion. Almost all of the papers presented aroused great interest among the participants at the conference. The Conference decided to improve the coordination of current research on alkali-halide crystals and to hold a second conference on the physics of alkali-halide crystals in the summer of 1961 in Riga.

TRANSLITERATION OF CYRILLIC CHARACTERS

used by the Optical Society of America

А	а	a	Р	р	r
Б	б	b	С	с	s
В	в	v	Т	т	t
Г	г	g	У	у	u
Д	д	d	Ф	ф	f
Е	е	e	Х	х	kh
Ж	ж	zh	Ц	ц	ts
З	з	z	Ч	ч	ch
И	и	i	Ш	ш	sh
Й	й	i	Щ	щ	shch
К	к	k	Ъ	ъ	″
Л	л	l	Ы	ы	y
М	м	m	Ь	ь	′
Н	н	n	Э	э	e
О	о	o	Ю	ю	yu
П	п	p	Я	я	ya

On the Correction for the Size of Exit Diaphragm in the Photoelectric Recording of Interference Bands of Equal Inclination . . . . . Yu. P. Efremov and Yu. P. Kanevskii 137
On the Semi-Empirical Calculation of the Ionization Potentials of Aliphatic Compounds . . . . . V. M. Baranov and T. K. Rebane 138
Change in the Infrared Absorption of Certain Semiconducting Adsorbents under Ultraviolet Illumination . . . . V. N. Filimonov 139
Superlinearity in Luminescence and Photoconductivity Phenomena and the Rose–Bube Theory . . . . . N. A. Tolstoi and A. I. Ryskin 141
Isotopic Effect of the Central Atom in the Vibrational Spectrum of Methane . . . . . R. R. Shvangiradze and Sh. Z. Jamagidze 142
On the Polarization of the Luminescence of ZnS Single Crystals . . . . . V. I. Gribkov and N. D. Zhevandrov 143
"Anisotropy" of the Light Pulse from a Polarized Electroluminescent Cell . . . . . V. L. Rabotkin and V. A. Sokolov 144
An Incandescent Lamp with a Mica Window for the Infrared Region of the Spectrum . . . . . E. N. Maleyev 144
The Channel Temperature of a Spark Discharge in Air . . . . . A. A. Mak 145
Reflexometer for the Vacuum Ultraviolet Region of the Spectrum with the Use of $CaSO_4$:Mn Phosphor . . . . . V. A. Arkhangel'skaya, B. I. Vainberg, and T. K. Razumova 146
On the Vibrational Analysis of the $A^2\pi - X^2\Sigma^-$ Band System of the OH Molecule . . . . . V. S. Yungman 147
Conference on the Physics of Alkali-Halide Crystals 148

EDITOR'S NOTE

Comments on the scientific content of the translated Russian articles published in OPTICS AND SPECTROSCOPY are invited. They should be addressed as a Letter to the Editor of the Journal of the Optical Society of America and forwarded to the Editor of that journal, Dr. W. R. Brode, National Bureau of Standards, Washington 25, D.C.

VOL. VIII, NO. 2 FEBRUARY 1960

Calculation of Photoionization Cross Sections of Aluminum and Gallium Atoms . . . . . L. A. Vainstein and G. E. Norman 79

The Contour of the H_δ Hydrogen Line Behind a Shock Wave in Argon . . . . . V. N. Alyamovskii and V. F. Kitaeva 80

On a Possible Mechanism of Electronic Excitation in Slow Atomic Collisions . . . . . E. E. Nikitin 82

Photoelectric Determination of the Excitation Functions of the Bands of the Negative System N_2^+ . . . . . S. M. Kishko 84

Effect of Interaction with the Environment on Fermi Resonance in Polyatomic Molecules . . . . . V. L. Strizhevsky 86

On the Theory of the Use of Dependent Coordinates in the Problem of Molecular Vibrations . . . . . I. V. Rigina and I. N. Godnev 89

Polarization of Harmonic Oscillator Luminescence . . . . . V. P. Gribkovskii and B. I. Stepanov 92

Theory of the Intensities of Infrared Spectra of Molecules, VI. BF_3, NF_3, SiF_4, and SF_6 . . . . . L. M. Sverdlov 96

New Variant of the Metallic Model of a Molecule . . . . . L. A. Borovinskii 99

Calculation of Frequency and Form Derivatives of Normal Vibrations of Molecules Possessing Symmetry . . . L. S. Mayants 102

Photoelectric Investigation of Raman Spectra of Gases at Low Pressures . . . . . P. A. Bazhulin and Iu. A. Lazarev 108

Total Luminescence Brightness of ZnS-Cu and ZnS-Cu, Mn Electroluminophors in a Pulsating Field . . . . . G. S. Kozina and L. P. Poskacheeva 110

Electroluminescence Light Pulses under the Simultaneous Action of dc and ac Voltage . . . . . G. S. Kozina, V. N. Favorin, and I. D. Anisimova 112

Polarization of Luminescence in a System of Particles with Three Energy Levels as a Function of the Exciting Light Intensity . . . . . B. I. Stepanov and V. P. Gribkovskii 114

Investigation of Reflectance and Luminescence Spectra of Copper Halides at Low Temperature . . . . . E. F. Gross, B. S. Razbirin, and R. I. Shekhmamet'ev 119

A Photographic Method of Measuring the Optical Constants of Metals . . . . . I. N. Shklyarevskii and A. I. Sharapov 122

The Determination of the Size of Particles by Scattering of Light. II. Determination of the Size of Globules of the Polychloroprene Latex by means of Optical and Electron-Microscope Methods . . . . . I. Ya. Slonim, N. M. Fodiman, and Z. M. Ustinova 124

Gas Characteristics of an Optico-Acoustic Gas Analyzer . . . . . A. O. Sall 126

SHORT COMMUNICATIONS

Relations Between the Infrared Band Intensities of Isotopic Molecules . . . . . L. M. Sverdlov 129

A Nomogram for Calculating the Diameter of Particles from Turbidity by Means of the Mie Equation . . . . . I. Ya. Slonim 130

Infrared Absorption Spectra of a Microporous Glass during Adsorption of Methanol and Phenol from Solutions in Carbon Tetrachloride . . . . . A. M. Bogomolny and Yu. A. Lyubimov 131

On the Causes of the Luminescence of Liquids under the Action of Hard Radiation . . . . . L. I. Al'perovich, I. D. Sherbaf, and R. Marupov 132

The Determination of the Order of Interference Bands by Means of a Monoprism and a Plate . . . . . V. G. Khomazuk 134

On the Interpretation of Pressure-Induced Infrared Spectra of Gases . . . . . E. E. Nikitin 135

(Contents continued on inside back cover)